Mitochondrial structure-function in health and disease

Mitchell Edison Allen

Dissertation submitted to the faculty of the Virginia Polytechnic Institute and State University in partial fulfillment of the requirements for the degree of

Doctor of Philosophy
In
Human Nutrition, Foods, and Exercise

David A. Brown, Committee Chair
Eva Schmelz
Steven Poelzing
Robert W. Grange

March 18, 2019
Blacksburg, Virginia

Keywords: mitochondria, cristae, bioenergetics, structure-function, ischemia reperfusion, elamipretide.

Mitochondrial structure-function in health and disease

Mitchell Edison Allen

ABSTRACT

Mitochondrial structure and function are inextricably linked ("structure-function"), with decrements in structure-function evident across diseases. Barriers to new therapies include a complete understanding of the underlying molecular culprits, as well as effective mitochondria-targeted therapies that mitigate injury. In these works, we investigate the role of cristae-shaping factors like cardiolipin in health and disease. In a series of studies, we tested the effects of the cell-permeable tetrapeptides, elamipretide and a postulated peptide, (arginine-tyrosine-lysine-phenylalanine; "RYKF"), on the recovery of mitochondrial structure-function after injury. Elamipretide is a clinical-stage compound currently under investigation for genetic and age-related mitochondrial diseases, yet the mechanism of action is not completely understood. We used a combination of physiological models, mitochondrial imaging, and biomimetic membrane studies to test the hypothesis that elamipretide and RYKF-cardiolipin interactions improved mitochondrial structure-function. Post-ischemic treatment with elamipretide sustained mitochondrial function across electron transport chain complexes. Endogenous RYKF expression similarly improved mitochondrial respiration after peroxide and hypoxia nutrient deprivation injuries. Using two parallel electron microscopy paradigms, we show elamipretide and RYKF treatment led to maintenance of mitochondrial ultrastructure and notably, improved cristae interconnectedness. Finally, we utilized a novel biomimetic membrane system to model the pathological mitochondrial membrane and found that elamipretide and RYKF both improved biophysical pressure-area relationships through a mechanism that appears

to involve aggregating cardiolipin. Our data indicate that targeting pathophysiological mitochondrial membranes with cationic, lipophilic peptides can improve bioenergetics by sustaining cristae networks and support interdependent relationships between mitochondrial structure and function.

Mitochondrial structure-function in health and disease

Mitchell Edison Allen

GENERAL AUDIENCE ABSTRACT

Mitochondria, the powerhouses of the cell, form energy networks that produce over 90% of the body's energy. Mitochondrial dysfunction is implicated across diseases, yet no FDA-approved treatments exist that improve mitochondrial energy production. In this study, we tested the effects of elamipretide, a peptide that localizes to mitochondria. Although elamipretide is currently in clinical trials for several diseases characterized by energetic deficiencies, its mechanism of action is not fully understood. Since mitochondrial structure and function are directly linked, we modeled heart attacks in cultured cells and rat hearts to test the hypothesis that elamipretide and a postulated analog, RYKF, glue damaged mitochondrial membranes back together to preserve structure and function during disease. In hearts subjected to a heart attack, elamipretide significantly protected mitochondrial energy production. Similarly, RYKF protected mitochondrial function in muscle cells exposed to peroxide stress. In damaged hearts imaged with electron microscopy, elamipretide and RYKF treatment significantly improved mitochondrial structure and notably, improved the interconnectedness of mitochondrial energy networks. Furthermore, elamipretide and RYKF improved the integrity of diseased mitochondrial membranes. Together, these data support our hypothesis that elamipretide and RYKF act as mitochondrial adhesion molecules to protect mitochondrial structure and sustain energy production during disease.

ACKNOWLEDGEMENTS

To DB, I am eternally grateful for providing me with the opportunity to work in your lab. You took on an immature and inexperienced student and molded me into a more well-rounded, confident scientist. Outside of the lab, you taught me the art of presentations, developed my work ethic, networked me with your colleagues, and showed me the importance of a healthy work life balance. You pushed me well beyond my perceived limits and along the way, showed me that hard work and dedication pays off in the long run. Today, I am a significantly better scientist than I was 4 years ago. In all, no words or number of thank you's can express my gratitude for your mentorship. Thank you and thank you again and again for all that you have done.

To Justin, you have been an incredible co-worker and friend over the last 4 years. I can't thank you enough for your patience in helping me develop the technical expertise needed to succeed in the lab. Without your guidance, there is absolutely no chance I'd be here today. Too, our similar timeline throughout this process made for thoughtful discussions and an ability to talk with someone who could relate to the ups and downs of this experience. You have been instrumental in my scientific development and in my overall success as a PhD student. I look forward to lifelong of friendship.

To Alex, Grace, and Abey, I am so happy we crossed paths at Virginia Tech. The support you all provided me was instrumental in completing this experience. The experience in helping you all grow into your prominent roles into the lab was the most rewarding aspect of my time as PhD student. You all made me a better person during this experience and for that, I am forever grateful. I wish you all nothing but a lifetime of happiness and success.

To Eva, You were the highlight of working at ILSB. You will never know how grateful I am that we worked together. Your technical expertise helped many of my imaging experiments and our thoughtful scientific discussions encouraged me to pursue the unknown. You were also a breath of fresh air on days I needed it most. If "shit hit the fan" I knew I could count on your enthusiasm to lift my spirits.

To Steve, You provided encouragement when I needed it most. Without your kind words and enthusiasm for science, my enthusiasm for the PhD process, imaging projects, and grants submissions would have sunk. You made the impossible possible for a number of experiments and analyses. I thoroughly enjoyed your mentorship and am grateful for all your support.

To Rob, I am grateful for your sustained support throughout this experience. Thank you for organizing seminars and providing opportunities to present my work. Without your encouragement, I would have never found my love for communicating science. I also thank you for the letter of support during the grant writing process. Your willingness to write your own letter was refreshing and it meant a lot that you wanted to share your own words of support on my behalf. I wish you, your grandchildren, and the rest of your family all the best going forward.

To Emily, there are no words to describe how grateful I am for you. I am forever indebted by your love, support, patience, and encouragement throughout this experience. You've been with me every step of the way and believed in me during the lowest of lows and celebrated with me during the highest of highs. You make me a better person every day, and I admire you more than you know. I can't wait for our next chapter together. I love you.

To my family, without your support, this experience would not have been possible. You all have been my rocks since day one. Thank you so much for providing me with ample opportunities to grow and for your unwavering support every day. I am so lucky I could count on you to help me preserve through some difficult stretches during the last few years. I can't wait to celebrate this achievement with you.

To my Blacksburg friends, Stephen, Burgy, Keagan, Sarah, Ayron, and Steve. You kept me sane throughout this entire process. You have no idea how much I enjoy hanging out with you all. I can't thank you enough for providing me with an outlet away from the lab. I look forward to lifetime of friendship with each of you.

TABLE OF CONTENTS

TABLE OF FIGURES

TABLE OF TABLES

Chapter 1

Introduction

Mitochondria are best known for their central involvement in ATP synthesis. Advances in biochemical assays and electron microscopy in the mid 20th century enabled scientists to study the structure and function of mitochondria for the first time. Mitochondrial structure is characterized by the presence of two membranes: the outer and inner membranes. Each membrane has a different composition, suggesting they play differing roles in mitochondrial function. Indeed, the inner membrane (IM) is characterized by the exclusive presence of cardiolipin (CL), a phospholipid that comprises ~18% of the total lipid composition [1].

CL has been purported to drive protein-protein interactions and membrane curvature [2, 3]. These findings are supported by studies reporting protein complexes assemble where CL is prevalent, specifically at the IM "curves" [4]. Additionally, CL is vital for the formation and maintenance of cristae, the IM "inward foldings" Palade first described in 1952 [5-7]. Cristae host the oxidative phosphorylation (OXPHOS) machinery, a system dependent on CL and comprised of protein complexes that couple the consumption of oxygen with the production of ATP [8]. The shape of cristae are dynamic as activation of OXPHOS shifts the IM from a contracted, "orthodox" state to a wider, "condensed" morphology [9, 10]. To this end, cristae have been called "dynamic biochemical reactors" capable of reorganizing their structure to facilitate the electrochemical processes needed to produce ATP [11]. In addition to CL, several proteins regulate cristae structure and function. These proteins have recently been identified and generally interact with CL to impart positive or negative membrane curvature. Disintegration of CL, these additional proteins, or a combination leads to cristae dysmorphology and impaired mitochondrial function.

Mitochondria are organized into a highly connected reticulum. The architecture of these networks varies depending on tissue type. Along this network, mitochondria are purported to exchange matrix contents, DNA, proteins, and electrical currents (protons) that distribute energy throughout the cell [12-14]. To support the transmission of contents, mitochondria are physically tethered to each other. At short distances (~50nm), mitochondria are connected by intermitochondrial junctions (IMJs) whereas those separated by ~1-5um can be linked by nanotunnels [15-17]. In tissues with increased energetic demands like cardiac and skeletal muscle, IMJs are abundant as mitochondria are packed together between myofibrils. IMJ formation is highly dynamic and is regulated by fusion and fission of the adjacent mitochondrial membranes.

Cristae density is increased at IMJs, a structural characteristic that results in trans mitochondrial cristae alignment [17]. These morphological features are purported to coordinate intermitochondrial networks and facilitate content exchange. Interestingly, cristae shaping factors have been demonstrated to support the exchange of protons between contiguous mitochondria [18]. Indeed, the loss of CL or proteins that regulate cristae ultrastructure causes mitochondrial network fragmentation [19]. These data are supported by emerging evidence demonstrating that cristae assembly factors are implicated in disease. For example, abhorrent cristae and mitochondrial fragmentation were observed in patients with Barth Syndrome, a mitochondrial disease characterized by the loss of CL [20]. These findings are corroborated by others demonstrating patients with mitochondrial diseases have significantly fragmented bioenergetic networks [21]. Taken together, these data suggest *agents that mimic or support cristae shaping factors* like CL may stabilize cristae, facilitate networking, and improve mitochondrial disease patient outcomes.

To our knowledge, therapeutics that enhance mitochondrial networking currently do not exist. A promising pre-clinical study reported that a novel drug-inducible linker system physically

tethers the outer membranes of adjacent mitochondria [17]. This linker technology reportedly recapitulated IMJ structures, increased cristae abundance at the adherent sites, and facilitated cristae alignment across multiple mitochondria. Although these data are exciting, whether or not the linker technology is protective in diseases characterized by fragmented networks is not presently known.

To date, treatments for patients with mitochondrial disease are largely directed at symptoms and often consist of a cocktail of supplements that do not significantly alter the course of the disease. Although multiple compounds are being used in clinical trials [22], the effects of most of these compounds on mitochondrial structure-function are not well-studied and have not been reviewed. Elamipretide, a cell-permeable tetrapeptide in clinical trials for genetic and age-related mitochondrial disease, has been reported to interact with CL, improve cristae morphology, and protect respiratory chain function [23]. Given the interrelated relationship between cristae shaping factors like CL, cristae morphology, mitochondrial networking, and health, elamipretide represents a promising therapeutic approach for bioenergetic disorders. Despite the use of this peptide across scores of studies, there has been uncertainty regarding the mechanism of action. It was originally described as a mitochondria-targeted antioxidant that scavenged reactive oxygen species (ROS) [24]. However, while elamipretide seems to decrease overall ROS levels from pathological mitochondria, the peptide does not affect ROS in healthy tissue or cell-free systems [25-27]. These data suggest elamipretide exerts protection by an alternative mechanism. Despite previous evidence indicating elamipretide interacts with CL, the physiological consequences of this interaction are not understood [28]. Additionally, other cationic, lipophilic peptides have been reported to localize to mitochondria. Nevertheless, it is not known if these peptides or analogs of elamipretide interact with CL to influence cristae structure and function[29].

Overall, the work described in the following chapters elucidates the role of mitochondrial structure-function in health and disease. A major focus of this work is mitochondrial cristae, the major regulators of cristae shape, and how cristae can be therapeutically targeted during disease. The second chapter reviews the literature pertaining to cristae shaping factors and how these contribute to health and disease. In chapters three and four, we provide evidence that two mitochondria-targeted peptides interact with CL, improve the biophysical properties of the inner membrane, and preserve cristae structure-function during disease. Finally, we describe the findings for their implications in the field, and provide future directions for the study of mitochondrial structure-function.

References

1. Horvath SE, D.G., *Lipids of mitochondria.* Progress in Lipid Research 2013. **52**(4): p. 590-614.

2. J, W., *Structural biology: Up close with membrane lipid-protein complexes.* Science, 2011. **334**: p. 320-321.
3. C, H.J.a.U., *Cellular microcompartments constitute general subcellular functional units in cells* Biological Chemistry, 2013. **394**: p. 151-161.
4. Bazán S, M.E., Mallampalli VK, Heacock P, Sparagna GC, Dowhan W, *Cardiolipin-dependent reconstitution of respiratory supercomplexes from purified Saccharomyces cerevisiae complexes III and IV.* Journal of Biological Chemistry, 2013. **288**(1): p. 401-411.
5. GE, P., *An electron miscroscope study of the mitochondrial structure* J Histrochem Cytochem, 1953. **1**(4): p. 188-211.
6. Khalifat N, F.J., Puff N, , *Lipid packing variations induced by pH in cardiolipin-containing bilayers: the driving force for the cristae-like shape instability.* Biochimica et Biophysica Acta, 2011. **1808**(11): p. 2724-2733.
7. Khalifat N, P.N., Monneau S, Fournier JB, Angelova MI, *Membrane deformation under local pH gradient: mimicking mitochondrial cristae dynamics.* Biphysical Journal 2008. **95**(10): p. 4924-4933.
8. Gilkerson RW, S.J., Capaldi, *The cristal membrane of mitochondria is the principal site of oxidative phosphorylation.* FEBS Letters, 2003. **546**: p. 355-358.
9. Hackenbrock, C., *Ultrastructural bases for metabolically linked mechanical activity in mitochondria* Journal of Cell Biology 1966. **2**: p. 269-297.
10. Hackenbrock, C., *Ultrastructural bases for metabolically linked mechanical activity in mitochondria. II. Electron transport-linked ultrastructural transformations in mitochondria.* Journal of Cell Biology 1968. **37**(2): p. 345-369.
11. Cogliati, E., Scorrano, *Mitochondrial Cristae: Where Beauty Meets Functionality.* Cell Press, 2016. **41**(3).
12. Amchenkova AA, B.L., Chentsov YS, Skulachev VP, Zorov DB, *Coupling membranes as energy-transmitting cables. I. Filamentous mitochondria in fibroblasts and mitochondrial clusters in cardiomyocytes.* Journal of Cell Biology, 1988. **107**(2): p. 481-495.
13. VP, S., *Mitochondrial filaments and clusters as intracellular power-transmitting cables.* Trends in Biochemical Sciences, 2001. **26**(1): p. 23-29.
14. Glancy, B., et al., *Mitochondrial reticulum for cellular energy distribution in muscle.* Nature, 2015. **523**(7562): p. 617-20.
15. Vincent AE, T.D., Eisner V, Hajnóczky G, Picard M, *Mitochondrial Nanotunnels.* Trends in Cell Biology, 2017. **27**(11): p. 787-799.
16. Lavorato M, I.V., Dewight W, Cupo RR, Debattisti V, Gomez L, De la Fuente S, Zhao YT, Valdivia HH, Hajnóczky G, Franzini-Armstrong *Increased mitochondrial nanotunneling activity, induced by calcium imbalance, affects intermitochondrial matrix exchanges.* Proceedings of the National Academy of Sciences, USA, 2017. **114**(5): p. E849-E858.
17. Picard M, M.M., Dorn GW, Wallace DC, et al, *Trans-mitochondrial coordination of cristae at regulated membrane junctions.* Nature Communications, 2015.
18. Santo-Domingo J, G.M., Poburko D, Scorrano L, Demaurex N, *OPA1 promotes pH flashes that spread between contiguous mitochondria without matrix protein exchange.* EMBO J, 2013. **32**(13): p. 1927-1940.
19. Weber TA, K.S., Heide H, Wittig I, Head B, van der Bliek A, Brandt U, Mittelbronn M, Reichart AS, *APOOL is a cardiolipin-binding constituent of the mitofilin/MINOS protein*

complex determining crisate morphology in mammalian mitochondria. Plos one, 2013. **8**(5).
20. Gonzalvez, F., et al., *Barth syndrome: cellular compensation of mitochondrial dysfunction and apoptosis inhibition due to changes in cardiolipin remodeling linked to tafazzin (TAZ) gene mutation.* Biochim Biophys Acta, 2013. **1832**(8): p. 1194-206.
21. Vincent AE, W.K., Davey T, Philips J, Ogden RT, Lawess C, Warren C, Hall MG, Ng YS, Falkous G, Holden T, Deehan D, Taylor RW, Turnbull DM, Picard M, *Quantitative 3D Mapping of the Human Skeletal Muscle Mitochondrial Network.* Cell Reports, 2019. **26**(4): p. 996-1009.
22. El-Hattab AW, Z.A., Almannai M, Scaglia F, *Therapies for mitochondrial diseases and current clinical trials.* Molecular Genetics and Metabolism, 2017. **122**(3): p. 1-9.
23. Birk, A.V., et al., *The Mitochondrial-Targeted Compound SS-31 Re-Energizes Ischemic Mitochondria by Interacting with Cardiolipin.* J Am Soc Nephrol, 2013.
24. Zhao, K., et al., *Cell-permeable peptide antioxidants targeted to inner mitochondrial membrane inhibit mitochondrial swelling, oxidative cell death, and reperfusion injury.* J Biol Chem, 2004. **279**(33): p. 34682-90.
25. Brown, D.A., et al., *Reduction of Early Reperfusion Injury With the Mitochondria-Targeting Peptide Bendavia.* J Cardiovasc Pharmacol Ther, 2013.
26. Dai, W., et al., *Bendavia, a mitochondria-targeting peptide, improves postinfarction cardiac function, prevents adverse left ventricular remodeling, and restores mitochondria-related gene expression in rats.* J Cardiovasc Pharmacol, 2014. **64**(6): p. 543-53.
27. Sabbah, H.N., et al., *Chronic Therapy With Elamipretide (MTP-131), a Novel Mitochondria-Targeting Peptide, Improves Left Ventricular and Mitochondrial Function in Dogs With Advanced Heart Failure.* Circ Heart Fail, 2016. **9**(2): p. e002206.
28. Birk, A.V., et al., *Targeting mitochondrial cardiolipin and the cytochrome c/cardiolipin complex to promote electron transport and optimize mitochondrial ATP synthesis.* Br J Pharmacol, 2014. **171**(8): p. 2017-28.
29. Horton KL, S.K., Froseca SB, Guo Q, Kelley S, *Mitochondria-Penetrating Peptides.* Cell Press, 2008 **15**: p. 375-382.

Chapter 2

Mitochondrial structure-function in health and disease: A comprehensive review of mitochondrial morphology and related mitochondria-targeted therapeutics

Mitchell E. Allen

The history of mitochondrial Structure-Function: The beginning

Mitochondrial characteristics may have first been published as early as the 1840s, yet anatomist Rudolf von Koeliker was most likely the first to describe mitochondria in 1857 as he called them "sarcosomes" while studying striated muscle. Thirty-three years later Altmann became the first to describe the structures as "bioblasts" and "elementary organisms" that live inside cells and carry out vital functions. Then, in 1898, Carl Benda coined the term "mitochondrion", which originates from the Greek words "mitos" (thread) and "chondros" (granule). At the turn of the century, mitochondrial research significantly increased as the first mitochondrial dye, Janus Green B, was identified by Michaelis and remarkably, in 1908, Regaud described the organelle as protein and lipid containing while suggesting they are "bearers of genes."

Many of these important early observations were almost exclusively based on morphological observations and without direct chemical evidence [1]. As Cowdry stated in 1924, "the investigation of mitochondria will never achieve the usefulness which it deserves […] until we know much more of their chemical constitution" [1, 2]. Soon after, Keilin described the cytochromes a "respiratory pigment" and a little over a decade later, Krebs detailed the citric acid cycle [3, 4].

The Middle

In the 1940s, Claude employed fractionation procedures to examine the size and shape of particles recovered from the fraction [5]. These experiments included a "large fraction" containing mitochondria and from these studies he concluded "the mechanism by which molecular oxygen is utilized [..] in the cell can be ascribed in large measure, if not entirely, to a definite morphological entity" [6]. These findings highlight one of the first comparisons of bioenergetic structure and function, and subsequently, led to optimized techniques that enabled the ability to study isolated, structurally-preserved mitochondria. Within half a decade, the respiratory control ratio (RCR) was developed and purported to be impaired when mitochondrial structure was compromised [7, 8]. Indeed, these data gave credence to Claude's findings and suggested oxidative phosphorylation required both the integrity of mitochondrial structure and functional respiratory enzymes.

Soon after methods were developed to isolate intact, functional mitochondria, Palade and Sjostrand published the first high resolution electron micrographs in 1953 [9-11]. These publications are hallmarks for identifying bioenergetic structures today as Palade became the first to identify and describe the matrix and cristae while Sjostrand noted the double membranes surrounding each mitochondrion. Using Palade's electron microscopy methods and isolation techniques first developed by Claude, Hackenbrock became the first to report that mitochondria undergo specific, morphological changes in response to substrate conditions [12, 13]. Indeed, these pioneering studies showed that mitochondrial structure is dynamic as the inner membrane (IM) switches between "orthodox" and "condensed" states. However, many scientists at the time believed these morphological transitions only occurred *in vitro*, and his findings were largely ignored for decades.

Present Day

In the last two decades, advances in microscopy have renewed interest in mitochondrial structure-function relationships. Today, Hackenbrock's studies are often regarded as the foundation of mitochondrial form and function studies. Recent advances employing high resolution, 3D imaging of mitochondria have confirmed Hackenbrock's findings and compliment the original electron micrographs produced by Palade and Sjostrand [14, 15]. These novel imaging technologies (namely FIB-SEM, SBF-SEM, and cryo-EM) permit deeper insights into mitochondrial structure than has ever been possible before. In conjunction with these imaging advancements, the development of genetic animal models has led to the identification of specific proteins and lipids that modulate mitochondrial structure-function. Indeed, emerging evidence suggests a variety of diseases ranging from cancer to heart failure are characterized by compromised bioenergetic structure-function. Thus, it is the purpose of this review to summarize how these morphological parameters influence mitochondrial form and function, contribute to health and disease, and can be targeted by developing therapies.

Cristae: Structure Meets Function

As first discovered by Sjostrand [10], mitochondria are composed of a limiting outer membrane (OM) and an inner membrane (IM) that encloses an enzymatic and mtDNA rich matrix. The IM is characterized by the presence of cardiolipin (CL), a mitochondrial specific lipid species found within the IM inner leaflet. CL has been purported to drive protein-protein interactions and membrane curvature [16, 17]. These findings are supported by studies reporting protein complexes assemble where CL is prevalent, namely at the IM "curves" [18]. Additionally, CL is vital for the formation and maintenance of cristae, the IM "inward foldings" Palade first described in 1952 [19-

21]. Cristae host the oxidative phosphorylation (OXPHOS) machinery, a system dependent on CL and comprised of protein complexes that couple the consumption of oxygen with the production of ATP [22]. The shape of cristae are dynamic as activation of OXPHOS shifts the IM from a contracted, "orthodox" state to a wider, "condensed" morphology [12, 13]. To this end, cristae have been called "dynamic biochemical reactors" capable of reorganizing their structure to facilitate the electrochemical processes needed to produce ATP [23]. In addition to CL, cristae form and function is regulated by a number of IM structures and proteins. Here, we review in detail how CL and these other shaping factors influence cristae structure-function and their implications in health and disease.

Dissecting Cristae Structure-Function

Cardiolipin (CL)

The IM is composed of ~ 40% phosphatidylcholine (PC), 34% phosphatidylethanolamine (PE), 18% cardiolipin (CL), and small amounts of phosphatidylserine (PS), phosphatidylinositol (PI), and cholesterol [24, 25]. Among the phospholipids within the IM, CL is the most unique. CL is a non-bilayer phospholipid exclusively found in the IM and has four fatty acyl chains that share a glycerol head group. The combination of two phosphatidyl moieties and the anionic head group create a cone-shaped structure that facilitates CL's ability to reside within the inner leaflet of the IM. Within the inner leaflet, CL imparts negative membrane curvature that stabilizes the cristae structure. In addition to maintaining structural stability of the membrane, CL is also important for preserving a variety of mitochondrial functions. For example, supercomplex assembly [26], complex I-dependent respiration [27], complex III-dependent respiration [27], complex IV-

dependent respiration [28], ADP-dependent respiration [29], ATP synthase activity [30], adenine nucleotide transporter (ANT) activity [31], and anchoring of cytochrome c [32] are a brief list of myriad CL-dependent functions. The role of CL in mitochondrial structure-function is well-known and has been extensively reviewed. For these reasons, we provide a brief description of CL and how it contributes to health and disease. For more in-depth analyses, we direct the reader to one of the many excellent review articles [23-25, 33-35].

While most phospholipids are synthesized in the ER, cardiolipin is produced in the IM. Precursor lipids like phosphatidic acid (PA) and diacylglyceral (DAG) are imported from the ER to the intermembrane space (IMS) via the protein complex PRELID1-TRIAP1 (Ups-Mdm35 in yeast) [36]. These precursor lipids are then converted into CL through a series of enzymatic reactions that are currently under investigation. Disruption of CL biosynthesis has vast consequences on cristae form and function that range from impaired morphology, dissipation of membrane potential, to decreased ATP production and supercomplex disassembly [37, 38].

CL loss and peroxidation is well-known to occur during diseases [35]. However, how these decrements influence the biophysical properties of the IM and contribute to disease progression is relatively unknown. A recent report concluded CL oxidation leads to conformational changes in both the head and backbone groups [39]. Indeed, CL oxidation was associated with bilayer thinning, decreased chain length, and CL “tilting” that affected the symmetrical properties of the membrane. This oxidation-induced reorganization of structure would conceivably impair CL-mediated cristae stabilization, membrane-respiratory protein interactions, and electron transport chain (ETC) function. Accordingly, diseases characterized by impaired mitochondrial structure-function such as Barth Syndrome, ischemia reperfusion (I/R), and aging are also defined by decrements in CL content and remodeling [35].

Mitochondrial-targeted therapeutics to preserve CL content, protect against peroxidation, and maintain its biophysical properties within the IM are under development. In pre-clinical models, exogenous administration of CL in the ischemia-reperfused rat heart improved decrements in complex I activity [40]. Although these results are encouraging, this paradigm has little to no translational relevance. More recently, an exciting method to deliver lipid-containing nanodiscs to mitochondrial membranes was reported [41]. Although this novel technique has promising therapeutic potential, whether or not the technology can deliver CL-containing nanodiscs to structurally compromised mitochondrial membranes and improve patient outcomes remains to be investigated.

Elamipretide (formerly Bendavia, SS-31, MTP-131) is a mitochondrial-targeted peptide currently in clinical development for mitochondrial diseases [42]. The peptide has been shown to localize to CL and improve mitochondrial structure-function in a variety of pre-clinical disease models [43-47]. Although the peptide has been called a "mitochondria-targeted antioxidant", cell-free studies recently concluded the peptide is not exerting cytoprotection by directly scavenging reactive oxygen species (ROS) [45]. Similarly, elamipretide has been reported to preserve CL content during disease, but these findings are not ubiquitous [44](Described in chapter 3). Instead, the peptide may exert protection via CL aggregation. As described in chapter 3, Elamipretide aggregates CL to maintain the biophysical and lipid packing properties of the IM. These data were associated with enhanced cristae ultrastructure, improved respiration across ETC complexes, and decreased ROS production. Taken together, these data suggest Elamipretide interacts with CL to preserve the integrity of the IM, which in turn, improves cristae form and mitochondrial function during disease.

Cristae Junctions

Cristae communicate with the inner boundary membrane (IBM), the matrix-facing side of the IM, through narrow, tubular cristae junctions (CJs). CJs physically connect the cristae to the IBM at a ~90° bend, and prevent the diffusion of cristae-bound, biochemical processes into the intermembrane space (IMS). Theoretical calculations have predicted spatially distinct solute concentrations between the cristae and IMS [48]. Furthermore, the integrity of CJs and the ability to induce significant curvature at the IBM is dependent on phospholipids like CL that reside in the elastic membrane environment [23, 25]. Under healthy, physiological conditions CJs are narrow (~20-40nm) and retain respiratory components within the cristae lumen. In contrast, CJs widen (~60nm) during disease and facilitate the release of respiratory factors like cytochrome c into the intermembrane space that subsequently, initiate a cascade of proapoptotic signaling events in the cytosol [49, 50]. Additionally, it is likely that lipid trafficking between the cristae and IMS is restricted at the CJ, and may explain the distinct lipid compositions between the OM and IM (i.e., the exclusive presence of CL in the IM) [51]. Thus, CJs have been described as "physical contacts that harbor functional significance" and "communication gates between the cytoplasm and mitochondrial matrix" [52]. Additionally, CJs most likely facilitate the exchange of metabolites, genetic information, and other content within and between mitochondria, although this has not been conclusively determined. Multiple protein complexes have been reported to exist at the contact sites, most notably the mitochondrial contact site and cristae organizing system (MICOS). Future studies should combine pre-clinical knockdown models of MICOS or other CJ components with pH-sensing probes [53] to determine how CJs aid in mitochondrial content exchange.

Mitochondrial Contact and Cristae Organizing System (MICOS)

MICOS is a 1279 kDa multiprotein complex located at the CJ and IBM intersection [54, 55]. Its role in mitochondrial structure-function is well documented and has been extensively reviewed. For these reasons, we have only provided a brief description of MICOS and its role in mitochondrial structure-function. For more in-depth description, we direct the reader to one the many excellent review articles [56-58]. Several MICOS subunits, termed "Mic plus a number," have recently been discovered. These subunits form complexes that are critical for CJ stability and cristae formation [55, 57, 59, 60]. Indeed, the Mic10/Mic12/Mic26 complex facilitates cristae junction formation and its assembly is CL-dependent [61]. Similarly, Mic26 (previously known as APOOL) directly binds CL to determine cristae morphology [62]. In contrast, the Mic60 complex has been described as OXPHOS and CL independent [61]. Mic19, which physically interacts with Mic60 in mammals, is critical for the formation of elongated mitochondria as its depletion has been reported to induce fragmentation and loss of cristae. These findings were associated with decreased basal and maximal respiration, suggesting Mic19 plays a crucial role in proper mitochondrial structure-function [63]. Similar results have been reported in human cell lines where depletion of MICOS subunits causes impaired respiration [62, 64]. Furthermore, the MICOS complex has been reported to interact with other IM proteins such as Aim24 [65]. In cells lacking Aim24 and modified MICOS subunits, cristae ultrastructure and super complex assembly were significantly impaired. These findings were associated with MICOS-dependent remodeling of CL to longer, more saturated acyl chains. Taken together, these data suggest MICOS affects the spatial organization of mitochondrial membrane lipids and subsequently influences cristae ultrastructure and respiratory complex assembly.

MICOS disruption has recently been reported in several pathologies. Loss of function of QIL1, a recently discovered MICOS subunit [66], has been reported to cause mitochondrial hepato-encephalopathy [67]. Parkinson's disease has also been characterized by CHCHD2 mutations and impaired respiratory function [68]. Interestingly, the mitochondria-targeting peptide, Elamipretide, was found to enhance CHCHD2 and OXPHOS enzymes in this neurodegenerative model. This study suggests mitochondria-targeted therapies may improve MICOS assembly and mitochondrial function during disease. However, these findings may not be ubiquitous across diseases, as studies have reported no differences in CJ width between healthy and Leigh Syndrome mitochondria, suggesting MICOS was not disrupted [69].

Today, it is clear MICOS is critical for proper mitochondrial structure-function. The field has made tremendous progress during the last decade to identify the MICOS components and define the phenotypic consequences of knocking down its constituents. However, characterizing how MICOS and the subsequent CJ assembly is affected during specific diseases is still relatively unknown. Future studies will need to employ animal and cell models of disease to further investigate the relationship between MICOS and conditions like cancer and heart failure. Additionally, mechanistic studies are needed to investigate how the MICOS subcomplexes communicate with the phospholipid environment to bind CL, stabilize CJs, and facilitate cristae formation. Interventions that promote MICOS-CL interactions may affect the spatial organization of the mitochondrial membrane. These membrane shaping interactions are attractive therapeutic targets, yet this area of research remains largely unexplored.

Optic Atrophy 1 (OPA1)

Optic Atrophy 1 (OPA) is a profusion dynamin-related protein located in the inner mitochondrial membrane. OPA1 is a potent regulator of cristae shape and its effects on mitochondrial structure-function have been extensively reviewed. Here, we provide a brief description of OPA1 and its implications in health and disease. For a more in-depth review we direct the reader to one of the excellent published review articles [23, 52, 70, 71]. OPA1 is comprised of long (L-OPA1) and short (S-OPA1) forms where the L-OPA1 is membrane-anchored and S-OPA1 is proteolytically cleavable [72]. Maintenance of cristae structure by OPA1 requires its oligomerization. Indeed, loss of OPA1 oligomers leads to widened CJs, cytochrome c release, apoptosis, impaired respiration, and decreased ATP synthase [49, 71, 73]. Furthermore, OPA1 knockout mice are embryonically lethal, highlighting the importance of the protein for viability and development. OPA1 overexpression *in vitro* and *in vivo* has been correlated with thinner cristae, narrower CJs, enhanced supercomplex assembly, improved respiration, and resistance to cell death [49, 74-76]. Although OPA1-mediated cristae remodeling is concomitant with its ability to fuse the IM, the observed antiapoptotic functions seem to be independent of fusion activity [49].

Interestingly, OPA1's position within the IM may promote interactions with other cristae shaping factors. Indeed, recent evidence suggests OPA1 is epistatic to MICOS in the regulation of cristae morphology [50]. This study concluded OPA1 physically interacts with Mic60 to form a multimer protein complex that controls CJ stability, and that OPA1 oligomers control both cristae and CJ width independent of Mic60. Similarly, OPA1-mediated fusion has been reported to be CL-dependent [72, 77] while others have suggested CL modulates OPA1 oligomerization and subsequently, cristae morphology [23, 78]. Recent *in vitro* evidence suggests L-OPA1 physically binds to CL-containing liposomes to drive membrane fusion whereas S-OPA1 does not fuse liposomes in the presence of CL [72]. These findings are supported by studies reporting CL

involvement in OPA1 assembly and subsequently, the protein's ability to hydrolyze GTP and stimulate membrane fusion [77-79]. Moreover, OPA1 has also been reported to interact with mitochondrial carrier and solute proteins like SLC25A [73]. These interactions enable OPA1 to sense fuel substrate changes and subsequently, remodel mitochondrial morphology by narrowing cristae and promoting ATP synthase dimerization. Taken together, these data highlight the ability of OPA1 to interact with IM proteins and lipids to dynamically influence cristae form and function.

OPA1 has been implicated in several diseases characterized by mitochondrial structure-function decrements. In pre-clinical models, OPA1 overexpression *in vivo* protects mice from muscular atrophy, cardiac ischemia-reperfusion injury, and liver damage [75]. These findings were associated with improved cristae ultrastructure and decreased cytochrome c release. Similarly, OPA1 overexpression protected two different mouse models of mitochondrial disease from deficiencies in complex I and IV, enhanced supercomplex formation, and corrected cristae dysmorphology [76]. In mice, cardiac-specific OPA1 proteolysis triggers mitochondrial fragmentation and subsequently causes dilated cardiomyopathy and heart failure [80]. Moreover, patients with a variety of neurological indications have been characterized by deficits in OPA1, including Alzheimer's [81] and Parkinson's Diseases [82].

OPA1 is undoubtedly a master regulator of cristae form and function. Although the field has made significant progress in establishing the structural and functional consequences of both ablating and overexpressing OPA1, there is still much to learn about this IM-fusing protein. Mechanistically, we know little about how OPA1 interacts with other membrane shaping factors like MICOS and CL. Animal and cell culture models employing a combination of OPA1-MICOS-CL mutations would elucidate specifically how these form factors contribute to cristae biogenesis and maintenance. Furthermore, with the exception of a few neurodegenerative indications, very

few data exist on how OPA1 is implicated in human disease. Clinicians and basic scientists alike need to collaborate to characterize how OPA1 could be involved in epidemics like cancer, heart failure, and diabetes.

Finally, research investigating how medicines can target OPA1 to improve cristae structure-function is non-existent to date. The pre-clinical evidence to date suggests medicines that increase the prevalence of OPA1 could be a viable therapeutic strategy for diseases characterized by cristae dysmorphology. Additionally, medicines that promote or mimic OPA1-SLC25A interactions may aid in stabilizing OPA1 oligomers and support dynamic cristae remodeling during disease. The SLC25A carrier proteins are comprised of three homologous amino acid repeats of largely cationic and lipophilic consensus motifs [83]. Medicines composed of alternating cationic, lipophilic amino acids may both localize to mitochondria [84], and support or mimic OPA1-SLC25A interactions to facilitate proper cristae structure-function during disease.

ATP Synthase

ATP synthase dimers are organized in helical rows along the cristae edges. Their "zipper-like" arrangement within the IM seems to be fundamental for the creation of a proton gradient that facilitates the flow of protons from the respiratory complexes back into the matrix via ATP synthases [85, 86]. The role of ATP dimer organization in imparting positive membrane curvature and facilitating proper mitochondrial structure-function has been extensively reviewed [14, 23, 52, 69, 88]. For these reasons, we only provide a brief overview of ATP synthase dimerization in mitochondrial form and function. The reader is directed to one of the excellent review articles cited above for a more in-depth analysis.

The ATP synthase is composed of F_1 and F_o monomers that assemble into dimers. F_1 is a catalytic sector that faces the matrix while the F_o sector is embedded into the IM [89]. Together, they form an intrinsic angle (40-70°) sufficient to induce positive curvature in the IM [52, 90, 91]. The subunits that comprise the two monomers are critical for dimerization and ultrastructure stability. Indeed, subunits e, g, and k within F_o have been reported to be essential for ATP dimer assembly and subsequent cristae structure-function in yeast mitochondria [92, 93]. Furthermore, in the absence of subunits e and g, abnormal, onion-like cristae form [90]. ATP synthase dimers may also constitute the calcium-sensitive mitochondrial permeability transition pore (mPTP) [94]. mPTP opening is well known to impair cristae ultrastructure, decrease mitochondrial respiration, release cytochrome c, and induce cell death. Taken together, these data highlight the critical role ATP synthase dimers play in proper membrane curvature and mitochondrial structure-function.

IM constituents like CL influence ATP synthase assembly and dimerization. As early as 1973, scientists reported correlations between CL degradation and loss of ATP synthase activity [95]. Two decades later Eble et al. reported the first evidence of physical CL-ATP synthase interactions using solid state NMR [30]. Today, we know CL specifically binds to the c-rings within F_o, which drives ATP synthase rotation and subsequent ATP production [96] (in the presence of sufficient membrane potential). Furthermore, recent studies reporting that CL deficiency disrupts ATP synthase assembly have complimented earlier findings [95, 97]. Taken together, these studies demonstrate the vital role CL plays in ATP synthase stability and support a model in which cristae-shaping proteins cooperate with IM lipids to determine cristae form and function.

A variety of diseases are characterized by ATP dimer impairment. Pre-clinical studies in yeast reported age-dependent dissociation of ATP synthase dimers that led to decreased cristae

[98]. Furthermore, an Alzheimer's Disease mouse model found disrupted ATP synthase dimers that caused reduced ATP production, increased oxidative stress, and mPTP opening [99]. Mitochondrial myopathy patients with the 8344A>G mutation (a gene important for mitochondrial protein assembly) contain onion-like cristae that are consistent with the dysmorphologies observed in mitochondria with F_0 mutations [93, 100]. Similar observations of disrupted ATP dimers, impaired cristae ultrastructure, and decreased ATP production have been reported in mitochondrial disease patients with Leigh's syndrome [69, 101]. Furthermore, enhanced mPTP opening is well characterized in a host of diseases including cardiac ischemia-reperfusion [102], diabetes [47], cancer [103], and Parkinson's Disease [104]. Advancements in biochemical assays and imaging modalities during the last two decades have revealed ATP synthase assembly and function is critically involved in bioenergetic health. Both pre-clinical and human studies have shown damage to ATP synthase dimers leads to compromised cristae structure-function that ultimately, causes a variety of diseases. Although the current evidence suggests ATP synthase dimers interact with IM lipids like CL, few data exist on whether ATP synthase coordinates with other membrane shaping proteins to influence cristae morphology. To this end, Rampelt et al. recently reported ATP dimers interact with the MICOS subunit Mic10 [105]. These data suggest the field is beginning to consider the cooperation between ATP synthase, MICOS, OPA1, and CL in regulating cristae shape, but more studies are certainly needed to investigate their interplay. Furthermore, the ATP synthase are often depicted at the cristae rims [23, 69]. The current literature suggests ATP synthases are located at CL-enriched domains around the curved regions of the IM. For these reasons, we hypothesize these dimers exist in rows ubiquitously expressed around the tubular edges as depicted in Muhleip et al. and are not exclusively found at the cristae rims [106]. Future studies employing the use of 3D microscopy are needed to confirm these hypotheses.

Lastly, medicines that stabilize ATP synthase assembly and promote proper cristae form and function are currently in development. Several therapies like cyclosporine A reduce mPTP opening and confer cellular protection in a host of pre-clinical disease models [107-112]. However, these medicines have had little success translating into the clinic [113-115]. Since the ATP synthase interacts with the IM lipid environment, another therapeutic strategy could be to target CL to indirectly stabilize ATP dimer assembly. Indeed, the cell-permeable, mitochondria-targeting peptide, Elamipretide (formerly SS-31, MTP-131, Bendavia), has been shown to localize to CL, preserve cristae architecture, improve ATP production, and desensitize mPTP opening in the diabetic rat heart [44, 47, 116]. Furthermore, Elamipretide treatment preserved complex V density after cardiac ischemia reperfusion injury (Described in chapter 3). In the clinic, Elamipretide treatment did not statistically decrease infarct size in patients with myocardial ischemia patients [117, 118]. However, Elamipretide treatment dose-dependently improved the distance primary mitochondrial disease patients walked in 6 minutes [42]. Taken together, these data suggest cationic, lipophilic peptides like Elamipretide target anionic cardiolipin head groups. In turn, the peptide-CL interactions may indirectly stabilize CL-ATP synthase interactions to preserve cristae form and mitochondrial function in pre-clinical and clinical settings.

Do current therapies for mitochondrial disease influence cristae structure-function?

The field has made tremendous growth in identifying cristae shaping factors that influence mitochondrial function. We are now beginning to understand the role these factors play in the development of mitochondrial disease as studies are reporting which structural defects accompany which disorders [69, 119]. However, more studies examining mitochondria from diseased patients

are needed to draw these conclusions. Defining the relationship between these disorders and their concomitant structural defects will support the development of therapeutics that are tailored to specific diseases. To date, treatments for mitochondrial patients are largely symptomatic and often consist of a cocktail of supplements that do not significantly alter the course of the disease [120]. Although these supplements and other developing compounds have been reported to improve bioenergetic function, their effects on mitochondrial structure are relatively unknown. As we learn more about which structural defects drive which diseases, physicians may be able to make patient-specific decisions regarding which therapies have the best chance of treating the underlying dysmorphology. In the next section we briefly review current and developing therapies for mitochondrial diseases. We compliment this existing knowledge by providing novel insight into how these therapeutics may influence bioenergetic structure, and subsequently, contribute evidenced-based recommendations for which compounds may potentially treat specific disorders for the first time. In doing so, we hope to accomplish two objectives. First, identify gaps in the literature where the effects of these therapies on mitochondrial structure are unknown. Second, improve mitochondrial disease patient outcomes by helping to tailor medicines to specific structure-function deficits. The therapeutics discussed below are compounds in clinical or preclinical development for bioenergetic disorders. For a more in depth review on these compounds and other nutritional supplements, we direct the interested reader to an excellent review of current therapies for mitochondrial disease [120].

Idebenone/CoQ_{10}

Idebenone and CoQ_{10} (ubiquinone) are mitochondrial treatments that aim to enhance electron transport chain (ETC) function. CoQ_{10} is an integral component of the ETC as it shuttles electrons from complexes I and II to III via the Q pool. CoQ_{10} deficiency is a mitochondrial disease that results from defective CoQ_{10} biosynthesis. A range of CoQ_{10} supplementation (5-30 mg/kg/day) has been shown to improve electron flow and clinical symptomology associated with this deficiency [120]. However, although CoQ_{10} is generally safe for patients, supplementation has not shown consistent benefits for other mitochondrial disorders.

To date, most of the literature has examined the effects of CoQ_{10} on mitochondrial function in a variety of pathological models while outcomes on structure are severely understudied. In one of the few studies investigating CoQ_{10} and mitochondrial morphology, CoQ_{10} treatment significantly prevented burn-induced swelling, cristae loss, cristae fragmentation, and super complex dissociation in mice [121]. Similarly, others have reported CoQ_{10} treatment in metabolically-stressed astrocytes preserves mitochondrial mass, cristae number, cristae width, and OXPHOS protein expression [122]. Interestingly, these findings were associated with increased levels of mitofilin, a MICOS component. These data suggest CoQ_{10} improves mitochondrial structure *in vitro*, perhaps by stabilizing cristae shaping factors like MICOS. Moreover, a recent study by Kaurola et al. demonstrated quinones interact with inner membrane lipid acyl groups and have little interaction with cardiolipin [123]. These data suggest CoQ_{10}-mediated protection is cardiolipin-independent and may aid in diseases characterized by the loss of cardiolipin like Barth Syndrome. Whether these quinone-lipid interactions cause inner membrane morphological changes is not presently known. More studies are warranted to corroborate these few reports of CoQ_{10} effects on mitochondrial structure and to determine whether CoQ_{10} modulates other cristae

shaping factors. Finally, investigations demonstrating how these effects translate to the clinic are needed.

Idebenone is a structural analog of CoQ_{10} with a more favorable pharmacokinetic profile [120]. Idebenone has been studied primarily as a therapeutic for Leber's hereditary optic neuropathy (LHON), a complex I mitochondrial disease characterized by vision loss. In LHON patient trials, 3 doses of 300mg idebenone prevented the loss of overall and color vision while failing to restore visual acuity toward healthy levels [124, 125]. In pre-clinical studies, idebenone has primarily been shown to exert protection through a mechanism purported to involve ROS scavenging, although our work indicates that idebenone acts by "bypassing" complex I of the ETC and is not a ROS scavenger (Perry, Allen, manuscript currently *in review*).

Despite promising clinical outcomes and substantial pre-clinical data demonstrating protection of bioenergetic function, there are no studies examining effects of idebenone on mitochondrial structure to our knowledge. Due to the similarity between idebenone and CoQ_{10}, we speculate that the effects of idebenone on cristae structure are analogous to the protection observed with CoQ_{10}. To this end, cristae dysmorphology observed in LHON patients (cristae loss and downregulation of mitofilin) is similar to the structural impairments CoQ_{10} has been reported to alleviate [126, 127]. Taken together, these data suggest idebenone may prevent abhorrent cristae remodeling in LHON patients, yet further study is needed to confirm this hypothesis.

EPI-743

EPI-743 is a para-benzoquinone analog. In comparison to CoQ_{10} and idebenone, EPI-743 is comprised of a *bis*-methyl substitution that changes the quinone ring structure and oxidation-reduction potential [128]. It is characterized as a mitochondrial antioxidant as it protects against

excessive ROS production and prevents depletion of reduced glutathione [128]. EPI-743 has been studied in a variety of mitochondrial diseases including Leigh syndrome, MELAS, Friedreich's Ataxia, LHON, and POLG deficiency. In a clinical trial of patients with genetically-confirmed mitochondrial disease, treatment generally slowed disease progression and improved clinical outcomes [129]. Other clinical studies of patients with Leigh syndrome and LHON have reported similar findings ranging from delayed or reversed disease progression to improvements in reduced glutathione levels [130-132].

Despite these promising clinical outcomes, to our knowledge no studies have examined the effects of EPI-743 on mitochondrial structure. Like CoQ_{10} and idebenone, EPI-743 is a quinone analog and it reportedly one thousand to ten thousand fold more potent than CoQ_{10} and idebenone in protecting patient fibroblasts from ROS [129]. Thus, it is likely EPI-743 affords similar or enhances the cristae protection observed with CoQ_{10} treatment. To this end, cristae dysmorphology observed in patients with LHON (cristae loss and downregulation of mitofilin) and Leigh syndrome (cristae loss, swollen matrix) are similar to the structural impairments CoQ_{10} has been reported to alleviate [69, 126, 127]. Taken together, these data suggest EPI-743 may delay or reverse the loss of cristae in patients with mitochondrial disease, but further studies are needed.

RTA-408

Omaveloxolone (RTA 408) is a semisynthetic oleanane triterpenoid that activates Nrf2 to promote antioxidant defense mechanisms [133]. Indeed, RTA 408 has been demonstrated to decrease ROS and increase glutathione levels [134]. Clinically, RTA 408 is safe for patients [133] and is currently being utilized in clinical trials for mitochondrial myopathies (https://clinicaltrials.gov/ct2/show/NCT02255422). In patients with Friedreich's Ataxia, RTA 408

dose-dependently improved neurological function as measured by the Friedreich Ataxia Rating Scale (mFARS) exam but did not meet its primary outcome of peak work during exercise testing [135].

To date, most pre-clinical data indicates RTA 408 protects against mitochondrial disease and ROS-induced mitochondrial dysfunction [136]. Despite promising pre-clinical and clinical studies demonstrating protection in Friedreich's Ataxia and other bioenergetic myopathies, no studies have investigated the effects of RTA 408 on mitochondrial structure to our knowledge. Additionally, few studies have reported how Friedreich's Ataxia affects mitochondrial structure. In one study, Friedreich's Ataxia patient-derived cells were characterized by abnormal cristae ultrastructure but specific alterations and quantitative data were not reported [137]. Due to the lack of evidence characterizing the effects of both RTA 408 and Friedreich's Ataxia on mitochondrial structure, it is difficult to hypothesize how RTA 408 impacts cristae morphology. Studies defining the relationships between mitochondrial structure, Friedreich's Ataxia, and RTA 408 are desperately needed. Additionally, more evidence is needed to confirm previous observations that RTA 408 is protective for patients with Friedreich's Ataxia and other mitochondrial disorders.

Elamipretide

Elamipretide (formerly SS-31, MTP-131, Bendavia) is a mitochondria-targeted tetrapeptide that is known to interact with cardiolipin (CL). Protection of mitochondrial structure-function with elamipretide has been demonstrated across a myriad of pre-clinical models [138, 139]. Elamipretide is reportedly safe and well-tolerated by patients [42, 118, 140] and is currently being used in clinical trials for genetic and age-related mitochondrial diseases. Namely, elamipretide is

being tested for primary mitochondrial myopathy, Barth Syndrome, LHON, and age-related macular degeneration. Given the dose-dependent improvement in walking distance observed in patients with primary mitochondrial myopathy, elamipretide represents a promising therapeutic for bioenergetic disorders.

Elamipretide has been demonstrated to improve cristae ultrastructure in several pre-clinical models characterized by mitochondrial dysmorphology. Notably, elamipretide prevents general cristae abnormalities and mitochondrial swelling while improving matrix density [44, 137, 141]. We recently reported elamipretide preserved cristae complexity, cristae junctions and networking despite sustained losses of CL (Described in chapter 3). These data suggest elamipretide may be beneficial for patients with Barth Syndrome. Despite the plethora of pre-clinical data demonstrating elamipretide confers protection against injuries that cause ultrastructure deficits, the effects of elamipretide on mitochondrial disease models are relatively unknown. However, the compound has been efficacious in clinical trials for patients with primary mitochondrial disease suggesting studies testing its effects in *in vitro* mitochondrial disease models are not warranted. Additionally, the observed protection of cristae number and networking in pre-clinical models supports its use in patients with LHON as the disease has been characterized by cristae loss and fragmentation [126, 127]. Elamipretide is perhaps the most studied compound of those reviewed here. However, further investigation is needed to determine if elamipretide-mediated protection of mitochondrial structure involves cristae shaping proteins in addition to its role in interacting with CL.

Conclusions

Mitochondrial diseases are debilitating disorders for which there are currently no FDA approved treatments. Several compounds are currently being developed to improve mitochondrial function. These therapeutics can improve electron flow through the respiratory chain, scavenge mitochondrial ROS, or stabilize mitochondrial lipids. Despite the differing mechanisms in which these therapies confer protection, they all represent promising approaches to treat mitochondrial diseases. However, the efficacy of these compounds is based on a limited number of studies and may only be beneficial in distinct mitochondrial disorders. To understand which therapeutics have the best opportunity to treat which diseases, further studies are desperately needed to define the relationships between specific morphological decrements, disease, and the reviewed therapies. As these investigations are realized, medicines can be tailored to specific diseases to improve patient outcomes.

References

1. S, E.L.a.G., *Mitochondria: A historical review* Journal of Cell Biology 1981. **91**(3): p. 227s-255s.
2. EV, C., ed. *In General Cytology* 1924, University Chicago Press: Chicago
3. WA, K.A.a.J., *Metabolism of ketonic acids in animal tissues* Biochem J, 1937. **31**(4): p. 645-660.
4. WB, K.D.a.H., *On cytochrome, a respiratory pigment, common to animals, yeast, and higher plants.* Proceedings of the Royal Society Biological Science, 1925. **98**(690).
5. A, C., *The constitution of mitochondria and microsomes, and the distribution of nucleic acid in the cytoplasm of a leukemic cell.* Journal of Experiments Medicine 1944. **80**(1): p. 19-29.
6. Hogeboom GH, C.A., Hotchkiss RD, *The distribution of cytochrome oxidase and succinoxidase in the cytoplasm of the mammaliam liver cell* J Biol Chem, 1946. **165**.
7. Niemyer H, C.R., Kennedy EP, Lipmann F, *Observations on respiration and phosphorylation with liver mitochondria of normal, hypo-, and hyperthyroid rats* Fed Proc, 1951.
8. H, L.H.a.W., *Oxidative phosporylations: role of inorganic phosphate and acceptor systems in control of metabolic rates* J Biol Chem, 1951 **195**: p. 215-224.
9. GE, P., *An electron microscope study of the mitochondrial structure.* Journal of Histochemistry and Cytochemistry 1953. **1**(4): p. 188-211.

10. FS, S., *Electron Microscopy of Mitochondria and Cytoplasmic Double Membranes: Ultra-Structure of Rod-shaped Mitochondria.* Nature, 1953. **171**: p. 30-31.
11. GE, P., *The fine structure of mitochondria* The Anatomical Record 1952. **114**(3): p. 427-451.
12. Hackenbrock, C., *Ultrastructural bases for metabolically linked mechanical activity in mitochondria* Journal of Cell Biology 1966. **2**: p. 269-297.
13. Hackenbrock, C., *Ultrastructural bases for metabolically linked mechanical activity in mitochondria. II. Electron transport-linked ultrastructural transformations in mitochondria.* Journal of Cell Biology 1968. **37**(2): p. 345-369.
14. Manella, C., *Structure and dynamics of the mitochondrial inner membrane cristae.* Biochimica et Biophysica Acta, 2006. **1763**: p. 542-548.
15. Mannella, C., *The relevance of mitochondrial membrane topology to mitochondrial function.* Biochimica et Biophysica Acta, 2005. **1762**(2): p. 140-147.
16. J, W., *Structural biology: Up close with membrane lipid-protein complexes.* Science, 2011. **334**: p. 320-321.
17. C, H.J.a.U., *Cellular microcompartments constitute general subcellular functional units in cells* Biological Chemistry, 2013. **394**: p. 151-161.
18. Bazán S, M.E., Mallampalli VK, Heacock P, Sparagna GC, Dowhan W, *Cardiolipin-dependent reconstitution of respiratory supercomplexes from purified Saccharomyces cerevisiae complexes III and IV.* Journal of Biological Chemistry, 2013. **288**(1): p. 401-411.
19. GE, P., *An electron miscroscope study of the mitochondrial structure* J Histrochem Cytochem, 1953. **1**(4): p. 188-211.
20. Khalifat N, F.J., Puff N, , *Lipid packing variations induced by pH in cardiolipin-containing bilayers: the driving force for the cristae-like shape instability.* Biochimica et Biophysica Acta, 2011. **1808**(11): p. 2724-2733.
21. Khalifat N, P.N., Monneau S, Fournier JB, Angelova MI, *Membrane deformation under local pH gradient: mimicking mitochondrial cristae dynamics.* Biphysical Journal 2008. **95**(10): p. 4924-4933.
22. Gilkerson RW, S.J., Capaldi, *The cristal membrane of mitochondria is the principal site of oxidative phosphorylation.* FEBS Letters, 2003. **546**: p. 355-358.
23. Cogliati, E., Scorrano, *Mitochondrial Cristae: Where Beauty Meets Functionality.* Cell Press, 2016. **41**(3).
24. Horvath SE, D.G., *Lipids of mitochondria.* Progress in Lipid Research 2013. **52**(4): p. 590-614.
25. Ikon, N. and R.O. Ryan, *Cardiolipin and mitochondrial cristae organization.* Biochim Biophys Acta, 2017. **1859**(6): p. 1156-1163.
26. Zhang M, M.E., Dowhan W, *Gluing the respiratory chain together. Cardiolipin is required for supercomplex formation in the inner mitochondrial membrane.* Journal of Biological Chemistry, 2002. **277**(46): p. 43553-43556.
27. Fry M, G.D., *Cardiolipin requirement for electron transfer in complex I and III of the mitochondrial respiratory chain.* Journal of Biological Chemistry, 1981. **256**(4): p. 1874-1880.
28. Fry M, G.D., *Cardiolipin requirement by cytochrome oxidase and the catalytic role of phospholipid.* Biochemical and Biophysical Research Communications, 1980. **93**(4): p. 1238-1246.

29. FL, H., *Cardiolipins and biomembrane function.* Biochem Biophys Acta, 1992. **1113**(1): p. 71-133.
30. Eble KS, C.W., Hantgan RR, Cunningham CC, *Tightly associated cardiolipin in the bovine heart mitochondrial ATP synthase as analyzed by 31P nuclear magnetic resonance spectroscopy.* Journal of Biological Chemistry, 1990. **265**(32): p. 19434-41940.
31. Beyer K, N.B., *Specific cardiolipin binding interferes with labeling of sulfhydryl residues in the adenosine diphosphate/adenosine triphosphate carrier protein from beef heart mitochondria.* Biochemistry 1996. **35**(49): p. 15784-15790.
32. Ott M, R.J., Gogvadze V, Zhivotovsky B, Orrenius S, *Cytochrome c release from mitochondria proceeds by a two-step process.* Proceedings of the National Academy of Sciences, USA, 2002. **99**(3): p. 1259-1263.
33. Ren M, P.C., Schlame M, *Metabolism and function of mitochondrial cardiolipin.* Progress in Lipid Research, 2014. **55**: p. 1-16.
34. Paradies G, P.V., De Benedictis V, Ruggiero FM, Petrosillo G, *Functional role of cardiolipin in mitochondrial bioenergetics.* Biochim Biophys Acta, 2014. **1837**(4): p. 408-417.
35. Chicco, A.J. and G.C. Sparagna, *Role of cardiolipin alterations in mitochondrial dysfunction and disease.* Am J Physiol Cell Physiol, 2007. **292**(1): p. C33-44.
36. Potting C1 Tatsuta T, K.T., Haag M, Wai T, Aaltonen MJ, Langer T, *TRIAP1/PRELI complexes prevent apoptosis by mediating intramitochondrial transport of phosphatidic acid.* Cell Metab, 2013. **18**(2): p. 287-295.
37. Xu Y, S.J., Plesken H, Kelley RI, Schlame M, *Characterization of lymphoblast mitochondria from patients with Barth syndrome.* Lab Investigations, 2005. **85**(6): p. 823-830.
38. Pfeiffer K, G.V., Stuart RA, Hunte C, Brandt U, Greenberg ML, Schägger H., *Cardiolipin stabilizes respiratory chain supercomplexes.* Journal of Biological Chemistry, 2003. **278**(52): p. 52873-52880.
39. Vähäheikkilä M, P.T., Róg T, Vazdar M, Pöyry S, Vattulainen I, *How cardiolipin peroxidation alters the properties of the inner mitochondrial membrane?* Chemistry and Physics of Lipids, 2018. **214**: p. 15-23.
40. Paradies, G., et al., *Decrease in mitochondrial complex I activity in ischemic/reperfused rat heart: involvement of reactive oxygen species and cardiolipin.* Circ Res, 2004. **94**(1): p. 53-9.
41. Malhotra, K. and N.N. Alder, *Reconstitution of Mitochondrial Membrane Proteins into Nanodiscs by Cell-Free Expression.* Methods Mol Biol, 2017. **1567**: p. 155-178.
42. Karaa, A., et al., *Randomized dose-escalation trial of elamipretide in adults with primary mitochondrial myopathy.* Neurology, 2018.
43. Birk, A.V., et al., *Targeting Mitochondrial Cardiolipin and the Cytochrome C/Cardiolipin Complex to Promote Electron Transport and Optimize Mitochondrial Atp Synthesis.* Br J Pharmacol, 2013.
44. Birk, A.V., et al., *The Mitochondrial-Targeted Compound SS-31 Re-Energizes Ischemic Mitochondria by Interacting with Cardiolipin.* J Am Soc Nephrol, 2013.
45. Brown, D.A., et al., *Reduction of Early Reperfusion Injury With the Mitochondria-Targeting Peptide Bendavia.* J Cardiovasc Pharmacol Ther, 2013.

46. Kloner RA, H.S., Dai W, Brown DA, et al. , *Reduction of Ischemia/Reperfusion Injury With Bendavia, a Mitochondria-Targeting Cytoprotective Peptide.* Journal of the American Heart Association 2012.
47. Sloan RC, M.F., Frasier CR, Patel HD, Bostian PA, Lust RM, Brown DA, *Mitochondrial permeability transition in the diabetic heart: contributions of thiol redox state and mitochondrial calcium to augmented reperfusion injury* Journal of Molecular and Cellular Cardiology 2012. **52**: p. 1009-1018.
48. Mannella CA, P.D., Bradshaw PC, Moraru II, Slepchenko B, Loew LM, Hsieh CE, Buttle K, Marko M., *Topology of the mitochondrial inner membrane: dynamics and bioenergetic implications.* IUBMB Life, 2001. **52**(3-5): p. 93-100.
49. Frezza C, C.A., Martin de Brito O, Micaroni M, Beznoussenko GV, Rudka T, Bartoli D, Polishuck RS, Danial NN, De Strooper B, Scorrano L, *OPA1 Controls Apoptotic Cristae Remodeling Independently from Mitochondrial Fusion.* Cell 2006. **126**(1): p. 177-189.
50. Glytsou C, C.E., Cogliati S, Mehrotra A, Anastasia I, Rigoni G, Raimondi A, Shintani N, Loureiro M, Vazquez J, Pellegrini L, Enriquez JA, Scorrano L, Soriano ME, *Optic Atrophy 1 Is Epistatic to the Core MICOS Component MIC60 in Mitochondrial Cristae Shape Control.* Cell Reports, 2016. **17**(11): p. 3024-3034.
51. Koob S, R.A., *Novel intracellular functions of apolipoproteins: the ApoO protein family as constituents of the Mitofilin/MINOS complex determines cristae morphology in mitochondria.* Biological Chemistry, 2014. **395**(3): p. 285-296.
52. Quintana-Cabrera, M., Rigoni, Soriano, *Who and how in the regulation of mitochondrial cristae shape and function.* Biochemical and Biophysical Research Communications, 2018. **500**: p. 94-101.
53. Santo-Domingo J, G.M., Poburko D, Scorrano L, Demaurex N, *OPA1 promotes pH flashes that spread between contiguous mitochondria without matrix protein exchange.* EMBO J, 2013. **32**(13): p. 1927-1940.
54. Jans DC, W.C., Riedel D, Wenzel D, Stagge F, Deckers M, Rehlling P, Jakobs S, *STED super-resolution microscopy reveals an array of MINOS clusters along human mitochondria.* Proceedings of the National Academy of Sciences, USA, 2013. **110**(22): p. 8936-8941.
55. V, K.-P., *The MICOS complex of human mitochondria.* Cell Tissue Research, 2017. **367**: p. 83-93.
56. Schorr S, v.d.L.M., *Integrative functions of the mitochondrial contact site and cristae organizing syste.* Seminars in cell and developmental biology 2018. **76**: p. 191-200.
57. Wollweber, F., K. von der Malsburg, and M. van der Laan, *Mitochondrial contact site and cristae organizing system: A central player in membrane shaping and crosstalk.* Biochim Biophys Acta, 2017. **1864**(9): p. 1481-1489.
58. Rampelt H, Z.R., van der Laan M, Pfanner N, *Role of the mitochondrial contact site and cristae organizing system in membrane architecture and dyanmics* Biochemica et biophysica acta, 2016. **1864**: p. 737-746.
59. Genin EC, P.M., Bannwarth S, Villa E, et al. , *CHCHD10 mutations promote loss of mitochondrial cristae junctions with impaired mitochondrial genome maintenance and inhibition of apoptosis.* EMBO Molecular Medicine 2016. **8**: p. 58-72.
60. Li H, R.Y., Zhang K, Jian F, Hu C, Mioa L, Gong L, Sun L, Zhnag X, Chen S, Chen H, Liu D, Sonh Z, *Mic60/Mitofilin determines MICOS assembly essential for mitochondrial dynamics and mtDNA nucleoid organization.* Cell Death and Differentiation, 2015. **23**(3).

61. Friedman JR, M.A., Yamada J, McCaffery JM, Nunnari J, *MICOS coordinates with respiratory complexes and lipids to establish mitochondrial inner membrane architecture.* eLife, 2015. **4**.
62. Weber TA, K.S., Heide H, Wittig I, Head B, van der Bliek A, Brandt U, Mittelbronn M, Reichart AS, *APOOL is a cardiolipin-binding constituent of the mitofilin/MINOS protein complex determining crisate morphology in mammalian mitochondria.* Plos one, 2013. **8**(5).
63. Darshi M1, M.V., Mackey MR, Murphy AN, Koller A, Perkins GA, Ellisman MH, Taylor SS., *ChChd3, an inner mitochondrial membrane protein, is essential for maintaining crista integrity and mitochondrial function.* Journal of Biological Chemistry, 2011. **286**(4): p. 2918-2932.
64. Anand R, S.V., Urbach J, Wittig I, Reichert AS, *Mic13 Is Essential for Formation of Crista Junctions in Mammalian Cells.* Plos one, 2016. **11**(8).
65. Harner ME1, U.A., Izawa T, Walther DM, Ozbalci C, Geimer S, Reggiori F, Brügger B, Mann M, Westermann B, Neupert W, *Aim24 and MICOS modulate respiratory function, tafazzin-related cardiolipin modification and mitochondrial architecture.* Elife, 2014. **1**(3).
66. Guarani V, M.E., Paulo JA, Huttlin EL, Fröhlich F, Gygi SP, Van Vactor D, Harper JW, *QIL1 is a novel mitochondrial protein required for MICOS complex stability and cristae morphology.* Elife, 2015. **21**(4).
67. V. Guarani, C.J., D. Chrétien, A. Lombès, P. Bénit, C. Labasse, E. Lacène,A. Bourillon, A. Imbard, J.-F. Benoist, I. Dorboz, M. Gilleron, E.S. Goetzman,P. Gaignard, A. Slama, M. Elmaleh-Bergès, N.B. Romero, P. Rustin, H. Ogier deBaulny, J.A. Paulo, et al., *QIL1mutation causes MICOS disassembly and earlyonset fatal mitochondrial encephalopathy with liver disease.* eLife, 2016. **5**.
68. Zhou W, M.D., Sun AX, Tran HD, Ma DL, Singh BK, Zhou J, Zhang J, Wang D, Zhao Y, Yen PM, Goh E, Tan EK., *PD-linked CHCHD2 mutations impair CHCHD10 and MICOS complex leading to mitochondria dysfunction.* Human Molecular Genetics, 2018.
69. Siegmund, F.e.a., *Three-Dimensional Analysis of Mitochondrial Crista Ultrastructure in a Patient with Leigh Syndrome by In Situ Cryoelectron Tomography.* Cell Press, 2018. **6**: p. 83-91.
70. Lee H, Y.Y., *Mitochondrial Membrane Dynamics—Functional Positioning of OPA1.* Antioxidants, 2018. **7**(12): p. 186.
71. Pernas L, S.L., *Mito-Morphosis: Mitochondrial Fusion, Fission, and Cristae Remodeling as Key Mediators of Cellular Function.* Annual Reviews in Physiology 2016. **78**: p. 505-531.
72. Ban T, K.H., Ishihara T, Ishihara N, *Relationship between OPA1 and cardiolipin in mitochondrial inner-membrane fusion.* Biochemica Biophysica Acta Bioenergetics, 2018. **1859**(9): p. 951-957.
73. Patten DA, W.J., Khacho M, Soubannier V, Mailoux RJ, Pilon-Larose K, MacLaurin JG, Park DS, McBride HM, Trinkle-Mulcahy L, Harper ME, Germain M, Slack RS, , *OPA1-dependent cristae modulation is essential for cellular adaptation to metabolic demand.* EMBO J, 2014. **33**: p. 2676-2691.
74. Cogliati, S., et al, *Mitochondrial Cristae Shape Determines Respiratory Chain Supercomplexes Assembly and Respiratory Efficiency.* Cell, 2013. **155**: p. 160-171.
75. Varanita T, S.M., Romanello V, Zaglia T, Quintana-Cabrera R, Semenzato M, Menabo R, Costa V, Civiletto G, Pesce P, Viscomi C, Zeviani M, Lisa FD, Mongillo M, Sandri M,

Scorrano L, *The Opa1-Dependent Mitochondrial Cristae Remodeling Pathway Controls Atrophic, Apoptotic, and Ischemic Tissue Damage.* Cell Metabolism, 2015. **21**(6).
76. Civiletto G, V.T., Cerutti R, Gorletta T, Barbaro S, Marchet S, Lamperti C, Viscomi C, Scorrano L, Zeviani M., *Opa1 overexpression ameliorates the phenotype of two mitochondrial disease mouse models.* Cell Metabolism, 2015 **21**(6): p. 845-854.
77. DeVay RM, D.-R.L., Lackner LL, Hoppins S, Stahlberg H, Nunnari J, *Coassembly of Mgm1 isoforms requires cardiolipin and mediates mitochondrial inner membrane fusion.* Journal of Cell Biology, 2009. **186**: p. 793-803.
78. Ban T, H.J., Song Z, Hinshaw JE, Chan DC., *OPA1 disease alleles causing dominant optic atrophy have defects in cardiolipin-stimulated GTP hydrolysis and membrane tubulation.* Human Molecular Genetics, 2010. **19**(11): p. 2113-2122.
79. Rujiviphat J, M.G., Rubinstein JL, McQuibban GA, *Phospholipid association is essential for dynamin-related protein Mgm1 to function in mitochondrial membrane fusion.* Journal of Biological Chemistry 2009. **284**(42): p. 28682-28686.
80. Wai T, G.-P.J., Baker MJ, Merkwirth C, Benit P, Rustin P, Rupérez FJ, Barbas C, Ibañez B, Langer T, *Imbalanced OPA1 processing and mitochondrial fragmentation cause heart failure in mice.* Science, 2015. **350**.
81. Wang X, S.B., Lee HG, Li X, Perry G, Smith MA, Zhu X, *Impaired balance of mitochondrial fission and fusion in Alzheimer's disease.* Journal of Neuroscience, 2009. **29**(28): p. 9090-9103.
82. Mortiboys H, J.K., Aasly JO, Bandmann O, *Mitochondrial impairment in patients with Parkinson disease with the G2019S mutation in LRRK2.* Neurology, 2010. **75**(22): p. 2017-2020.
83. SJ, N.D.a.F., *Bioenergetics 4*. 2013, London: Academic Press.
84. Horton KL, S.K., Froseca SB, Guo Q, Kelley S, *Mitochondria-Penetrating Peptides.* Cell Press, 2008 **15**: p. 375-382.
85. Davies KM, S.M., Daum B, Kief JH, Osiewacz HD, Rycovska A, Zickermann V, and Kühlbrandt W, *Macromolecular organization of ATP synthase and complex I in whole mitochondria.* Proceedings of the National Academy of Sciences, USA, 2011. **108**(34): p. 14121-14126.
86. RD, A., *Membrane tubulation and proton pumps.* Protoplasma, 1995. **189**(102): p. 1-8.
87. Rieger B, J.W., Busch K., *Lateral pH gradient between OXPHOS complex IV and F(0)F(1) ATP-synthase in folded mitochondrial membranes.* Nature Communications, 2014. **5**(3103).
88. Jayashankar V, M.I., Rafelski SM, *Shaping the multi-scale architecture of mitochondria.* Current Opinions in Cell Biology 2016. **38**: p. 45-51.
89. JE, W., *The ATP synthase: the understood, the uncertain and the unknown.* Biochemical Society Transactions 2013. **41**(1): p. 1-16.
90. Patrick Paumard, J.V., Bénédicte Coulary, Jacques Schaeffer, Vincent Soubannier, David M. Mueller, Daniel Brèthes, Jean-Paul di Rago, and Jean Velours, *The ATP synthase is involved in generating mitochondrial cristae morphology.* EMBO J, 2002. **21**(3): p. 221-230.
91. Dudkina NV, H.J., Keegstra W, Boekema EJ, Bruan HP, *Structure of dimeric ATP synthase from mitochondria: An angular association of monomers induces the strong curvature of the inner membrane.* Federation of European Biochemical Societies 2005. **579**: p. 5769-5772.

92. Arnold I, P.K., Neupert W, Stuart RA, Schägger H, *Yeast mitochondrial F1F0-ATP synthase exists as a dimer: identification of three dimer-specific subunits.* EMBO J, 1998. **17**(24): p. 7170-7178.
93. Arselin G, V.J., Salin B, Schaeffer J, Giraud MF, Dautant A, Brèthes D, Velours J, *The modulation in subunits e and g amounts of yeast ATP synthase modifies mitochondrial cristae morphology.* Journal of Biological Chemistry, 2004. **279**(39): p. 40392-40399.
94. Giorgio V, v.S.S., Antoniel M, Fabbro A, Fogolari F, Forte M, Glick GD, Petronilli V, Zoratti M, Szabó I, Lippe G, Bernardi P, *Dimers of mitochondrial ATP synthase form the permeability transition pore.* Proceedings of the National Academy of Sciences, USA, 2013. **110**(15): p. 5887-1592.
95. Santiago E, L.-M.N., Segovia JF., *Correlation between losses of mitochondrial ATPase activity and cardiolipin degradation.* Biochemical and Biophysical Research Communications, 1973. **53**(2): p. 439-445.
96. Duncan AL, R.A., Walker JE, *Cardiolipin binds selectively but transiently to conserved lysine residues in the rotor of metazoan ATP synthases.* Proceedings of the National Academy of Sciences, USA, 2016. **113**: p. 8687–8692.
97. Acehan D, M.A., Xu Y, Ren M, Stokes DL, Schlame M, *Cardiolipin Affects the Supramolecular Organization of ATP Synthase in Mitochondria.* Biophysics Journal, 2011. **100**(9): p. 2184–2192.
98. Daum B, W.A., Horst A, Osiewacz HD, Kühlbrandt W, *Age-dependent dissociation of ATP synthase dimers and loss of inner-membrane cristae in mitochondria.* Proceedings of the National Academy of Sciences, USA, 2013. **110**(38): p. 15301-15306.
99. Beck SJ, G.L., Phensy A, Tian J, Wang L, Tandon N, Gauba E, Lu L, Pascual JM, Kroener S, Du H, *Deregulation of mitochondrial F1FO-ATP synthase via OSCP in Alzheimer's disease.* Nature Communications, 2016. **7**(11483).
100. Vincent, A.E., et al., *The Spectrum of Mitochondrial Ultrastructural Defects in Mitochondrial Myopathy.* Sci Rep, 2016. **6**: p. 30610.
101. Barca E, G.R., Potluri P, Juanola-Falgarona M, Gai X, Li D, Jalas C, Hirsch Y, Emmanuele V, Tadesse S, Ziosi M, Akman HO, Chung WK, Tanji K, McCormick EM, Place E, Consugar M, Pierce EA, Hakonarson H, Wallace DC, Hirano M, Falk MJ, *USMG5 Ashkenazi Jewish founder mutation impairs mitochondrial complex V dimerization and ATP synthesis.* Human Molecular Genetics, 2018. **27**(19): p. 3305-3312.
102. Kloner, R.A., et al., *New and revisited approaches to preserving the reperfused myocardium.* Nat Rev Cardiol, 2017.
103. Xue L, L.X., Wang Q, Liu CQ, Chen Y, Jia W, Hsie R, Chen Y, Luh F, Zheng S, Yen Y, *Ribonucleotide reductase subunit M2B deficiency leads to mitochondrial permeability transition pore opening and is associated with aggressive clinicopathologic manifestations of breast cancer.* American Journal of Translational Research, 2018. **10**(11): p. 3635-3649.
104. Guo JD, Z.X., Li Y, Li GR, Liu XL, *Damage to dopaminergic neurons by oxidative stress in Parkinson's disease (Review).* International Journal of Molecular Medicine, 2018. **41**(4): p. 1817-1825.
105. Rampelt H, B.M., Zerbes RM, Horvath SE, Warscheid B, Pfanner N, van der Laan M, *Mic10, a Core Subunit of the Mitochondrial Contact Site and Cristae Organizing System, Interacts with the Dimeric F1Fo-ATP Synthase.* Journal of Molecular Biology, 2017. **429**(8): p. 1162-1170.

106. Mühleip AW, J.F., Wigge C, Frangakis AS, Kühlbrandt W, Davies KM, *Helical arrays of U-shaped ATP synthase dimers form tubular cristae in ciliate mitochondria.* Proceedings of the National Academy of Sciences, USA, 2016. **113**(30): p. 8442-8447.
107. Kon N, S.A., Miyoshi N, *A small-molecule DS44170716 inhibits Ca2+-induced mitochondrial permeability transition.* Scientific Reports, 2017. **7**(1): p. 3864.
108. Ikeda G, M.T., Nakano Y, Nagaoka K, Ishikita A, Nakano K, Funamoto D, Sunagawa K, Egashira K, *Nanoparticle-Mediated Targeting of Cyclosporine A Enhances Cardioprotection Against Ischemia-Reperfusion Injury Through Inhibition of Mitochondrial Permeability Transition Pore Opening.* Scientific Reports, 2016. **6**.
109. Salameh A, K.M., Dähnert I, Dhein S, *Olesoxime Inhibits Cardioplegia-Induced Ischemia/Reperfusion Injury. A Study in Langendorff-Perfused Rabbit Hearts.* Frontiers in Physiology, 2017. **8**(324).
110. Jahandiez V, Cour M, Bochaton T, Abrial M, Loufouat J, Gharib A, Varennes A, Ovize M, Argaud L, *Fast therapeutic hypothermia prevents post-cardiac arrest syndrome through cyclophilin D-mediated mitochondrial permeability transition inhibition.* Basic Research in Cardiology 2017. **112**(4).
111. Kharechkina ES, N.A., Teplova VV, Odinokova IV, Krestinina OV, Baburina YL, Kruglova SA, Kruglov AG, *Regulation of permeability transition pore opening in mitochondria by external NAD(H).* Biochim Biophys Acta Gen Subj, 2019. **1863**(5): p. 771-783.
112. Gräb J, S.I., van Gumpel E, Winter S, Schreiber F, Esser A, Hölscher C, Fritsch M, Herb M, Schramm M, Wachsmuth L, Pallasch C, Pasparakis M, Kashkar H, Rybniker J, *Corticosteroids inhibit Mycobacterium tuberculosis-induced necrotic host cell death by abrogating mitochondrial membrane permeability transition.* Nature Communications, 2019. **10**(1): p. 688.
113. Sacchetti M, M.F., Lambiase A, Mastropasqua A, Merlo D, Bonini S, *Systematic review of randomised clinical trials on topical ciclosporin A for the treatment of dry eye disease.* Brain Journal of Ophthalmology, 2014. **98**(8): p. 1016-1022.
114. Song K, W.S., Qi D, *Effects of Cyclosporine on Reperfusion Injury in Patients: A Meta-Analysis of Randomized Controlled Trials.* Oxidative Medicine and Cellular Longevity 2015.
115. Ottani F, L.R., Staszewsky L, La Vecchia L, Locuratolo N, Sicuro M, Masson S, Barlera S, Milani V, Lombardi M, Costalunga A, Mollichelli N, Santarelli A, De Cesare N, Sganzerla P, Boi A, Maggioni AP, Limbruno U, *Cyclosporine A in Reperfused Myocardial Infarction: The Multicenter, Controlled, Open-Label CYCLE Trial.* Journal of the American College of Cardiology 2016. **67**(4): p. 365-374.
116. Birk, A.V., et al., *Targeting mitochondrial cardiolipin and the cytochrome c/cardiolipin complex to promote electron transport and optimize mitochondrial ATP synthesis.* Br J Pharmacol, 2014. **171**(8): p. 2017-28.
117. Chakrabarti, A.K., et al., *Rationale and design of the EMBRACE STEMI Study: A phase 2a, randomized, double-blind, placebo-controlled trial to evaluate the safety, tolerability and efficacy of intravenous Bendavia on reperfusion injury in patients treated with standard therapy including primary percutaneous coronary intervention and stenting for ST-segment elevation myocardial infarction.* Am Heart J, 2013. **165**(4): p. 509-514 e7.

118. Gibson, C.M., et al., *EMBRACE STEMI study: a Phase 2a trial to evaluate the safety, tolerability, and efficacy of intravenous MTP-131 on reperfusion injury in patients undergoing primary percutaneous coronary intervention.* Eur Heart J, 2015.
119. Vincent AE, N.Y., White K, Davey T, Turnbull DM, Picard M *The spectrum of mitochondrial ultrastructure defects in mitochondrial myopathy* Scientific Reports 2016.
120. El-Hattab AW, Z.A., Almannai M, Scaglia F, *Therapies for mitochondrial diseases and current clinical trials.* Molecular Genetics and Metabolism, 2017. **122**(3): p. 1-9.
121. Nakazawa H, I.K., Shinozaki S, Yasuhara S, Yu YM, Martyn JAJ, Tompkins RG2, Yorozu T, Inoue S, Kaneki *Coenzyme Q10 protects against burn-induced mitochondrial dysfunction and impaired insulin signaling in mouse skeletal muscle.* FEBS Open Bio, 2019. **9**(2): p. 348-363.
122. Y H Noh, K.-Y.K., M S Shim, S-H Choi, S Choi, M H Ellisman, R N Weinreb, G A Perkins, and W-K Ju, *Inhibition of oxidative stress by coenzyme Q10 increases mitochondrial mass and improves bioenergetic function in optic nerve head astrocytes.* Cell Death Discovery, 2013. **4**(10).
123. Kaurola P, S.V., Vonk A, Vattulainen I, Róg T, *Distribution and dynamics of quinones in the lipid bilayer mimicking the inner membrane of mitochondria.* Biochim Biophys Acta, 2016. **1858**(9): p. 2116-2122.
124. Klopstock T, Y.-W.-M.P., Dimitriadis K, Rouleau J, Heck S, Bailie M, Atawan A, Chattopadhyay S, Schubert M, Garip A, Kernt M, Petraki D, Rummey C, Leinonen M, Metz G, Griffiths PG, Meier T, Chinnery PF, *A randomized placebo-controlled trial of idebenone in Leber's hereditary optic neuropathy.* Brain, 2011. **134**: p. 2677-2686.
125. Rudolph G, D.K., Büchner B, Heck S, Al-Tamami J, Seidensticker F, Rummey C, Leinonen M, Meier T, Klopstock T, *Effects of idebenone on color vision in patients with leber hereditary optic neuropathy.* Journal of Neuroophthalmology, 2013. **33**(1): p. 30-36.
126. Uittenbogaard M, B.C., Fang Z, Wong LJ, Gropman A, Chiaramello A, *The m.11778 A > G variant associated with the coexistence of Leber's hereditary optic neuropathy and multiple sclerosis-like illness dysregulates the metabolic interplay between mitochondrial oxidative phosphorylation and glycolysis.* Mitochondrion, 2018.
127. Aung Win Tun, S.C., 2 Supannee Kaewsutthi, Wanphen Katanyoo, Wanicha Chuenkongkaew, Masayoshi Kuwano, Takeshi Tomonaga, Chayanon Peerapittayamongkol, Visith Thongboonkerd, and Patcharee Lertrit *Profiling the Mitochondrial Proteome of Leber's Hereditary Optic Neuropathy (LHON) in Thailand: Down-Regulation of Bioenergetics and Mitochondrial Protein Quality Control Pathways in Fibroblasts with the 11778G>A Mutation.* Plos one, 2014. **9**(9).
128. Shrader WD, A.A., Barnes A, Enns GM, Hinman A, Jankowski O, Kheifets V, Komatsuzaki R, Lee E, Mollard P, Murase K, Sadun AA, Thoolen M, Wesson K, Miller G, *α-Tocotrienol quinone modulates oxidative stress response and the biochemistry of aging.* Bioorganic and Medicinal Chemistry Letters, 2011. **21**(12): p. 3693-3698.
129. Enns GM, K.S., Perlman SL, Spicer KM, Abdenur JE, Cohen BH, Amagata A, Barnes A, Kheifets V, Shrader WD, Thoolen M, Blankenberg F, Miller G, *Initial experience in the treatment of inherited mitochondrial disease with EPI-743.* Molecular Genetics and Metabolism, 2012. **105**(1): p. 91-102.
130. Martinelli D, C.M., Piemonte F, Pastore A, Tozzi G, Dionisi-Vici C, Pontrelli G, Corsetti T, Livadiotti S, Kheifets V, Hinman A, Shrader WD, Thoolen M, Klein MB, Bertini E, Miller G, *EPI-743 reverses the progression of the pediatric mitochondrial disease--*

genetically defined Leigh Syndrome. Molecular Genetics and Metabolism, 2012. **107**(3): p. 383-388.
131. Pastore A, P.S., Tozzi G, Carrozzo R, Martinelli D, Dionisi-Vici C, Di Giovamberardino G, Ceravolo F, Klein MB, Miller G, Enns GM, Bertini E, Piemonte F, *Glutathione: a redox signature in monitoring EPI-743 therapy in children with mitochondrial encephalomyopathies.* Molecular Genetics and Metabolism, 2013. **109**(2): p. 208-214.
132. Sadun AA, C.C., Ross-Cisneros FN, Barboni P, Thoolen M, Shrader WD, Kubis K, Carelli V, Miller G, *Effect of EPI-743 on the clinical course of the mitochondrial disease Leber hereditary optic neuropathy.* Archives of Neurology, 2012. **69**(3): p. 331-338.
133. Ben C Creelan, D.I.G., Jhanelle E Gray, Charles C Williams, Tawee Tanvetyanon, Eric B Haura, Jeffrey S Weber, Geoffrey T Gibney, Joseph Markowitz, Joel W Proksch, Scott A Reisman, Mark D McKee, Melanie P Chin, Colin J Meyer, and Scott J Antonia, *Safety, pharmacokinetics, and pharmacodynamics of oral omaveloxolone (RTA 408), a synthetic triterpenoid, in a first-in-human trial of patients with advanced solid tumors.* Onco Targets Ther, 2017. **10**: p. 4239–4250.
134. Neymotin A, C.N., Wille E, Naseri N, Petri S, Damiano M, Liby KT, Risingsong R, Sporn M, Beal MF, Kiaei M, *Neuroprotective effect of Nrf2/ARE activators, CDDO ethylamide and CDDO trifluoroethylamide, in a mouse model of amyotrophic lateral sclerosis.* Free Radic Biol Med, 2011. **51**(1): p. 88-96.
135. Lynch DR, F.J., Hauser L, Blair IA, Wang QQ, Mesaros C, Snyder N, Boesch S, Chin M, Delatycki MB, Giunti P, Goldsberry A, Hoyle C, McBride MG, Nachbauer W, O'Grady M, Perlman S, Subramony SH, Wilmot GR, Zesiewicz T, Meyer C, *Safety, pharmacodynamics, and potential benefit of omaveloxolone in Friedreich ataxia.* Annals of Clinical and Trasnlational Neurology 2018. **6**(1): p. 15-26.
136. Abeti R, B.A., Esteras N, Giunti P, *Novel Nrf2-Inducer Prevents Mitochondrial Defects and Oxidative Stress in Friedreich's Ataxia Models.* Frontiers in Cellular Neuroscience, 2018. **12**(188).
137. Zhao, H., et al., *Peptide SS-31 upregulates frataxin expression and improves the quality of mitochondria: implications in the treatment of Friedreich ataxia.* Sci Rep, 2017. **7**(1): p. 9840.
138. Brown, D.A., H.N. Sabbah, and S.R. Shaikh, *Mitochondrial inner membrane lipids and proteins as targets for decreasing cardiac ischemia/reperfusion injury.* Pharmacol Ther, 2013.
139. Szeto, H.H., *Pharmacologic Approaches to Improve Mitochondrial Function in AKI and CKD.* J Am Soc Nephrol, 2017. **28**(10): p. 2856-2865.
140. Daubert, M.A., et al., *Novel Mitochondria-Targeting Peptide in Heart Failure Treatment: A Randomized, Placebo-Controlled Trial of Elamipretide.* Circ Heart Fail, 2017. **10**(12).
141. Sweetwyne, M.T., et al., *The mitochondrial-targeted peptide, SS-31, improves glomerular architecture in mice of advanced age.* Kidney Int, 2017. **91**(5): p. 1126-1145.

Chapter 3

Mitochondrial cristae networks in the post-ischemic heart: mitigation of ultrastructural and functional derangements with a cardiolipin-aggregating peptide

Mitchell E. Allen[1], Justin B. Perry[1], Edward Ross Pennington[2,3], Sahil Dadoo[3], Marina Makrecka-Kuka[4], Maja Dombrova[4], Fatiha Moukdar[5], Hetal D. Patel[5], Xianlin Han[6], Grahame K. Kidd[7,8], Emily K. Benson[8], Webster L. Santos[9,10], Tristan B. Raisch[13,14], Steven Poelzing[13,14], Saame Raza Shaikh[3], and David A. Brown[1,10,11,12]

[1]Department of Human Nutrition, Foods, and Exercise, Virginia Tech, Blacksburg, VA; [2]Department of Biochemistry and Molecular Biology, East Carolina University, Greenville, NC; [3]Department of Nutrition, Gillings School of Global Public Health and School of Medicine, University of North Carolina, Chapel Hill, NC; [4]Latvian Institute for Organic Synthesis Riga Latvia; [5]Department of Physiology, East Carolina University, Greenville NC; [6]Barshop Institute for Longevity and Aging Studies, University of Texas Health Science Center, San Antonio TX; [7]Department of Neurosciences, Cleveland Clinic, Cleveland OH; [8]Renovo Neural Inc, Cleveland OH; [9]Department of Chemistry, Virginia Tech, Blacksburg VA; [10]Virginia Tech Center for Drug Discovery, [11]Virginia Tech Faculty of Health Sciences, and [12]Virginia Tech Metabolic Phenotyping Core Virginia Tech, Blacksburg VA. [13]Virginia Tech Carilion Research Institute, Virginia Tech. [14]Translational Biology, Medicine and Health, Virginia Tech.

Corresponding Author
David A. Brown, Ph.D.
Virginia Tech Corporate Research Center
1981 Kraft Drive
1035 Integrated Life Sciences Building
Blacksburg, VA 24060
540-231-8146 (phone)
brownda@vt.edu

Abstract

Mitochondrial dysfunction is a well-established contributor to a wide variety of diseases, including various cardiac pathologies. Barriers to new therapies include a complete understanding of the underlying molecular culprits, as well as effective mitochondria-targeted therapies that mitigate injury. In this study we investigated the effects of the cell-permeable tetrapeptide elamipretide on recovery of mitochondrial structure-function after acute ischemia-reperfusion. Elamipretide is a clinical-stage compound currently under investigation for genetic and age-related mitochondrial diseases, yet the mechanism of action is not completely understood. We used a combination of physiological models, mitochondrial imaging, and biomimetic membrane studies to test the hypothesis that elamipretide-cardiolipin interactions improved mitochondrial function and structure, which are inter-related. Post-ischemic treatment with elamipretide sustained mitochondrial function in intact hearts and permeabilized fibers, with improvements noted across electron transport complexes. Myofiber anoxia-reoxygenation studies conducted in parallel indicated a reduction in H_2O_2 production with elamipretide treatment, ostensibly related to a measured decrease in reverse electron transport. Using two parallel electron microscopy paradigms, elamipretide led to maintenance of mitochondrial ultrastructure, notably improving cristae interconnectedness. Structural stabilization was also confirmed using blue-native PAGE, where elamipretide preserved the integrity of complex V. Mass spectrometry studies indicated a loss of cardiolipin with ischemia-reperfusion, which was not abrogated with elamipretide treatment. Finally, we used a novel biomimetic membrane system to model the pathological mitochondrial membrane, and found that elamipretide improved biophysical pressure-area relationships through a mechanism that appears to involve aggregating cardiolipin. Our data indicate that targeting mitochondrial membranes can improve pathological bioenergetics by

sustaining cristae networks, this supporting inter-related properties of mitochondrial structure and function.

Introduction

The biophysical organization of the mitochondrial inner membrane regulates bioenergetics. Studies spanning fifty years have described the intertwined relationship between mitochondrial structure and function[1, 2], bolstered in more recent years by advances in imaging modalities [3-5]. Energy-transducing membranes within mitochondria are held within cristae, invaginations of the inter-membrane space that are surrounded by a gel-like matrix. The composition of inner membranes is unique, comprised predominantly by phosphatidylethanolamine, phosphatidylcholine, and the notable presence of cardiolipin. Cardiolipin represents a structurally distinct anionic phospholipid found predominately in the mitochondrial inner membrane [6, 7]. Mitochondrial cardiolipin is postulated to exist in clustered microdomains that influence mitochondrial structure-function[8]. Specifically, cardiolipin is often found at negatively curved regions of the inner membrane, including cristae contact sites with the boundary membrane and along the inner leaflet of cristae tubules. Cardiolipin is essential for protein localization and assembly, profoundly influencing mitochondrial dynamics, energetics, and network continuity [9, 10]. Previous studies have established oxidation and subsequent loss of cardiolipin across cardiac pathologies, including acute I/R [11, 12] and heart failure [13-15]. Aside from exogenous perfusion with cardiolipin[16], which may only be applicable in experimental settings, there are currently no therapies that can improve mitochondrial function by targeting cardiolipin.

A number of cell permeable, mitochondria-targeting peptides have emerged over the last two decades. This class of peptides typically contain residues of alternating cationic-aromatic motifs ranging from 4-16 amino acids, and have been explored for a variety of pre-clinical models (reviewed in [17]). Elamipretide (MTP-131, Bendavia) is a cell-permeable peptide currently being tested in several clinical trials to mitigate mitochondrial dysfunction associated with genetic- and age-related mitochondrial diseases. This peptide is a structural analog to the SS-31 peptide [18], and consists of a tetrapeptide sequence of D-arginine-dimethyltyrosine-lysine-phenylalanine. Pre-clinical studies spanning numerous models and laboratories have demonstrated preserved mitochondrial function and cytoprotection with this peptide (reviewed in [19-21]), although the mechanism of action of the peptide has remained elusive.

Previous work has indicated that elamipretide can interact with cardiolipin[22], yet the physiological consequences of this interaction are not understood. In this study, we utilized comprehensive and complimentary approaches to determine novel decrements in mitochondrial structure-function after ischemia-reperfusion injury. We tested the hypothesis that elamipretide would improve post-ischemic mitochondrial structure-function by aggregating mitochondrial cardiolipin domains.

Methods

Animals. Male Sprague-Dawley rats (aged 2-3 months) were used in the study. All procedures received prior approval from the Institutional Animal Care and Use Committees at East Carolina University, Latvian Institute for Organic Synthesis, and Virginia Tech. Animals were housed in a temperature and light-controlled environment and received food and water ad libitum. Prior to excision of the heart, animals received an i.p. injection of ketamine/xylazine (90mg/kg/10mg/kg,

respectively), and hearts were excised (after the diminution of animal reflexes) via midline thoracotomy and placed in ice-cold saline.

*Materials***.** All phospholipids were purchased from Avanti Polar Lipids Inc. Elamipretide and the TAMRA-elamipretide conjugate were synthesized by New England Peptide. All organic solvents were HPLC grade and all other reagents were purchased from either Fisher Scientific or Sigma.

Ischemia-Reperfusion. Excised hearts were perfused on one of four modified Langendorff apparatus (AD Instruments) per our established protocols[23, 24]. Hearts were exposed to 20/120 minutes of global ischemia/reperfusion, respectively. For the elamipretide treatment, hearts received 10uM elamipretide beginning at the onset of reperfusion, which is a well-established cardioprotective paradigm in our models[19, 25-27]. Myocardial oxygen consumption was measured at the end of reperfusion in a subset of hearts per our established protocols [28]. At the end of reperfusion, hearts were split into the experimental groups described below.

High-resolution respirometry in Permeabilized Ventricular Fibers. Two different protocols were employed to determine mitochondrial function after ischemic stress in ventricular muscle fibers. The first set determined mitochondrial function in fibers isolated *after* cardiac ischemia-reperfusion ("post I/R Studies"). The second set of studies isolated cardiac fibers from a freshly isolated (normoxic) heart, and then induced anoxia-reoxygenation on the isolated fibers ("A/R Studies").

For post I/R studies, the left ventricle was dissected after the end of reperfusion and placed on a petri dish containing ice-cold buffer containing in (mM): 7.2 K_2EGTA, 2.8 CaK_2EGTA, 20

Imidazole, 20 Taurine, 5.7 ATP, 14.3 Phosphocreatine, 6.6 $MgCl_2$-$6H_2O$ and 50 MES; pH 7.1. All fat and connective tissues were removed under a dissecting microscope, and small cardiac fiber bundles (5-7 mg of wet weight) were prepared. Fiber bundles were permeabilized using 50µg/ml saponin at 4°C for 20 min. Permeabilized fiber bundles were then washed, 3 times for 5 min each, in ice-cold buffer Z containing in (mM): 110 K-MES, 35 KCL, 1 EGTA, 5 K_2HPO_4, 3 $MgCl_2$-$6H_2O$, and 5 mg/ml BSA; pH 7.4. The fiber bundles were kept at 4°C in buffer Z until analysis.

All experiments were conducted at 37°C in presence of 20 µM blebbistatin to prevent contraction. Five Oroboros High-resolution Respirometers (Oroboros Instruments, Innsbruck, Austria) in the Virginia Tech Metabolism Core were used in parallel to measure O_2 consumption and/or H_2O_2 emission per established protocols[29]. Buffer Z was used as respiration medium and O_2 consumption was monitored during a substrate-inhibitor titration ("SUIT") protocol to obtain a step-by-step analysis of various components of the mitochondrial respiratory chain as described by Kuznestov et al.[30]. The addition of substrates and inhibitors was done in the following sequence: glutamate/malate (10mM/5mM), ADP (2 mM), rotenone (0.5µM), succinate (10mM), antimycin A (5µM), N,N,N',N'-tetramethyl-p-phenylenediamine (TMPD)/ascorbate (0.5mM/2mM), cytochrome C (10µM), and FCCP (1µM). At the end of each experiment the fiber bundles were washed with distilled water and lyophilized in a freeze-dryer (Labconco, Kansas City, MO) for 3 hours and then weighed on a microsclae (Mettler-Toledo XS3DU). O_2 consumption is expressed in pmol/min*mg dry wt. FCCP data were excluded from 3 fibers because they were statistical outliers, with values greater than two standard deviations away from the group mean. Respiratory control ratio in permeabilized fibers was calculated as the ratio of ADP-stimulated respiration divided by respiration with glutamate/malate before the addition of ADP.

For A/R studies in ventricular fibers, mitochondrial respiration and H_2O_2 flux following anoxia-reoxygenation were performed using the Oxygraph-2k platform with established protocols [31-33]. Cardiac fiber bundles were permeabilized using 50μg/ml saponin and 0.5 mg/ml collagenase at 4ºC in 1 ml of buffer A (20mM imidazole, 0.5mM dithiothreitol, 20mM taurine, 7.1mM $MgCl_2$, 50 mM MES, 5 mM ATP, 15 mM phosphocreatine, 2.6 mM CaK_2EGTA, 7.4 mM K_2EGTA, pH 7.0 at 4ºC). After 15 min incubation, fibers were washed for 15 min in 2 ml of buffer B (20mM imidazole, 0.5mM dithiothreitol, 20mM taurine, 1.6mM $MgCl_2$, 100mM MES, 3mM KH_2PO_4, 2.9mM CaK_2EGTA, 7mM K_2EGTA, pH 7.1 at 37ºC) supplemented with elamipretide (100nM) or vehicle. State 3 respiration was stimulated with succinate (10mM), rotenone (0.5μM), and ADP (5mM), and the fiber bundle was left to consume all O_2 in the respiratory chamber (typically within 10-20 min) for the induction of anoxia. After 30 min anoxia, O_2 was reintroduced to the chamber by opening the chamber to achieve reoxygenation. After 8 min of reoxygenation, the chamber was closed and O_2 flux monitored for 2 min. At the end of the experiment, antimycin A (2.5μM) was added to determine mitochondrial-independent residual oxygen consumption. H_2O_2 flux was measured with 10μM Amplex Red, 1 U/mL horseradish peroxidase (HRP) and 5 U/mL superoxide dismutase (SOD), and H_2O_2 was calibrated using serial 0.1 H_2O_2 μM titrations.

Isolated Mitochondria. Mitochondria were isolated from the left ventricle and succinate-derived reverse electron transport determined using our established protocols[34].

Electron microscopy of mitochondria. A subset of hearts exposed to ischemia-reperfusion (as described above) were imaged by electron microscope (Virginia Tech Morphology Service Core Laboratory, Virginia-Maryland College of Veterinary Medicine). Images were obtained with

slight modifications to published protocols [35, 36]. Briefly, the left ventricle was isolated after I/R and sectioned into 3x3mm pieces. Sectioned tissue was chemically fixed with 3% glutaraldehyde for 24 hours and then washed twice in 0.1M Na-cacodylate for 15 minutes. Following the washes, tissue was post-fixed in 1% osmium tetroxide in 0.1M Na-cacodylate for 1 hour to fix membrane lipids. Samples were dehydrated in graded ethanol solutions of increasing concentrations (15%, 30%, 50%, 70%, 95%, and 100%) for 15 minutes, followed by a 15-minute submersion in propylene oxide. Dehydrated tissue was infiltrated with a 50:50 propylene oxide:Poly/Bed 812 solution for 12 hours. This step was followed by a 12-hour infiltration protocol of 100% Poly/Bed 812, so that the sample resin was polymerized into a hard plastic suitable for microtome sectioning. Samples were embedded into molds and cured at 60°C for 48 hours, and then sectioned into 90nm slices using a microtome. Slices were loaded into metal grids and stored in 100% ethanol until ready for use. For imaging, sections were air-dried and then stained with 2% uranyl acetate followed by lead citrate to enhance nucleic acid and cell membrane structure contrasts, respectively. Samples were loaded onto a plate adapter and imaged using transmission electron microscopy (JEOL JEM-1400) with a magnification of 25,000X and resolution of 0.0022um x 0.0022um. Images were processed in Gatan Inc. software and stored on a personal computer. Contact image analysis, sarcomere length measurements, mean mitochondrial Feret diameter [37], cristae complexity index [38], and electron density were performed with ImageJ. For about one-half of the images collected, resolution was insufficient to accurately measure cristae complexity, but mitochondrial morphology and electron density could still be obtained. Similarly, not all images that contained mitochondria contained measurable sarcomeres, also reflected by differing n's in the analysis.

Serial Block Face Scanning Electron Microscopy. A subset of hearts was fixed with electron microscopy-grade buffer (4% paraformaldehyde, 2.5% glutaraldehyde, 0.2M sodium cacodylate, pH =7). Tissues were stained and imaged by Renovo Neural Inc. (Cleveland, Ohio). Briefly, the samples were washed, stained with 1% tannic acid for 30 mins and then incubated successively with osmium ferrocyanide, thiocarbohydrazide, osmium tetroxide, uranyl acetate and lead aspartate, as previously described[39]. Tissues were dehydrated and embedded in Epon resin (Electron Microscopy Sciences).

Trimmed samples were imaged using either a ThermoFisher VolumeScope system on a Teneo SEM platform, or a Zeiss Sigma VP scanning electron microscope equipped with a Gatan 3View in-chamber ultramicrotome stage with Gatan low-kV backscattered electron detector. On both systems, stacks of digital images were acquired at 6.0 nm/pixel resolution (x,y) at 2.0 kV, using 65 nm steps (z); these are standard settings that approximate TEM-based imaging. Each resulting serial image stack contained ~500 images (~33µm deep, 49µm high x 49µm wide). Images were scaled and sub-stacks were generated and aligned using Image J software with the FIJI plugin suite. To augment the distinction between the mitochondrial cristae and matrix, slices were contrast enhanced to 0.5%, CLAHE filtered (511 block size, 512 histogram bins), and rendered using a 0.5 gamma processing setting.

For analyses and 3D reconstructions, the 5-10th slices of mitochondria (325-650nm deep) were used across treatment groups. Cristae contact site analyses were performed after contrast enhancement by calculating the percentage of cristae networks adhered to the intermitochondrial junction on the 5th slice (325nm deep) of all mitochondria across treatments (number of cristae within a cristae network ultimately contacting an intermitochondrial junction / total number of

cristae). All cristae longer than 100nm were included in the contact site analyses. A cristae contact site was considered to be present if a cristae longer than 100nm was adhered to a IMJ.

To measure intermitochondrial network connectivity, we analyzed a subset of mitochondrial images with 3-7 interconnected mitochondria. In these images, we utilized the flood-fill macro (ImageJ) to highlight inter-connected contrast. A single flood-fill click on an internal (in between adjacent mitochondria) intermitochondrial junction was performed to initiate intermitochondrial connectivity. The yellow highlighted contrast was subsequently separated from the rest of the network using the color threshold tool (0/38 hue, 0/255 saturation, 0/255 brightness, mean threshold method, black color, HSB color space, dark background). Yellow highlighted networks were then converted to white and the mean grey value was calculated. The percent connectivity was measured by dividing the thresholded mean grey value by the total network's mean grey value (i.e., the grey value before employing flood-fill).

Separation of Native Mitochondrial Respiratory Chain Complexes by Blue-Native Polyacrylamide Gel Electrophoresis (BN-PAGE). Separation of mitochondrial respiratory chain complexes was performed using BN-PAGE according to methods described by Schägger et al.[40, 41]. Based on established protocols that differentiate between supercomplexes and individual ETC complexes[42, 43], mitochondrial membranes were solubilized using either digitonin (digitonin:mitochondrial protein ratio was 8:1 (w/w)) for isolation of mitochondrial supercomplexes, or DDM (DDM:protein ratio of 2:1) for native complexes I, III, and V in sample buffer. After solubilization, the samples were centrifuged for 30 min at 20,000 x g, and protein content of the supernatant was determined using bicinchoninic acid (BCA protein assay reagent, Thermo Scientific, Rockford, IL, USA). Coomassie G-250 was added to each sample in a ratio

detergent-to-dye of 8:1 (w/w), and 35 µg total protein from each sample were separated on a Native PAGE 3-12% Bis-Tris (Life Technologies, Carlsbad, CA, USA) at 4°C. Running buffer was supplemented with 0.02% Coomassie G-250 to allow visualization of protein bands. The stained bands were scanned using the Odyssey Infrared Imaging system (LI-COR Biosciences, Lincoln, NB), and the densitometric analysis was performed blinded using Image J software (National Institutes of Health).

Mass Spectrometry. A subset of hearts was taken immediately at the end of reperfusion and the left ventricle was snap frozen and pulverized using a liquid nitrogen-cooled mortar/pestle. Thirty mg of powdered ventricular tissue was used for shotgun lipidomics, with each sample blinded to the lipidomics core. Frozen heart samples were weighed, lyophilized, pulverized, and homogenized in 500 µl of ice-cold diluted phosphate-buffered saline (0.1X PBS) on a cooling tissue homogenizer (Cryolys Precellys Evolution Homogenizer). Protein assays on individual homogenates were performed using a BCA protein assay kit (Pierce, Rockford, IL, USA). Lipids were extracted by a modified procedure of Bligh and Dyer extraction as described previously[44, 45] in the presence of an internal standard (tetra14:1 cardiolipin, 2 nmol/mg protein) which was added based on total protein content of the sample. Each lipid extract was resuspended into a volume of 200µL of chloroform/methanol (1:1, v/v) per mg of protein and flushed with nitrogen, capped, and stored at −20 °C for lipid analysis. For electrospray ionization (ESI) direct infusion analysis, lipid extract was further diluted to a final concentration of ~500 fmol/µL by $CHCl_3$/MeOH/isopropanol (1:2:4, v/v/v), and the mass spectrometric analysis was performed on a Q-Exactive mass spectrometer (Thermo Scientific, San Jose, CA) equipped with an automated nanospray device (TriVersa NanoMate, Advion Bioscience Ltd., Ithaca, NY) and operated with

Xcalibur software. Identification and quantification of cardiolipin molecular species were performed as previously described [46] using an automated software program [47]. The determined cardiolipin levels were normalized to the protein content of individual samples.

Construction of biomimetic lipid monolayers for pressure-area studies. All phospholipids were handled with extreme care to prevent oxidation under low light conditions and a gentle stream of nitrogen gas using established protocols [48]. Fresh lipid stocks in chloroform (HPLC grade, Fisher Scientific) were used for all studies. Biomimetic mitochondrial lipid monolayers were generated by co-dissolving lipids (40 mol% 18:0-22:6 PC, 30.0 mol% 16:0-20:4 PE, 20 mol% $(18:2)_4$CL, 5 mol% $(18:1)_2$PI, 3 mol% $(18:1)_2$PS, 2 mol% cholesterol) in chloroform (10 μg/μL). The trough was washed three times with 70% ethanol, Milli-Q water, and subphase prior to collecting pressure-area isotherms. Lipid monolayers were constructed by spotting 10 μg of lipid on a subphase of 10 mM sodium phosphate buffer (pH 7.4). Pressure-area isotherms were generated using a Mini Langmuir-Blodgett Trough (KSV NIMA, Biolin Scientific, Paramus, NJ) as previously demonstrated [49]. The area per molecule was calculated at a physiological surface pressure of 30 mN/m as previously shown [49].

Construction of Biomimetic Giant Unilamellar Vesicles (GUVs) for Imaging Microdomains. GUVs were constructed via electroformation as previously described [48], and contained 39.9 mol% 18:0-22:6 PC, 30.0 mol% 16:0-20:4 PE, 20 mol% $(18:2)_4$CL, 5 mol% $(18:1)_2$PI, 3 mol% $(18:1)_2$PS, 2 mol% cholesterol, and 0.1 mol% nonyl acridine orange (NAO). Briefly, 10 μg of total lipid was spread onto the conductive side of an indium tin oxide coated glass slide. The lipid-coated slide was subjected to dark vacuum for 1 hr to remove excess solvent. Electroformation

occurred at room temperature using a buffer containing 10 mM HEPES (pH 7.4) and 250 mM sucrose. Upon completion, samples were prepared for microscopy as previously described [48]. For select experiments, the total CL concentration was decreased 25-50% by mass. The addition of peptide occurred after monolayer construction or immediately prior to imaging.

Cardiolipin Lipid Vesicle Aggregation Assays. Multilamellar vesicles (MLVs) of varying composition were made as previously described by our groups[50]. Briefly, all lipids (1mg) were co-dissolved in HPLC-grade chloroform, extensively dried and re-suspended in 1 ml of 80 mM sodium phosphate buffer, pH = 7.4. The resuspension in buffer was conducted above the phase transition temperature (T_m) to ensure complete hydration. The aqueous dispersions were then put through three freeze-thaw cycles using dry ice and a water bath set above the T_m of the lipids. Stringent precautions including the use of low-light conditions were implemented to prevent oxidation of the lipids. As cardiolipin-enriched MLVs precipitate out of solution upon the addition of elamipretide, we devised a simple absorbance assay to quantify the extent of cardiolipin-elamipretide precipitate using an absorbance wavelength of 300nm. Titrations of elamipretide were introduced by calculating the molar ratios of elamipretide to cardiolipin. Elamipretide also precipitated cardiolipin-containing MLVs when the studies were repeated using higher salt (150mM) buffers (data not shown).

Cristae width. A custom Matlab program, previously described [51], was modified and combined with a blob algorithm [52] to quantify mitochondrial cristae width. The program calculated, in pixels, the maximal horizontal distance between each side of the cristae. These

values were then averaged over the entire array to produce an average mitochondrial cristae width value. The blob algorithm was utilized to weigh the averages by blob size and reduce human intervention in the analysis while quantifying mitochondrial cristae. Furthermore, the blob algorithm was utilized to calculate the total area occupied by networked or orphaned cristae (in pixels).

Statistical analyses. All data were analyzed using GraphPad Prism and are presented as mean ± sem. We ensured the data were distributed normally, which allowed for parametric analyses. Statistical analyses were conducted using a one-way ANOVA followed by a student t-test, with p values ≤ 0.05 considered significant. One trace from RET studies was excluded because the hydrogen peroxide emission was greater than two standard deviations away from the mean.

Results

Protection of mitochondrial energetics with elamipretide is not electron transport complex-dependent. We first confirmed myocardial uptake and mitochondrial localization using a novel TAMRA-conjugated elamipretide (Supplemental Figure S1). Mitochondrial functional studies are presented in Figure 1. In permeabilized ventricular fibers isolated after reperfusion ("Post-I/R" Fibers), respiratory control ratios (RCR; using glutamate/malate substrate) fell from 3.6 ± 0.2 in normoxic fibers to 1.9 ± 0.1 after I/R. This decrement was partially blunted with peptide treatment, with elamipretide leading to a post-I/R RCR of 2.5 ± 0.1. The substrate-uncoupler-inhibitor-titration (SUIT) protocol employed indicated significant decrements in mitochondrial respiration across complexes I-IV after ischemia-reperfusion. Post-ischemic administration of elamipretide improved mitochondrial respiration in both complexes I and II ($P<0.05$ compared to ischemia-reperfusion alone, Figure 1A), and trended to improve complex IV-dependent

respiration. Improved mitochondrial bioenergetics was also supported by higher myocardial oxygen consumption in the intact heart in post-ischemic hearts receiving elamipretide.

Elamipretide-mediated reductions in H_2O_2 emission. A major limitation to using fibers in the above paradigm (isolating fibers from the heart *after* I/R) is that one cannot determine whether the observed protection of mitochondrial energetics is a cause versus a consequence of cardioprotection. Accordingly, we next devised a series of studies to determine the efficacy of elamipretide in models where energetics can be measured *during* the insult. Permeabilized ventricular fibers (from normoxic hearts) were placed in a high-resolution respirometry chamber and respired (saturating ADP present, "State 3") until they consumed all of the oxygen in the chamber, thus making themselves anoxic. To account for variability, each fiber preparation was normalized to its own pre-anoxia, normoxic values. There was an observable burst of H_2O_2 at the onset of reoxygenation, and elamipretide significantly reduced fiber H_2O_2 emission (Figure 1B). This effect persisted whether H_2O_2 rates were expressed alone or when normalized to the fiber's simultaneous oxygen consumption rate.

We then determined if the mechanism of elamipretide involved reduction in ROS emission through reverse electron transfer (RET), presented in Figure 1C-E. There was a modest but statistically significant reduction in succinate-derived RET when mitochondria were treated acutely with elamipretide. This was reflected whether the H_2O_2 emission was integrated over a five-minute timespan after succinate addition (Figure 1D) or normalized to simultaneous oxygen flux (Figure 1E). As expected, treatment with rotenone abolished almost all RET. After rotenone treatment there were no differences in the rates of H_2O_2 production between the saline and elamipretide-treated mitochondria (Figure 1E).

These mitochondrial function studies were accompanied by complimentary studies using blue-native PAGE, (Supplemental Figure S2). We did not observe a discernible decrease in mitochondrial supercomplex density after I/R (Figure S2A and S2C). However, there was a decrease in the supercomplex coupling (flux control factor) after I/R, which was significantly improved with elamipretide (Figure S2D). There was a profound decrease in native Complex V after I/R, which was abrogated with elamipretide

(Figure S2B and S2E). Although previous studies have extracted supercomplex bands from the gel and measured discernible respiration[36], in our hands the changes in respiration when substrates were given appeared to be an artifact as it was observed even when non-loaded acrylamide gel was placed into the respirometer (data not shown).

Protection of mitochondrial ultrastructure. Given the integral relationships between mitochondrial function and structure [4, 37], we employed two different electron microscopy imaging modalities to determine mitochondrial morphology in our studies. Results from transmission electron microscopy are presented in Figure 2, with representative images in Figure 2A and Supplemental Figure S3. Ischemia-reperfusion induced modest mitochondrial swelling, with I/R-saline treated hearts having a significantly greater Feret Diameter when compared to normoxic hearts (Figure 2B, $P<0.05$ versus control). Treatment with elamipretide did not markedly influence mitochondrial swelling based on TEM imaging. Ischemia-reperfusion induced a substantial decrease in mitochondrial electron density ($P<0.05$, Figure 2C), which was attenuated with elamipretide treatment. Sarcomeric contracture (z-band width) was prominent with ischemia-reperfusion (Figure 3A and 3D), and was not affected by post-ischemic elamipretide treatment. Mitochondrial cristae complexity index was significantly lowered after reperfusion, and this decrease in cristae complexity was attenuated with elamipretide (Figure 2E). Cristae width averaged 25.0±1.8nm in normoxic mitochondria (n=189) and was not influenced by ischemia-reperfusion (cristae width: 25.4±0.7nm; n=178) or elamipretide treatment (26.7±0.5nm; n=172).

Higher resolution serial block face scanning electron microscopy (SBF-SEM) was employed to obtain more advanced structural insight. These data are presented in Figures 3 and 4 (along with reconstructed three-dimensional movies in Figures S4-S6). Under normoxic conditions, approximately 65% of cristae were physically adhered to the inner boundary membrane, termed “contact sites”. I/R injury led to a significant decrease in the number of cristae contact sites (Figure 3A and 3B; $P<0.05$ versus normoxia). Post-ischemic administration of elamipretide blunted the loss of cristae adhered to contact sites

(Figure 3B; $P<0.05$ versus I/R alone). Among adjoining mitochondria, inter-mitochondrial cristae network connectivity analysis indicated a substantial loss in network connectivity *between* mitochondria (presented in Figure 3C and 3D). Inter-mitochondrial cristae connectivity improved in post-ischemic hearts perfused with elamipretide (Figure 3C and 3D).

Separate SBF-SEM analyses were conducted to determine the extent of intra-mitochondrial cristae network connectivity. In these studies, we mapped the connectivity of cristae *inside* a subset of mitochondria using the rationale that contiguous cristae facilitate efficient energy transfer. We termed cristae that were interconnected "networked cristae", versus cristae that were disconnected from the network as "orphaned cristae". From our analysis we rendered networked cristae yellow color, and orphaned cristae red color. These data are presented in Figure 4 (with reconstructed three-dimensional movies in Supplemental Figures S7-S9). Interestingly, in normoxic hearts nearly all cristae appeared to be networked with one another (Figure 4B-4D). Matrix volume swelling and a substantial loss of cristae volume were prominent after reperfusion, which were not prevented with elamipretide (Figure 4A-C). However, elamipretide significantly increased the number of "connected cristae" versus cristae that were orphaned from the network (Figure 4A and 4D). Taken together, elamipretide did not prevent mitochondrial swelling or the loss of total cristae at reperfusion, but significantly improved cristae contact sites with the boundary membrane and reticular connectivity among the cristae network.

Cardiolipin content and composition from mass spectrometry. The functional and structural importance of cardiolipin led us to conduct shotgun lipidomics studies for cardiolipin content and acyl chain composition. These data are presented in Figure 5A-B, with the 25 most abundant cardiolipin species from the lipidomics studies presented in Table 1. There was a significant decrease in the total amount of cardiolipin after ischemia-reperfusion, as well as a significant decline in the most abundant cardiolipin species (tetralinolyl cardiolipin; $[18:2]_4$). The acute administration of elamipretide at the onset of reperfusion did not abrogate

the loss of cardiolipin, the decrease in $(18:2)_4$ cardiolipin, or significantly alter any of the other cardiolipin species examined in the study (Figures 5A-B and Table 1).

Biophysical studies of elamipretide with mitochondrial membranes. To better understand the biophysical interaction of elamipretide with cardiac mitochondrial membranes, we synthesized biomimetic membranes of the inner mitochondrial membrane. The advantage of this model is that it allowed us to tightly control lipid composition. Mitochondrial models were composed of physiological species of membrane lipids (described in methods), and a cardiolipin content that represented 20% of the total lipids (consistent with the content range seen across mammalian mitochondria [38]). Informed by our cardiolipin lipidomics studies (Figure 5A-B), we modeled the effects of cardiolipin loss after ischemia-reperfusion in biomimetic mitochondrial membranes by examining the biophysical interactions using a Langmuir trough (which provides mean molecular area-pressure isotherms of compressed lipid monolayer films). A 25% loss of cardiolipin ("I/R model") resulted in a significant reduction in the mean molecular area at a physiological membrane pressure of 30 mN/m (Figure 5D), consistent with a loss of membrane density as seen by our electron microscopy imaging modalities. Acute addition of elamipretide to I/R model membranes restored the mean molecular area in vesicles with reduced cardiolipin, suggesting a molecular interaction whereby elamipretide expands the 'footprint' from cardiolipin-enriched domains. We also modeled severe CL loss (50%, more comparable to chronic diseases and also saw an improvement (albeit not restoring the area to the non-pathological membrane levels). Notably, elamipretide treatment of biomimetic monolayers without cardiolipin present had no discernible effect on membrane behavior (Figure 5D, left panel).

To compliment the monolayer studies, we synthesized biomimetic mitochondrial lipid vesicles of similar composition. In the absence of peptide, cardiolipin fluorescence (assessed by NAO localization) is uniform across the vesicle membrane and is accompanied by no observable aggregation of adjacent vesicles. Upon the addition of elamipretide to biomimetic vesicles, the NAO signal clustered into enriched domains. This cardiolipin clustering co-localized with fluorescent TAMRA-elamipretide (Figure 5C),

providing a complement to our imaging in intact cells (Figure S1). Furthermore, addition of elamipretide promoted aggregation of adjacent lipid vesicles (Figure 5C). This aggregation effect was not seen in vesicles devoid of cardiolipin, and our previous work has shown that proteins that do not associate with cardiolipin do not have this effect on CL domains [35]. Additionally, we serendipitously discovered that cardiolipin-containing vesicles and elamipretide precipitate when in solution together (Supple Figure S10). Titration studies indicated that elamipretide aggregated cardiolipin-enriched vesicles, essentially saturating the signal at a molar ratio of one peptide to two cardiolipin (Supplemental Figure S10).

Discussion

In this study we used comprehensive approaches to advance our understanding of mitochondrial structure-function in hearts exposed to ischemia-reperfusion. To the best of our knowledge, several aspects of our study represent novel findings to the field. First, we found parallel decrements in mitochondrial cristae structure and respiratory function noted across electron transport system complexes after ischemia-reperfusion. Second, we have provided an innovative new approach to map mitochondrial network connectivity in the heart, discovering decrements among and between mitochondrial cristae networks after ischemia-reperfusion. Third, our studies elucidate new mechanistic insight into elamipretide, a clinical-stage peptide that appears to aggregate cardiolipin and improve mitochondrial membrane structure and bioenergetic function without preventing acute cardiolipin loss. Finally, we highlight the potential of utilizing biomimetic model membranes to directly quantify membrane-dependent effects of pathologies and putative therapeutics.

Targeting mitochondria in ischemia-reperfusion. Mitochondrial dysfunction is widely observed in cardiac pathologies, making the mitochondrial network an attractive target for novel adjuvant therapies[21, 39]. The mitochondrial panoply responsible for bioenergetics impairments include: reactive oxygen species production that exceeds endogenous scavenging capacity, matrix calcium overload, imbalances in substrate

content/composition, inner membrane uncoupling, membrane lipid oxidation/degradation, inefficient electron flux, opening of energy-dissipating channels/pores, and collapse(s) in mitochondrial membrane potential (reviewed in [8, 40, 41]). A number of different pharmacological approaches have been explored to target these aspects of dysfunction, with several compounds progressing to clinical trials (reviewed in [42]). In this study, we sought to improve mitochondrial function by targeting mitochondrial cardiolipin, with the hypothesis that restoring membrane structural organization would lead to downstream bioenergetic improvements.

Cardiolipin and structural anomalies in pathological mitochondria. The dynamic link between mitochondrial function and structure has been known for half a century [1, 2], strengthened in recent years with augmented imaging modalities [3, 4]. Mitochondrial ultrastructure is undoubtedly complex, encompassing processes involving various membrane lipids, nuclear- and mitochondria-encoded proteins, and lipid-protein interactions. In this study we focused primarily on cardiolipin, a non-bilayer-forming, cone-shaped inner membrane phospholipid with two very well-described roles: influencing mitochondrial structure and function.

Cardiolipin contributes to inner membrane structure by imparting negative membrane curvature[43] found at cristae junctions and along the inner leaflet of cristae membranes (depicted in Figure 6). Cardiolipin also serves as a membrane anchor for mitochondrial proteins essential for the cristae assembly/morphology, including ATP synthase dimers [44-48], OPA1 [48-51], mitoregulin [52], and components of the mitochondrial contact site and cristae organizing system (MICOS) [10, 53-57]. Although the role of proteins in influencing cristae structure cannot be understated, proton-dependent cristae formation can be observed in inner mitochondrial

membrane lipid vesicles containing cardiolipin yet devoid of any proteins[58]. Cardiolipin is also essential for the activity of a myriad of proteins involved in bioenergetic function [6, 7, 12, 16], making it a central player in trying to improve structure-function decrements across bioenergetic diseases.

The loss of total and tetralinolyl cardiolipin that we observed corroborates findings from a number of previous studies ([12, 16, 59, 60]). Likewise, mitochondrial ultrastructural defects similar to what we observed have been noted across other pathologies[37] characterized by loss of cardiolipin and corresponding cristae [7]. Cardiolipin replacement strategies have been tested and include direct perfusion of cardiolipin to isolated rat hearts [16] and utilization of cardiolipin-containing nanodiscs [61]. While promising, the translational relevance of these paradigms for patients remains to be demonstrated.

Mitigation of bioenergetic dysfunction in post-ischemic mitochondria. Dysfunction along the electron transport system is widely observed across models of ischemia-reperfusion injury. Our finding of multi-complex dysfunction after ischemia-reperfusion compliments previous studies noting decrements in complex activity, subunit oxidation, and augmented ROS production along the electron transport system [41, 62-71]. In this study we utilized a cell-permeable, mitochondria-targeting peptide to determine the efficacy in improving mitochondrial structure-function. Mitochondria-targeting peptides represent an emerging class of therapeutics that are being tested across disease indications. These peptides share structural homology with endogenous mitochondria-targeting sequences, which are both amphipathic and cationic[72]. Likewise, most mitochondria-targeting peptides contain alternating cationic-aromatic amino acid motifs [17, 73, 74]. Mitochondria-targeted peptides appear to be lipophilic enough to cross membrane barriers, typically contain arginine (especially the D-isomer for enzymatic stability), and are postulated to hone to mitochondria based on the negative membrane potential, the presence of anionic phospholipids (such as cardiolipin), or combinations thereof.

To determine if a mitochondria-targeted peptide could improve mitochondrial structure-function, we utilized the tetrapeptide elamipretide (D-arginine-dimethyltyrosine-lysine-phenylalanine). Elamipretide (MTP-131 or Bendavia) is a salt-variant of the SS-31 peptide first serendipitously discovered by Szeto and Schiller [75] in their search for novel opioid receptor ligands. This peptide has shown protective efficacy across myriad preclinical studies (reviewed in [8, 20]) and is currently being tested in multiple clinical trials (addressed in more detail below).

Improved post-ischemic respiratory function with elamipretide was observed across complexes, which corroborates previous studies where elamipretide improved activity or expression of several different electron transport complexes [15, 76-78]. These data suggest that elamipretide's mechanism of action does not depend on one particular protein or complex. The improved bioenergetic function across complexes was suggested by studies examining the existence of native protein complexes. Supercomplex coupling control factor, a functional measure of the 'intactness' of respirasomes (Chatfield et al.), and native complex V structure were both impaired after ischemia-reperfusion and improved with elamipretide. We did not find evidence of robust decreases in supercomplex density after ischemia-reperfusion. These results are consistent with other studies examining supercomplexes after acute cardiac ischemia-reperfusion [79, 80], which generally show extremely modest effects of ischemia-reperfusion on supercomplex band density (<15% reductions band density). These findings also corroborate previous work where cardioprotection was not associated with augmented supercomplex band density [81]. Given the sensitivity of native protein complexes to detergent conditions[82-84], and the issue of sample bias in isolating mitochondrial supercomplexes from infarcted myocardium (i.e. isolation procedures enrich for healthy mitochondria), future studies are warranted to better understand the relevance of blue-native supercomplexes in models of cardiac pathology.

Reduction of mitochondrial ROS emission without direct scavenging. Despite the use of this peptide across scores of studies, there has been uncertainty regarding the mechanism of action. The SS-31 peptide was originally described as a "scavenger" of reactive oxygen species. While it is clear that elamipretide can reduce overall ROS *levels* from *pathological* mitochondria ([15, 25]), several lines of evidence suggest that it is not scavenging ROS. We previously showed that the peptide was not scavenging either superoxide or hydrogen peroxide as compared to several positive controls using cell-free model systems[19]. Other groups have found that elamipretide-mediated reductions in ROS are observed in diseased tissues but not healthy tissues[76, 85], also suggesting that the peptide is reducing pathological production of ROS and not scavenging *per se.* Preconditioning of the heart, which has been shown to involve small bursts of ROS that

trigger adaptive responses and is typically abolished with "ROS scavengers", was not abolished with elamipretide treatment[26]. Our finding of reduced ROS emission in permeabilized ventricular fibers and a modest reduction in reverse electron transfer (RET) [86] provides further evidence that the peptide may be reducing succinate-derived RET early in reperfusion. Interestingly, elamipretide-mediated reductions in ROS production by the ETC were not observed downstream of ubiquinone (Figure 1), suggesting an alternative mechanism than one involving cytochrome c-mediated injury [87, 88].

Targeting cardiolipin to attenuate pathological structure-function. Using innovative biophysical models of the inner mitochondrial membrane we observed interactions between elamipretide and cardiolipin, corroborating findings first made by Birk et al.[22, 88]. Among endogenous proteins, arginine and lysine amino acid residues are both known to bind with cardiolipin [52], and this interaction was confirmed in our studies showing cardiolipin-dependent lipid aggregation. Another novel aspect of our study was that acute elamipretide treatment at reperfusion did not prevent cardiolipin loss observed after acute ischemia-reperfusion. While longer term administration of elamipretide ($\geq$4 weeks) has shown to normalize aberrant cardiolipin in canine models of heart failure [15] and pigs with metabolic syndrome[78], our data indicate that the peptide has robust, acute activity to preserve mitochondrial structure-function even in the presence of cardiolipin deficiencies. This beneficial, acute activity suggest that the peptide may be effective in diseases characterized by loss of cardiolipin (such as genetic mitochondrial diseases and/ or Barth Syndrome).

We used our mass spectrometry data to synthesize biomimetic membranes of the post-ischemic inner membrane. The loss or oxidation of cardiolipin modeled after ischemia-reperfusion led to a discernible change in the membrane structure, notably a decreased area per molecule, which is a measure of membrane packing (Figure 5). Elamipretide promoted a physical 'aggregation' of cardiolipin domains, where the peptide is acting like a *membrane adhesion factor* for the cardiolipin that is present (even if it is oxidized). As it is virtually impossible to study mammalian mitochondria devoid of cardiolipin, our finding

from the models that elamipretide-mediated lipid aggregation is not present without cardiolipin highlights the preferential nature of this interaction.

We observed mutual benefits for mitochondrial structure and function in pathological (post-reperfusion) mitochondria. Our finding of improved mitochondrial ultrastructure with elamipretide in cardiac ischemia-reperfusion injury corroborates previous work where elamipretide improved mitochondrial morphology in other disease states [78, 88, 89]. In this study we provide advanced insight into mitochondrial structure using higher resolution, SBF-SEM. To the best of our knowledge, this is the first time this technology has been employed to map mitochondrial cristae ultrastructural networks in cardiac health and pathology. These studies found that cristae contact sites are disrupted in the post-ischemic heart, novel findings that compliment altered contact sites seen in other diseases [90, 91]. We observed that elamipretide did not prevent the loss in total cristae with reperfusion, consistent with a lack of protection against cardiolipin loss (Figures 4L and 5A-B), as these are inter-related [58, 92]. A major advancement using this technology is that elamipretide, which appears to aggregate cardiolipin domains, partially restored the cristae network connectivity. This may help explain the robust protection of ATP synthase dimers with elamipretide, as ATP synthase and cristae architecture have shown inter-dependent declines in other pathologies [46]. Likewise, the modest reduction in RET that we observed was also associated with improved cristae ultrastructure, and succinate accumulation has previously been shown to induce mitochondrial fragmentation [93].

If any generalizations can be made about elamipretide's mechanism across studies to date, it is that this peptide appears to exert biological effects *predominantly* when there is an underlying pathological burden present. The ability of elamipretide to prolong PTP opening [15, 19], improve exercise capacity[85], promote cardiolipin remodeling[15, 78], reduce apoptotic signaling[94], stimulate state 3 respiration[87], or improve the activity of several different ETC complexes [15, 76-78] is only observed in diseased, aged, or damaged (respiratory control ratio <2) mitochondria. There appears to be translational support for this concept, as a recent clinical trial with elamipretide showed the greatest 6-minute-walk benefit in patients who began the study with the largest functional impairments (those who walked <350m before the study

saw the greatest benefit) [95]. As the sequence of elamipretide contains two non-natural amino acids, there is no known homology between this peptide and endogenous assembly or mitochondrial fusion factors, although the up-regulation of cristae assembly factors (such as OPA1) has been recently observed after elamipretide treatment [96, 97].

Given the cationic and aromatic repeats, and that many mitochondrial assembly proteins have conserved RYL or RYK motifs [52, 98-101], it is tempting to speculate that the peptide is acting as an enzymatically resistant, cell-permeable analog of an endogenous assembly factor(s). Such a mechanism may explain why there are little/no observable effects in healthy mitochondria across studies with elamipretide as noted above. Healthy inner membranes may be sufficiently intact such that the addition of an adhesion factor has a negligible effect. This type of mechanism may also promote the utility of this peptide (and related analogs) across mitochondrial pathologies that share the commonality of structural abnormalities[3, 4]. Clearly further testing is warranted to better elucidate the efficacy of elamipretide across other pathologies.

Elamipretide in the clinic. As a therapeutic in development, elamipretide appears to be safe and well-tolerated by patients [95, 102, 103], and recently showed promise in improving functional parameters in adults with primary mitochondrial myopathies[95]. A Phase 2 clinical trial using elamipretide in STEMI patients was conducted in 2015 [102]. Despite some interesting trends to reduce events associated with congestive heart failure, there was no significant effect of peptide treatment[104]. The major limitation to this study was that ~40% of patients had to be excluded due to open arteries at the time of reperfusion. Pre-clinical studies have indicated that post-ischemic perfusion of elamipretide is no longer efficacious if started >10 minutes after reperfusion, ostensibly to attenuate structure-function decrements that occur in the first few minutes of reperfusion[19].

Conclusions

In this study we provide unprecedented insight into mitochondrial structure-function derangements in acute ischemia-reperfusion. We have combined comprehensive functional measurements in mitochondria, fibers, and the intact heart, with innovative new imaging modalities examining cristae architecture. Or data indicate that while elamipretide does not prevent the loss of cardiolipin, post-ischemic treatment can improve a variety of functional and morphological characteristics of mitochondria even with cardiolipin loss. Our new approaches to synthesize biomimetic models that recapitulate inner membrane lipids has profound potential to expand our understanding of the consequences of phospholipid alterations. Future studies utilizing these complimentary approaches will continue to advance the development of mitochondria-targeting strategies.

Limitations

We acknowledge that there are limitations to our SBF-SEM imaging studies. The number of experimental replicates (n=8-10) is somewhat low for these data. Hundreds of hours were spent reconstructing high resolution, 3D mitochondria and their networks from each treatment group. For these reasons, we complemented these data with transmission electron microscopy images (n=59-70 mitochondria from 3 hearts per treatment group), and demonstrate similar findings across imaging modalities.

Conclusions

Abhorrent cristae ultrastructure underlies the pathology associated with mitochondrial dysfunction and disease. Despite sustained losses in cardiolipin and cristae volume, elamipretide preserved respiratory function across complexes, inner membrane biophysical integrity, and cristae connectivity. This has potential implications for several mitochondrial diseases characterized by

the loss of cardiolipin and cristae, i.e., Barth Syndrome. To this end, our study supports the continued clinical development for elamipretide as a therapeutic for patients with mitochondrial disease. Future studies should continue to investigate the effects of other cationic, lipophilic peptides on mitochondrial structure-function and how they contribute to health and disease.

Acknowledgements

We are very grateful for the support provided by Kathy Lowe of the Virginia Tech Electron Microscopy Core. Without her guidance and technical expertise, our electron microscopy studies and morphological analyses would not have been possible. We'd also like to acknowledge the contributions of Ella Maru Studio and the outstanding animations depicted in Figure 6.

Funding

These studies were supported by research grants from the National Institutes of Health, NHLBI 1R01HL123647 (to SRS and DAB), Stealth BioTherapeutics (to DAB and SRS), USDA National Institute of Food and Agriculture Hatch Project 1017927 (to DAB), and a Translational Obesity Research Fellowship from the Virginia Tech Interdisciplinary Graduate Education Program (to MEA).

Acknowledgements

We are very grateful for the support provided by Kathy Lowe of the Virginia Tech Electron Microscopy Core. Without her guidance and technical expertise, our electron microscopy studies and morphological analyses would not have been possible. We'd also like to acknowledge the contributions of Ella Maru Studio and the outstanding animations depicted in Figure 6.

Conflict of Interest

DAB has received consulting income and research grants from Stealth Biotherapeutics.

References

1. Hackenbrock, C.R., *Ultrastructural bases for metabolically linked mechanical activity in mitochondria. I. Reversible ultrastructural changes with change in metabolic steady state in isolated liver mitochondria.* J Cell Biol, 1966. **30**(2): p. 269-97.
2. Hackenbrock, C.R., *Ultrastructural bases for metabolically linked mechanical activity in mitochondria. II. Electron transport-linked ultrastructural transformations in mitochondria.* J Cell Biol, 1968. **37**(2): p. 345-69.
3. Mannella, C.A., *Structural diversity of mitochondria: functional implications.* Ann N Y Acad Sci, 2008. **1147**: p. 171-9.
4. Mannella, C.A., W.J. Lederer, and M.S. Jafri, *The connection between inner membrane topology and mitochondrial function.* J Mol Cell Cardiol, 2013. **62**: p. 51-7.
5. Glancy, B., et al., *Mitochondrial reticulum for cellular energy distribution in muscle.* Nature, 2015. **523**(7562): p. 617-20.
6. Schlame, M. and M. Ren, *The role of cardiolipin in the structural organization of mitochondrial membranes.* Biochim Biophys Acta, 2009. **1788**(10): p. 2080-3.
7. Chicco, A.J. and G.C. Sparagna, *Role of cardiolipin alterations in mitochondrial dysfunction and disease.* Am J Physiol Cell Physiol, 2007. **292**(1): p. C33-44.
8. Brown, D.A., H.N. Sabbah, and S.R. Shaikh, *Mitochondrial inner membrane lipids and proteins as targets for decreasing cardiac ischemia/reperfusion injury.* Pharmacol Ther, 2013.
9. Schlame, M. and M.L. Greenberg, *Biosynthesis, remodeling and turnover of mitochondrial cardiolipin.* Biochim Biophys Acta, 2017. **1862**(1): p. 3-7.
10. Wollweber, F., K. von der Malsburg, and M. van der Laan, *Mitochondrial contact site and cristae organizing system: A central player in membrane shaping and crosstalk.* Biochim Biophys Acta, 2017. **1864**(9): p. 1481-1489.
11. Kim, J., et al., *Cardiolipin: characterization of distinct oxidized molecular species.* J Lipid Res, 2011. **52**(1): p. 125-35.

12. Paradies, G., et al., *Role of cardiolipin peroxidation and Ca2+ in mitochondrial dysfunction and disease.* Cell Calcium, 2009. **45**(6): p. 643-50.
13. Sparagna, G.C., et al., *Quantitation of cardiolipin molecular species in spontaneously hypertensive heart failure rats using electrospray ionization mass spectrometry.* J Lipid Res, 2005. **46**(6): p. 1196-204.
14. Chatfield, K.C., et al., *Dysregulation of cardiolipin biosynthesis in pediatric heart failure.* J Mol Cell Cardiol, 2014. **74**: p. 251-9.
15. Sabbah, H.N., et al., *Chronic Therapy With Elamipretide (MTP-131), a Novel Mitochondria-Targeting Peptide, Improves Left Ventricular and Mitochondrial Function in Dogs With Advanced Heart Failure.* Circ Heart Fail, 2016. **9**(2): p. e002206.
16. Paradies, G., et al., *Decrease in mitochondrial complex I activity in ischemic/reperfused rat heart: involvement of reactive oxygen species and cardiolipin.* Circ Res, 2004. **94**(1): p. 53-9.
17. Horton, K.L., et al., *Tuning the activity of mitochondria-penetrating peptides for delivery or disruption.* Chembiochem, 2012. **13**(3): p. 476-85.
18. Zhao, K., et al., *Cell-permeable peptide antioxidants targeted to inner mitochondrial membrane inhibit mitochondrial swelling, oxidative cell death, and reperfusion injury.* J Biol Chem, 2004. **279**(33): p. 34682-90.
19. Brown, D.A., et al., *Reduction of Early Reperfusion Injury With the Mitochondria-Targeting Peptide Bendavia.* J Cardiovasc Pharmacol Ther, 2013.
20. Szeto, H.H., *Pharmacologic Approaches to Improve Mitochondrial Function in AKI and CKD.* J Am Soc Nephrol, 2017. **28**(10): p. 2856-2865.
21. Brown, D.A., et al., *Expert consensus document: Mitochondrial function as a therapeutic target in heart failure.* Nat Rev Cardiol, 2016.
22. Birk, A.V., et al., *Targeting Mitochondrial Cardiolipin and the Cytochrome C/Cardiolipin Complex to Promote Electron Transport and Optimize Mitochondrial Atp Synthesis.* Br J Pharmacol, 2013.
23. Brown, D.A., et al., *Effects of 4'-chlorodiazepam on cellular excitation-contraction coupling and ischaemia-reperfusion injury in rabbit heart.* Cardiovasc Res, 2008. **79**(1): p. 141-9.
24. Brown, D.A., et al., *Cardiac arrhythmias induced by glutathione oxidation can be inhibited by preventing mitochondrial depolarization.* J Mol Cell Cardiol, 2010. **48**(4): p. 673-9.
25. Kloner, R.A., et al., *Reduction of ischemia/reperfusion injury with bendavia, a mitochondria-targeting cytoprotective Peptide.* J Am Heart Assoc, 2012. **1**(3): p. e001644.
26. Frasier, C.R., et al., *Redox-dependent increases in glutathione reductase and exercise preconditioning: role of NADPH oxidase and mitochondria.* Cardiovasc Res, 2013. **98**(1): p. 47-55.
27. Sloan, R.C., et al., *Mitochondrial permeability transition in the diabetic heart: Contributions of thiol redox state and mitochondrial calcium to augmented reperfusion injury.* J Mol Cell Cardiol, 2012. **52**(5): p. 1009-18.
28. Liu, T., D.A. Brown, and B. O'Rourke, *Role of mitochondrial dysfunction in cardiac glycoside toxicity.* J Mol Cell Cardiol, 2010. **49**(5): p. 728-36.
29. Perry, C.G., et al., *Inhibiting myosin-ATPase reveals a dynamic range of mitochondrial respiratory control in skeletal muscle.* Biochem J, 2011. **437**(2): p. 215-22.

30. Kuznetsov, A.V., et al., *Analysis of mitochondrial function in situ in permeabilized muscle fibers, tissues and cells.* Nat Protoc, 2008. **3**(6): p. 965-76.
31. Makrecka-Kuka, M., G. Krumschnabel, and E. Gnaiger, *High-Resolution Respirometry for Simultaneous Measurement of Oxygen and Hydrogen Peroxide Fluxes in Permeabilized Cells, Tissue Homogenate and Isolated Mitochondria.* Biomolecules, 2015. **5**(3): p. 1319-38.
32. Kuka, J., et al., *The cardioprotective effect of mildronate is diminished after co-treatment with L-carnitine.* J Cardiovasc Pharmacol Ther, 2012. **17**(2): p. 215-22.
33. Makrecka, M., et al., *Mildronate, the inhibitor of L-carnitine transport, induces brain mitochondrial uncoupling and protects against anoxia-reoxygenation.* Eur J Pharmacol, 2014. **723**: p. 55-61.
34. Dai, W., et al., *Cardioprotective Effects of Mitochondria-Targeted Peptide SBT-20 in two Different Models of Rat Ischemia/Reperfusion.* Cardiovasc Drugs Ther, 2016.
35. Fujioka, H., B. Tandler, and C.L. Hoppel, *Mitochondrial division in rat cardiomyocytes: an electron microscope study.* Anat Rec (Hoboken), 2012. **295**(9): p. 1455-61.
36. Lee, H.L., et al., *Biphasic modulation of the mitochondrial electron transport chain in myocardial ischemia and reperfusion.* Am J Physiol Heart Circ Physiol, 2012. **302**(7): p. H1410-22.
37. Federico, M., et al., *Calcium-calmodulin-dependent protein kinase mediates the intracellular signalling pathways of cardiac apoptosis in mice with impaired glucose tolerance.* J Physiol, 2017. **595**(12): p. 4089-4108.
38. Williams, P.A., et al., *Retinal ganglion cell dendritic degeneration in a mouse model of Alzheimer's disease.* Neurobiol Aging, 2013. **34**(7): p. 1799-806.
39. Mukherjee, K., et al., *Analysis of Brain Mitochondria Using Serial Block-Face Scanning Electron Microscopy.* J Vis Exp, 2016(113).
40. Schagger, H., *Respiratory chain supercomplexes of mitochondria and bacteria.* Biochim Biophys Acta, 2002. **1555**(1-3): p. 154-9.
41. Schagger, H., W.A. Cramer, and G. von Jagow, *Analysis of molecular masses and oligomeric states of protein complexes by blue native electrophoresis and isolation of membrane protein complexes by two-dimensional native electrophoresis.* Anal Biochem, 1994. **217**(2): p. 220-30.
42. Gomez, L.A., et al., *Supercomplexes of the mitochondrial electron transport chain decline in the aging rat heart.* Arch Biochem Biophys, 2009. **490**(1): p. 30-5.
43. Wittig, I., H.P. Braun, and H. Schagger, *Blue native PAGE.* Nat Protoc, 2006. **1**(1): p. 418-28.
44. Han, X., *Lipidomics: Comprehensive Mass Spectrometry of Lipids*. 2016, Hoboken, New Jersey: John Wiley & Sons, Inc. 496.
45. Han, X., *Comprehensive Mass Spectrometry of Lipids*. 2016: John Wiley & Sons, Inc.
46. Han, X., et al., *Shotgun lipidomics of cardiolipin molecular species in lipid extracts of biological samples.* J Lipid Res, 2006. **47**(4): p. 864-79.
47. Yang, K., et al., *Automated lipid identification and quantification by multi-dimensional mass spectrometry-based shotgun lipidomics.* Anal. Chem., 2009. **81**: p. 4356-4368.
48. Sullivan, E.M., et al., *Docosahexaenoic acid lowers cardiac mitochondrial enzyme activity by replacing linoleic acid in the phospholipidome.* J Biol Chem, 2018. **293**(2): p. 466-483.

49. Pennington, E.R., et al., *Distinct membrane properties are differentially influenced by cardiolipin content and acyl chain composition in biomimetic membranes.* Biochim Biophys Acta, 2017. **1859**(2): p. 257-267.
50. Shaikh, S.R., et al., *Oleic- and docosahexaenoic acid-containing phosphatidylethanolamines differentially phase separate from sphingomyelin.* Biochim Biophys Acta, 2009. **1788**(11): p. 2421-6.
51. Raisch, T., M. Khan, and S. Poelzing, *Quantifying Intermembrane Distances with Serial Image Dilations.* Journal of Visualized Experiments, 2018. **139**.
52. Analyst, I., *Image Segmentation Tutorial.* 2015.
53. Smith, R.A., R.C. Hartley, and M.P. Murphy, *Mitochondria-targeted small molecule therapeutics and probes.* Antioxid Redox Signal, 2011. **15**(12): p. 3021-38.
54. Yousif, L.F., et al., *Mitochondria-penetrating peptides: sequence effects and model cargo transport.* Chembiochem, 2009. **10**(12): p. 2081-8.
55. Alta, R.Y., et al., *Mitochondria-penetrating peptides conjugated to desferrioxamine as chelators for mitochondrial labile iron.* PLoS One, 2017. **12**(2): p. e0171729.
56. Maranzana, E., et al., *Mitochondrial respiratory supercomplex association limits production of reactive oxygen species from complex I.* Antioxid Redox Signal, 2013. **19**(13): p. 1469-80.
57. Schagger, H. and K. Pfeiffer, *Supercomplexes in the respiratory chains of yeast and mammalian mitochondria.* EMBO J, 2000. **19**(8): p. 1777-83.
58. Acin-Perez, R., et al., *Respiratory active mitochondrial supercomplexes.* Mol Cell, 2008. **32**(4): p. 529-39.
59. Vincent, A.E., et al., *The Spectrum of Mitochondrial Ultrastructural Defects in Mitochondrial Myopathy.* Sci Rep, 2016. **6**: p. 30610.
60. Paradies, G. and F.M. Ruggiero, *Age-related changes in the activity of the pyruvate carrier and in the lipid composition in rat-heart mitochondria.* Biochim Biophys Acta, 1990. **1016**(2): p. 207-12.
61. Pell, V.R., et al., *Moving Forwards by Blocking Back-Flow: The Yin and Yang of MI Therapy.* Circ Res, 2016. **118**(5): p. 898-906.
62. Walters, A.M., G.A. Porter, Jr., and P.S. Brookes, *Mitochondria as a drug target in ischemic heart disease and cardiomyopathy.* Circ Res, 2012. **111**(9): p. 1222-36.
63. Murphy, E. and C. Steenbergen, *Mechanisms underlying acute protection from cardiac ischemia-reperfusion injury.* Physiol Rev, 2008. **88**(2): p. 581-609.
64. Kloner, R.A., et al., *New and revisited approaches to preserving the reperfused myocardium.* Nat Rev Cardiol, 2017.
65. Ikon, N. and R.O. Ryan, *Cardiolipin and mitochondrial cristae organization.* Biochim Biophys Acta, 2017. **1859**(6): p. 1156-1163.
66. Paradies, G., et al., *Mitochondrial bioenergetics and cardiolipin alterations in myocardial ischemia/reperfusion injury. Implications for pharmacological cardioprotection.* Am J Physiol Heart Circ Physiol, 2018.
67. Malhotra, K. and N.N. Alder, *Reconstitution of Mitochondrial Membrane Proteins into Nanodiscs by Cell-Free Expression.* Methods Mol Biol, 2017. **1567**: p. 155-178.
68. Szeto, H.H. and A.V. Birk, *Serendipity and the discovery of novel compounds that restore mitochondrial plasticity.* Clin Pharmacol Ther, 2014. **96**(6): p. 672-83.
69. Horton, K.L., et al., *Mitochondria-penetrating peptides.* Chem Biol, 2008. **15**(4): p. 375-82.

70. Kelley, S.O., K.M. Stewart, and R. Mourtada, *Development of novel peptides for mitochondrial drug delivery: amino acids featuring delocalized lipophilic cations.* Pharm Res, 2011. **28**(11): p. 2808-19.
71. Chakrabarti, A.K., et al., *Rationale and design of the EMBRACE STEMI Study: A phase 2a, randomized, double-blind, placebo-controlled trial to evaluate the safety, tolerability and efficacy of intravenous Bendavia on reperfusion injury in patients treated with standard therapy including primary percutaneous coronary intervention and stenting for ST-segment elevation myocardial infarction.* Am Heart J, 2013. **165**(4): p. 509-514 e7.
72. Karaa, A., et al., *Randomized dose-escalation trial of elamipretide in adults with primary mitochondrial myopathy.* Neurology, 2018.
73. Daubert, M.A., et al., *Novel Mitochondria-Targeting Peptide in Heart Failure Treatment: A Randomized, Placebo-Controlled Trial of Elamipretide.* Circ Heart Fail, 2017. **10**(12).
74. Gibson, C.M., et al., *EMBRACE STEMI study: a Phase 2a trial to evaluate the safety, tolerability, and efficacy of intravenous MTP-131 on reperfusion injury in patients undergoing primary percutaneous coronary intervention.* Eur Heart J, 2015.
75. Dai, W., et al., *Bendavia, a mitochondria-targeting peptide, improves postinfarction cardiac function, prevents adverse left ventricular remodeling, and restores mitochondria-related gene expression in rats.* J Cardiovasc Pharmacol, 2014. **64**(6): p. 543-53.
76. Siegel, M.P., et al., *Mitochondrial-targeted peptide rapidly improves mitochondrial energetics and skeletal muscle performance in aged mice.* Aging Cell, 2013. **12**(5): p. 763-71.
77. Birk, A.V., et al., *Targeting mitochondrial cardiolipin and the cytochrome c/cardiolipin complex to promote electron transport and optimize mitochondrial ATP synthesis.* Br J Pharmacol, 2014. **171**(8): p. 2017-28.
78. Birk, A.V., et al., *The Mitochondrial-Targeted Compound SS-31 Re-Energizes Ischemic Mitochondria by Interacting with Cardiolipin.* J Am Soc Nephrol, 2013.
79. Zhao, H., et al., *Peptide SS-31 upregulates frataxin expression and improves the quality of mitochondria: implications in the treatment of Friedreich ataxia.* Sci Rep, 2017. **7**(1): p. 9840.
80. Yuan, F., et al., *Mitochondrial targeted peptides preserve mitochondrial organization and decrease reversible myocardial changes in early swine metabolic syndrome.* Cardiovasc Res, 2018. **114**(3): p. 431-442.
81. Petrosillo, G., et al., *Decreased complex III activity in mitochondria isolated from rat heart subjected to ischemia and reperfusion: role of reactive oxygen species and cardiolipin.* FASEB J, 2003. **17**(6): p. 714-6.
82. Nickel, A.G., et al., *Reversal of Mitochondrial Transhydrogenase Causes Oxidative Stress in Heart Failure.* Cell Metab, 2015. **22**(3): p. 472-84.
83. Sweetwyne, M.T., et al., *The mitochondrial-targeted peptide, SS-31, improves glomerular architecture in mice of advanced age.* Kidney Int, 2017. **91**(5): p. 1126-1145.
84. Khalifat N, F.J., Puff N, , *Lipid packing variations induced by pH in cardiolipin-containing bilayers: the driving force for the cristae-like shape instability.* Biochimica et Biophysica Acta, 2011. **1808**(11): p. 2724-2733.
85. Khalifat N, P.N., Monneau S, Fournier JB, Angelova MI, *Membrane deformation under local pH gradient: mimicking mitochondrial cristae dynamics.* Biphysical Journal 2008. **95**(10): p. 4924-4933.

86. Frezza C, C.A., Martin de Brito O, Micaroni M, Beznoussenko GV, Rudka T, Bartoli D, Polishuck RS, Danial NN, De Strooper B, Scorrano L, *OPA1 Controls Apoptotic Cristae Remodeling Independently from Mitochondrial Fusion.* Cell 2006. **126**(1): p. 177-189.
87. Glytsou C, C.E., Cogliati S, Mehrotra A, Anastasia I, Rigoni G, Raimondi A, Shintani N, Loureiro M, Vazquez J, Pellegrini L, Enriquez JA, Scorrano L, Soriano ME, *Optic Atrophy 1 Is Epistatic to the Core MICOS Component MIC60 in Mitochondrial Cristae Shape Control.* Cell Reports, 2016. **17**(11): p. 3024-3034.
88. Gadicherla AK, S.D., Antholine WE, Yang M, Camara AK, *Damage to mitochondrial complex I during cardiac ischemia reperfusion injury is reduced indirectly by anti-anginal drug ranolazine.* Biochim Biophys Acta, 2012. **1817**(3): p. 419-429.
89. Jang S, L.T., Powers C, Khuchua Z, Baines CP, Wipf P, Javadov S, *Elucidating Mitochondrial Electron Transport Chain Supercomplexes in the Heart During Ischemia-Reperfusion.* Antioxid Redox Signal, 2017. **27**(1): p. 57-69.
90. Chouchani ET, P.V., Gaude E, Aksentijević D, Sundier SY, Robb EL, Logan A, Nadtochiy SM, Ord ENJ, Smith AC, Eyassu F, Shirley R, Hu CH, Dare AJ, James AM, Rogatti S, Hartley RC, Eaton S, Costa ASH, Brookes PS, Davidson SM, Duchen MR, Saeb-Parsy K, Shattock MJ, Robinson AJ, Work LM, Frezza C, Krieg T, Murphy MP, *Ischaemic accumulation of succinate controls reperfusion injury through mitochondrial ROS.* Nature, 2014. **515**(7527): p. 431-435.
91. Wong, R., et al., *Cardioprotection leads to novel changes in the mitochondrial proteome.* Am J Physiol Heart Circ Physiol, 2010. **298**(1): p. H75-91.
92. Lu YT, L.L., Yang YL, Yin X, Liu Q, Zhang L, Liu K, Liu B, Li J, Qi LW, *Succinate induces aberrant mitochondrial fission in cardiomyocytes through GPR91 signaling.* Cell death and Disease, 2018. **9**(6).
93. Anand R, S.V., Urbach J, Wittig I, Reichert AS, *Mic13 Is Essential for Formation of Crista Junctions in Mammalian Cells.* Plos one, 2016. **11**(8).
94. Kojima R, K.Y., Furuta S, Itoh K, Sesaki H, Endo T, Tamura Y., *Maintenance of Cardiolipin and Crista Structure Requires Cooperative Functions of Mitochondrial Dynamics and Phospholipid Transport.* Cell Reports, 2019. **26**(3): p. 518-528.
95. Quintana-Cabrera, M., Rigoni, Soriano, *Who and how in the regulation of mitochondrial cristae shape and function.* Biochemical and Biophysical Research Communications, 2018. **500**: p. 94-101.
96. Manella, C., *Structure and dynamics of the mitochondrial inner membrane cristae.* Biochimica et Biophysica Acta, 2006. **1763**: p. 542-548.
97. Siegmund, F.e.a., *Three-Dimensional Analysis of Mitochondrial Crista Ultrastructure in a Patient with Leigh Syndrome by In Situ Cryoelectron Tomography.* Cell Press, 2018. **6**: p. 83-91.
98. Jayashankar V, M.I., Rafelski SM, *Shaping the multi-scale architecture of mitochondria.* Current Opinions in Cell Biology 2016. **38**: p. 45-51.
99. Cogliati, E., Scorrano, *Mitochondrial Cristae: Where Beauty Meets Functionality.* Cell Press, 2016. **41**(3).
100. Genin EC, P.M., Bannwarth S, Villa E, et al. , *CHCHD10 mutations promote loss of mitochondrial cristae junctions with impaired mitochondrial genome maintenance and inhibition of apoptosis.* EMBO Molecular Medicine 2016. **8**: p. 58-72.

101. Li H, R.Y., Zhang K, Jian F, Hu C, Mioa L, Gong L, Sun L, Zhnag X, Chen S, Chen H, Liu D, Sonh Z, *Mic60/Mitofilin determines MICOS assembly essential for mitochondrial dynamics and mtDNA nucleoid organization.* Cell Death and Differentiation, 2015. **23**(3).
102. V, K.-P., *The MICOS complex of human mitochondria.* Cell Tissue Research, 2017. **367**: p. 83-93.
103. Jans DC, W.C., Riedel D, Wenzel D, Stagge F, Deckers M, Rehlling P, Jakobs S, *STED super-resolution microscopy reveals an array of MINOS clusters along human mitochondria.* Proceedings of the National Academy of Sciences, USA, 2013. **110**(22): p. 8936-8941.
104. Friedman JR, M.A., Yamada J, McCaffery JM, Nunnari J, *MICOS coordinates with respiratory complexes and lipids to establish mitochondrial inner membrane architecture.* eLife, 2015. **4**.
105. Weber TA, K.S., Heide H, Wittig I, Head B, van der Bliek A, Brandt U, Mittelbronn M, Reichart AS, *APOOL is a cardiolipin-binding constituent of the mitofilin/MINOS protein complex determining crisate morphology in mammalian mitochondria.* Plos one, 2013. **8**(5).
106. Genin EC, B.S., Lespinasse F, Ortega-Vila B, Fragaki K, Itoh K, Villa E, Lacas-Gervais S, Jokela M, Auranen M, Ylikallio E, Mauri-Crouzet A, Tyynismaa H, Vihola A, Augé G, Cochaud C, Sesaki H, Ricci JE, Udd B, Vives-Bauza C, Paquis-Flucklinger V, *Loss of MICOS complex integrity and mitochondrial damage, but not TDP-43 mitochondrial localisation, are likely associated with severity of CHCHD10-related diseases.* Neurobiology of Disease, 2018. **119**: p. 159-171.
107. Cogliati, S., et al, *Mitochondrial Cristae Shape Determines Respiratory Chain Supercomplexes Assembly and Respiratory Efficiency.* Cell, 2013. **155**: p. 160-171.
108. Ban T, K.H., Ishihara T, Ishihara N, *Relationship between OPA1 and cardiolipin in mitochondrial inner-membrane fusion.* Biochemica Biophysica Acta Bioenergetics, 2018. **1859**(9): p. 951-957.
109. DeVay RM, D.-R.L., Lackner LL, Hoppins S, Stahlberg H, Nunnari J, *Coassembly of Mgm1 isoforms requires cardiolipin and mediates mitochondrial inner membrane fusion.* Journal of Cell Biology, 2009. **186**: p. 793-803.
110. Kumar R, B.M., Wider JM, Reynolds CA, Calo L, Lepore B, Tousignant R, Jones M, Przyklenk K, Sanderson TH. , *Mitochondrial Dynamics Following Global Cerebral Ischemia.* Molecular and Cell Neuroscience 2016 **76**: p. 68-75.
111. Santo-Domingo J, G.M., Poburko D, Scorrano L, Demaurex N, *OPA1 promotes pH flashes that spread between contiguous mitochondria without matrix protein exchange.* EMBO J, 2013. **32**(13): p. 1927-1940.
112. Patten DA, W.J., Khacho M, Soubannier V, Mailoux RJ, Pilon-Larose K, MacLaurin JG, Park DS, McBride HM, Trinkle-Mulcahy L, Harper ME, Germain M, Slack RS, , *OPA1-dependent cristae modulation is essential for cellular adaptation to metabolic demand.* EMBO J, 2014. **33**: p. 2676-2691.
113. SJ, N.D.a.F., *Bioenergetics 4*. 2013, London: Academic Press.

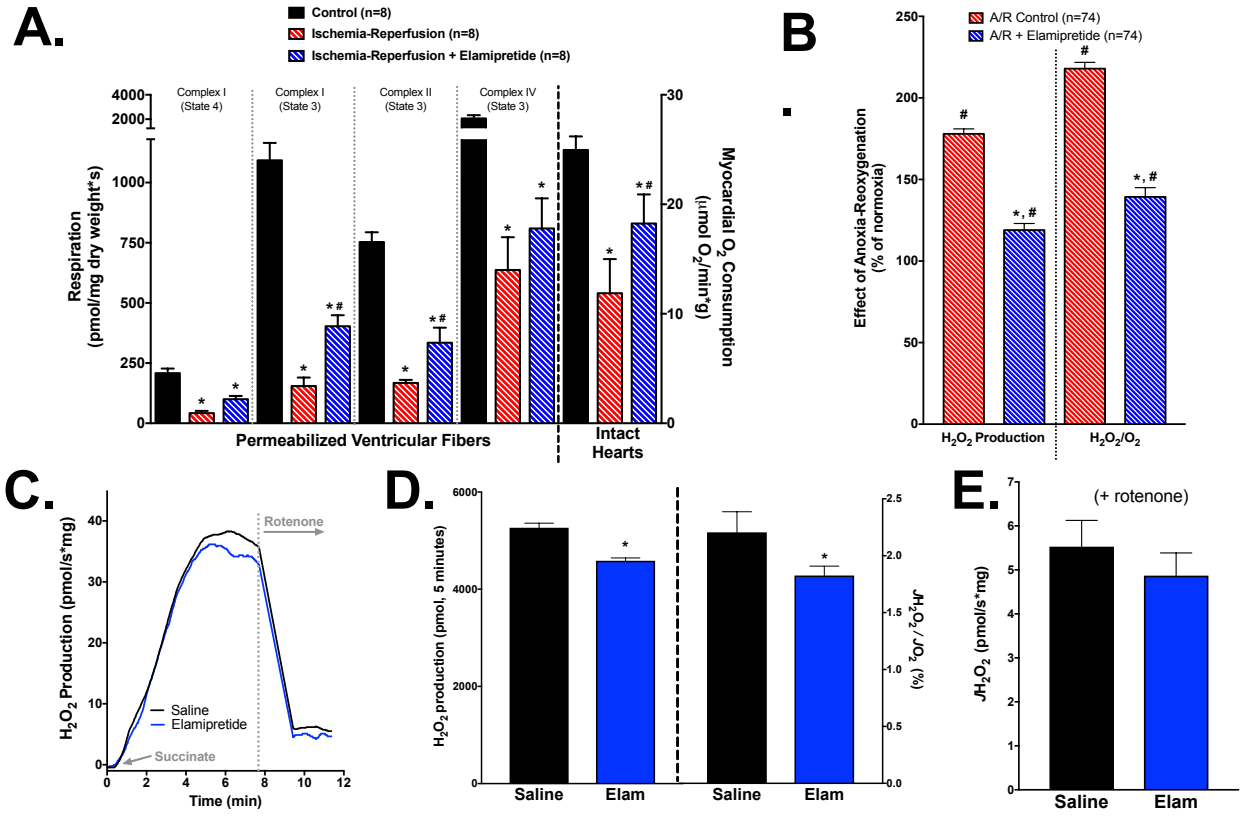

Figure 1: Improvement of mitochondrial function with elamipretide. (A) Decrements in mitochondrial respiration were seen across different mitochondrial complexes and substrate conditions in permeabilized fibers and intact hearts, with elamipretide providing improved function across complexes. (B) In permeabilized ventricular fibers, elamipretide reduced H_2O_2 emission associated with reoxygenation. (C-E) Effects of elamipretide on reverse electron transport (RET) stimulated by succinate administration. Effects of elamipretide on reverse electron transport (RET) stimulated by succinate administration. (C) Representative trace of succinate-supported RET. (D) Elamipretide led to modest reductions in RET whether analyzed as an integrated response after succinate or steady-state. (E) Rotenone substantially reduced H2O2 emission, with no differences between saline and elamipretide groups. *, P<0.05 versus normoxic; #, P<0.05 versus saline.

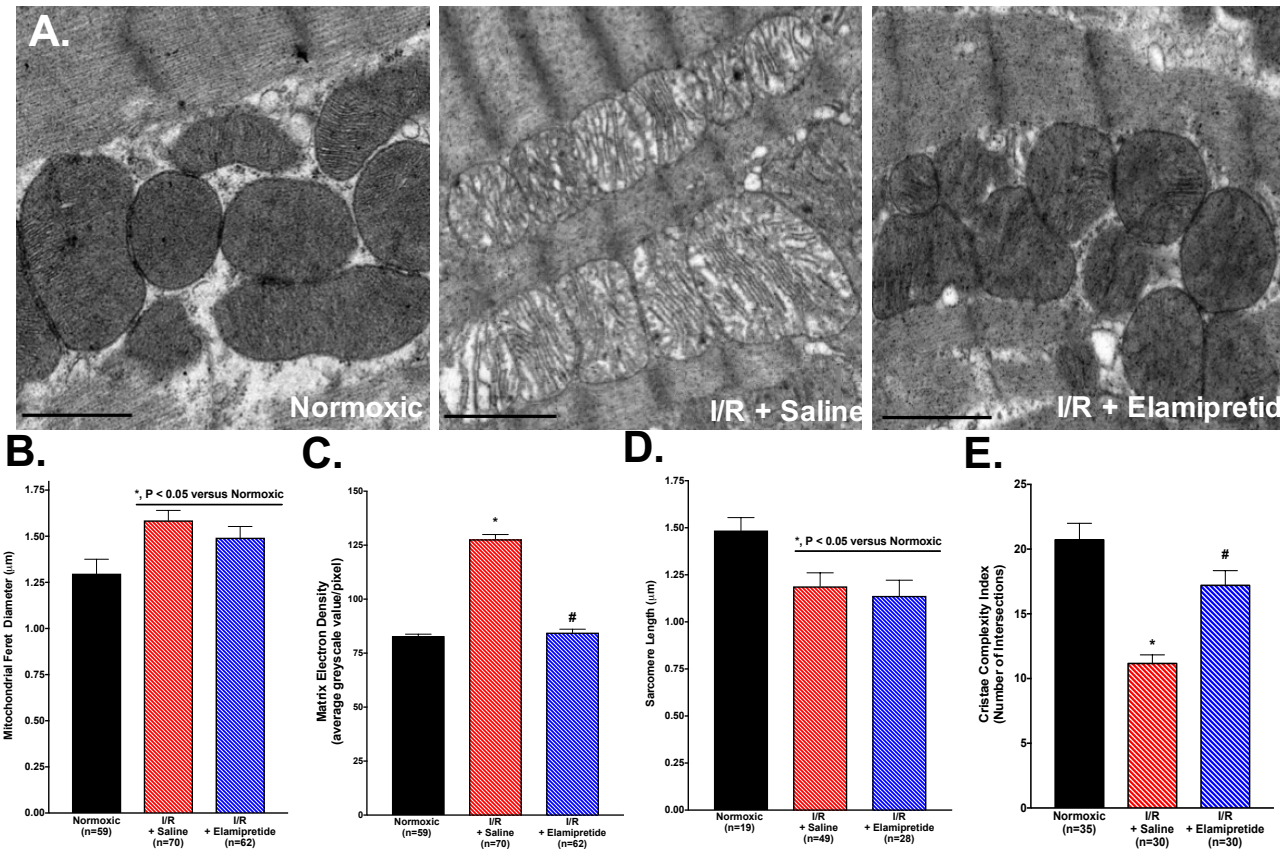

Figure 2: TEM data from hearts in the study. (A) Representative images from experimental groups. Images were analyzed for mitochondrial feret diameter (B), matrix electron density (C), sarcomere length (D), and cristae complexity index (E). *, P<0.05 v normoxic; #, P<0.05 versus I/R + Saline. Scale bar represents 2um.

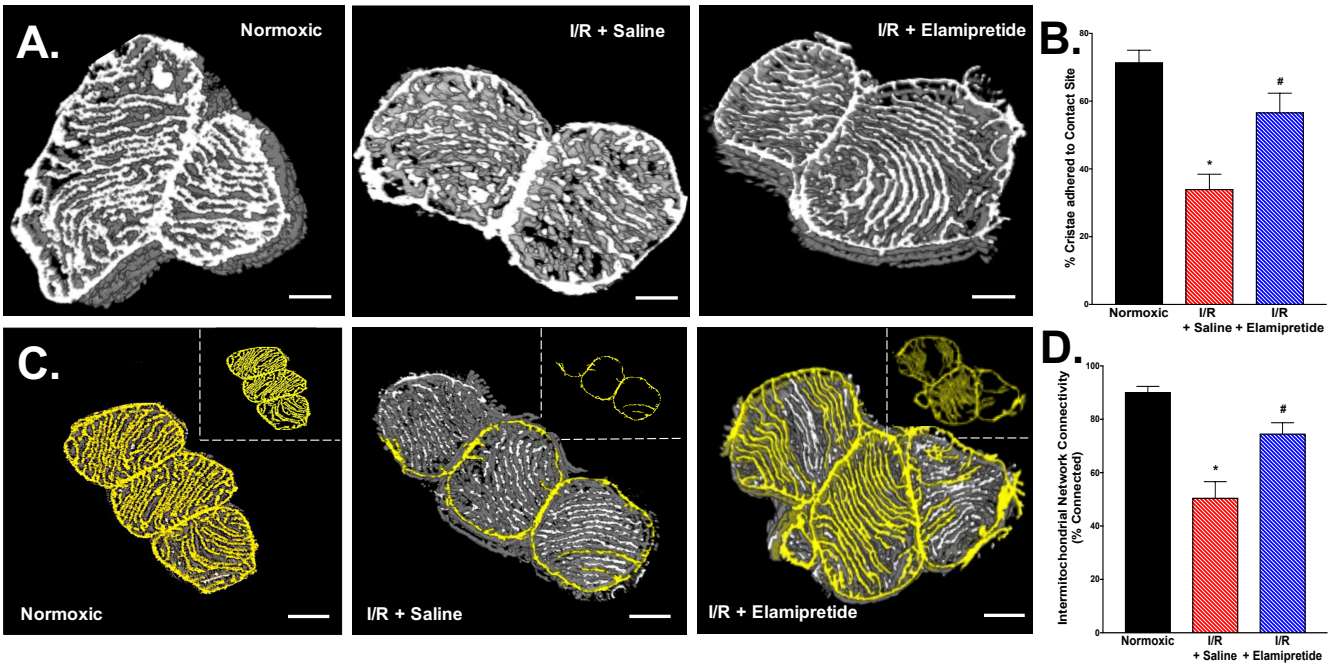

Figure 3: Serial block-face scanning electron microscopy images of mitochondrial ultrastructure in the experimental groups. Mitochondria were analyzed for contract site analysis (A) and intermitochondrial network connectivity (C), with quantified data in panels (B) and (D), respectively. *, P < 0.05 versus normoxic, #, P<0.05 versus I/R saline. Three-dimensional reconstructions of these images are presented in the Supplemental Figures, Figure S5. Scale bar represents 500nm.

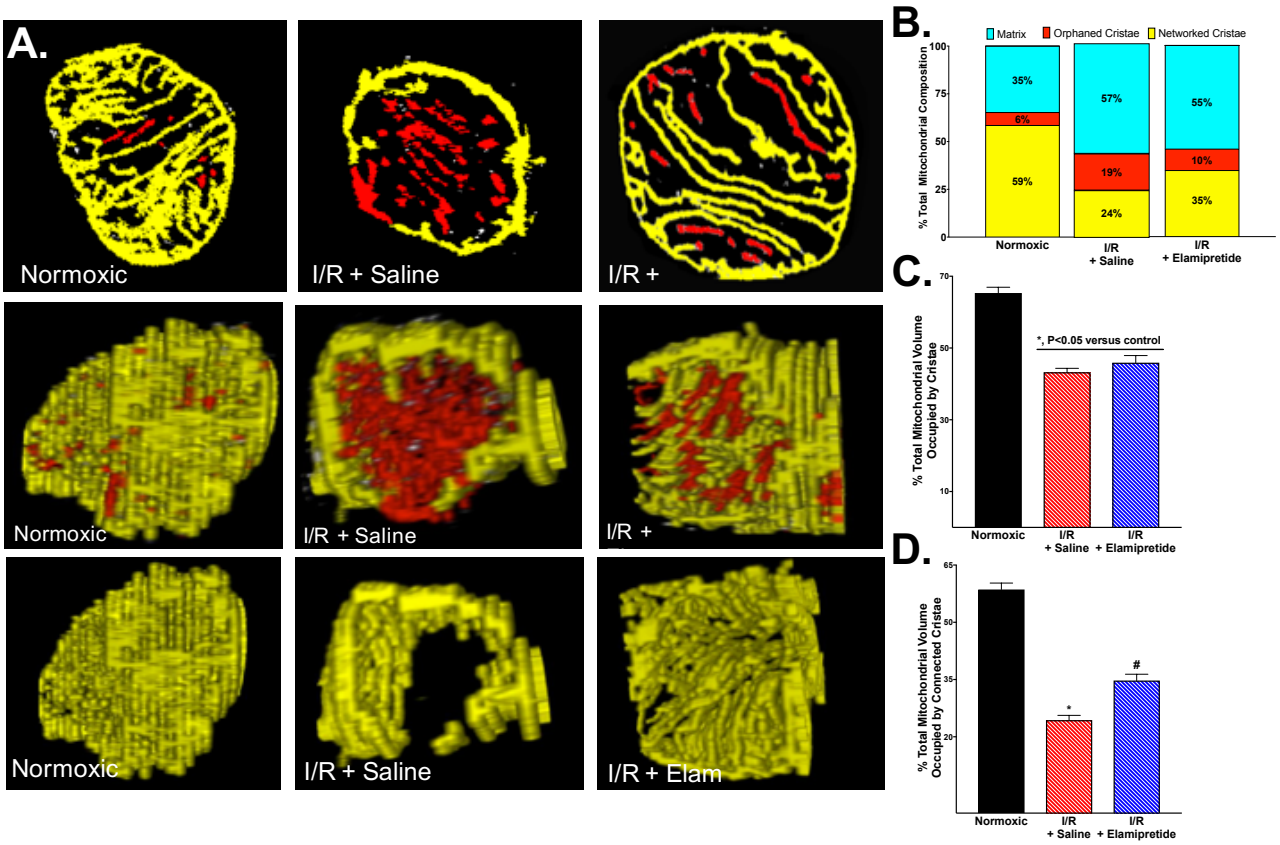

Figure 4: Serial block-face scanning electron microscopy images of single mitochondrial ultrastructure in the experimental groups. Mitochondria were analyzed for cristae connectivity. (A) Top Panel: individual slices from SBF-SEM imaging showing cristae networking. Middle Panel: cross-section of composite stacks indicating networked (yellow) and orphaned cristae (red). Bottom Panel: mitochondrial cross-section showing only networked cristae (from middle panel). Composition of total mitochondrial volume (B) total cristae volume (C) and connected cristae volume were measured in each experimental groups. *, P<0.05 versus normoxic; #, P<0.05 versus I/R.

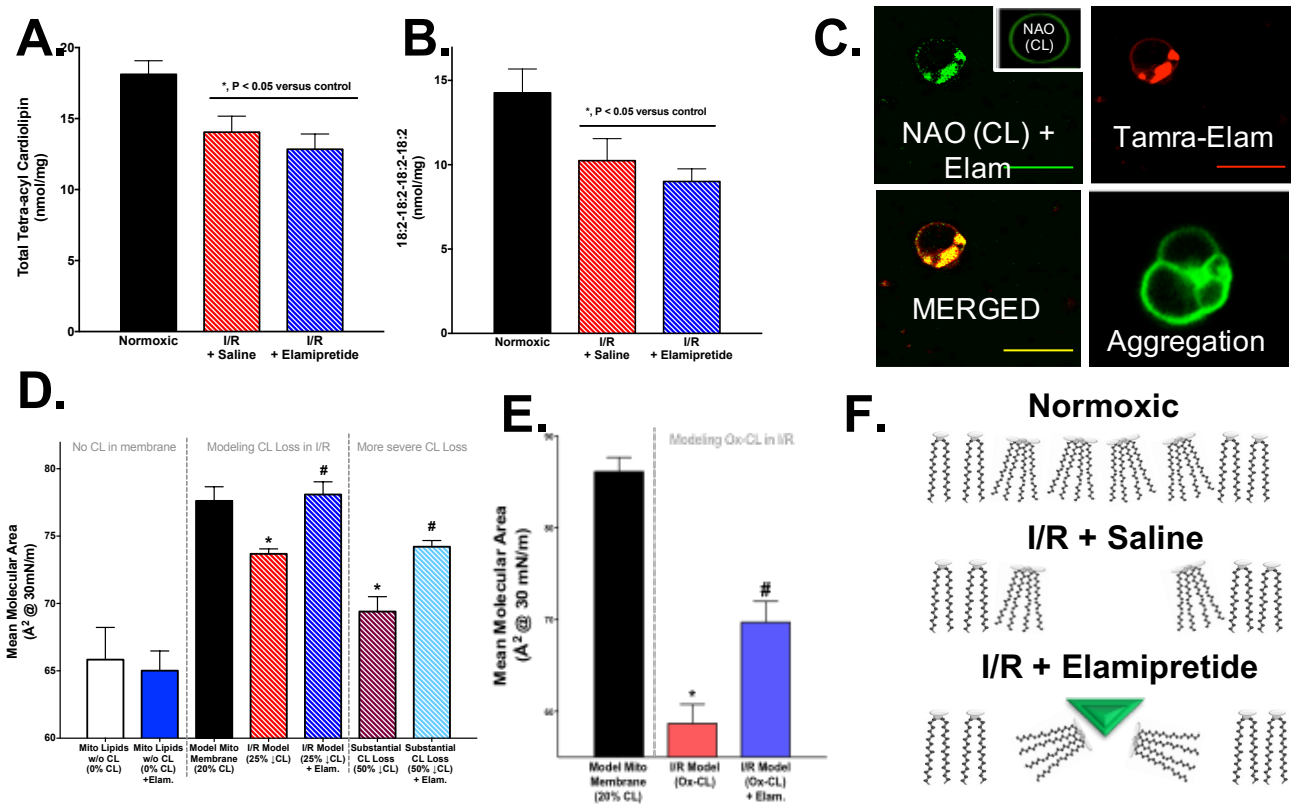

Figure 5: Elamipretide-mediated protection of mitochondrial function was observed despite sustained declines in total cardiolipin (A) and tetra-linolyl cardiolipin (B) after ischemia-reperfusion (assessed by mass spec). This loss in CL content was recapitulated by creating models of mitochondrial inner membrane lipids (C-F). (C) GUV imaging of mitochondrial CL with NAO and fluorescent TAMRA-elamipretide, as well as elamipretide-mediated vesicle aggregation. (D) Pressure-area isotherms at physiological membrane pressure (30mN/m) showing effects of losing CL content and elamipretide interactions to augment lipid area despite CL losses. This was observed in our I/R model and with severe (50%) declines in total CL. (E) Isotherms from model membrane studies looking at the effects of CL oxidation and Elam on pressure-area relationships (F) Proposed model in which elamipretide aggregates CL to preserve inner mitochondrial membrane integrity. *, P<0.05 v control, #, P<0.05 v. I/R.

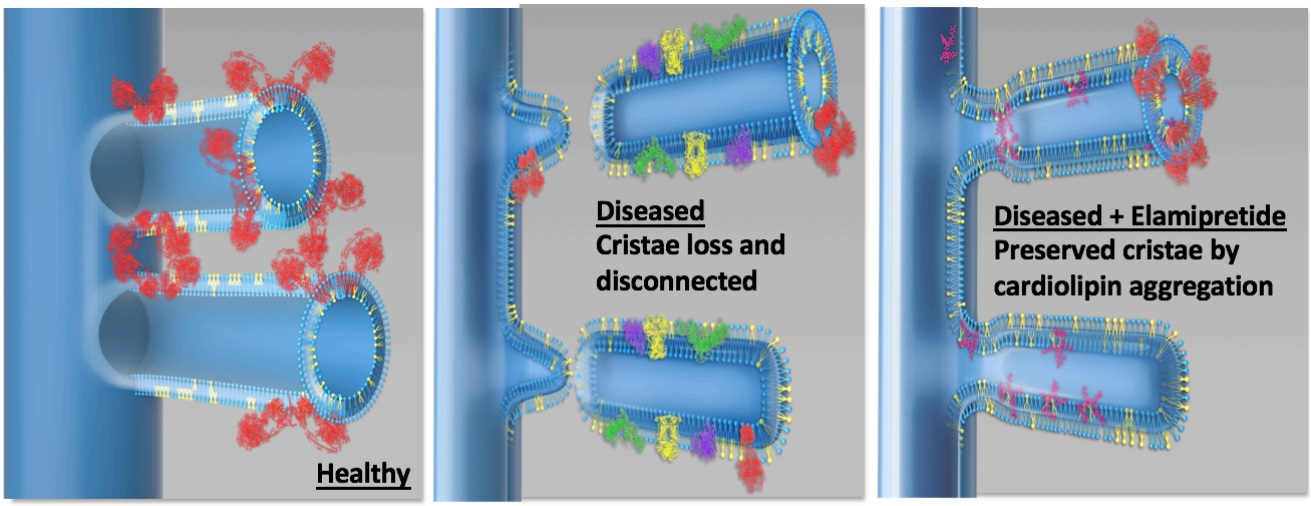

Figure 6: Proposed model in which Elamipretide aggregates cardiolipin to preserve cristae ultrastructure in diseased mitochondria. Therapeutic approaches that target cardiolipin may conserve inner mitochondrial membrane integrity, maintain cristae contact sites, sustain intra and intermitochondrial networks, and improve mitochondrial function during disease states.

Supplemental Figures

Cardiolipin Species	Control	Ischemia-Reperfusion	Ischemia-Reperfusion + Elamipretide
18:2-18:2-18:2-18:2	74.36 ± 4.38	68.17 ± 3.47	65.58 ± 3.03
18:2-18:2-18:2	4.47 ± 0.33	4.69 ± 0.63	5.78 ± 0.35
18:2-18:2-18:2-22:6	3.53 ± 0.70	3.80 ± 0.47	3.82 ± 0.62
18:2-18:2-18:2-20:3	2.91 ± 0.08	2.98 ± 0.14	2.96 ± 0.15
18:2-18:2-18:2-20:4	2.30 ± 0.27	3.12 ± 0.22	3.05 ± 0.22
18:2-18:2-18:2-22:5 **18:1-18:2-18:2-22:6**	1.63 ± 0.26	2.05 ± 0.20	1.99 ± 0.19
18:2-18:2-18:2-20:2	1.40 ± 0.13	1.56 ± 0.07	1.49 ± 0.10
18:2-18:3-18:2-18:2	1.23 ± 0.06	1.03 ± 0.07	1.06 ± 0.06
18:2-18:2-18:2-16:1	1.17± 0.10	1.53 ± 0.05	1.28 ± 0.03
18:1-18:2-18:2-20:2	0.37 ± 0.04	0.40 ± 0.03	0.38 ± 0.04
18:1-18:2-18:2-22:5 **18:1-18:1-18:2-22:6**	0.35 ± 0.06	0.51 ± 0.05	0.49 ± 0.04
14:0-16:1-16:1-16:1	0.29 ± 0.04	0.24 ± 0.06	0.07 ± 0.03
18:2-18:2-18:2-16:0	0.29 ± 0.02	0.36 ± 0.03	0.32 ± 0.03
18:2-18:1-18:1-16:1 **18:2-18:2-18:1-16:0**	0.17 ± 0.03	0.24 ± 0.03	0.21 ± 0.03
18:2-18:2-16:1-16:1	0.16 ± 0.01	0.22 ± 0.01	0.19 ± 0.01
18:2-18:2-18:1	0.15 ± 0.04	0.22 ± 0.05	0.26 ± 0.03
16:1-18:1-18:1-18:1	0.12 ± 0.03	0.21 ± 0.03	0.17 ± 0.03
18:2-18:3-18:2-20:4 **18:2-18:2-16:1-22:6**	0.07 ± 0.02	0.10 ± 0.01	0.10 ± 0.02
18:2-18:2-20:3 **18:2-18:1-20:4**	0.07 ± 0.01	0.11 ± 0.02	0.14 ± 0.01
18:2-18:3-18:2-16:1	0.03 ± 0.01	0.04 ± 0.01	0.04 ± 0.01

Table 1: Myocardial cardiolipin levels after ischemia-reperfusion, expressed as a percentage of total cardiolipin per sample (data are the top 25 most prevalent cardiolipin isoforms from mass spectrometry studies).

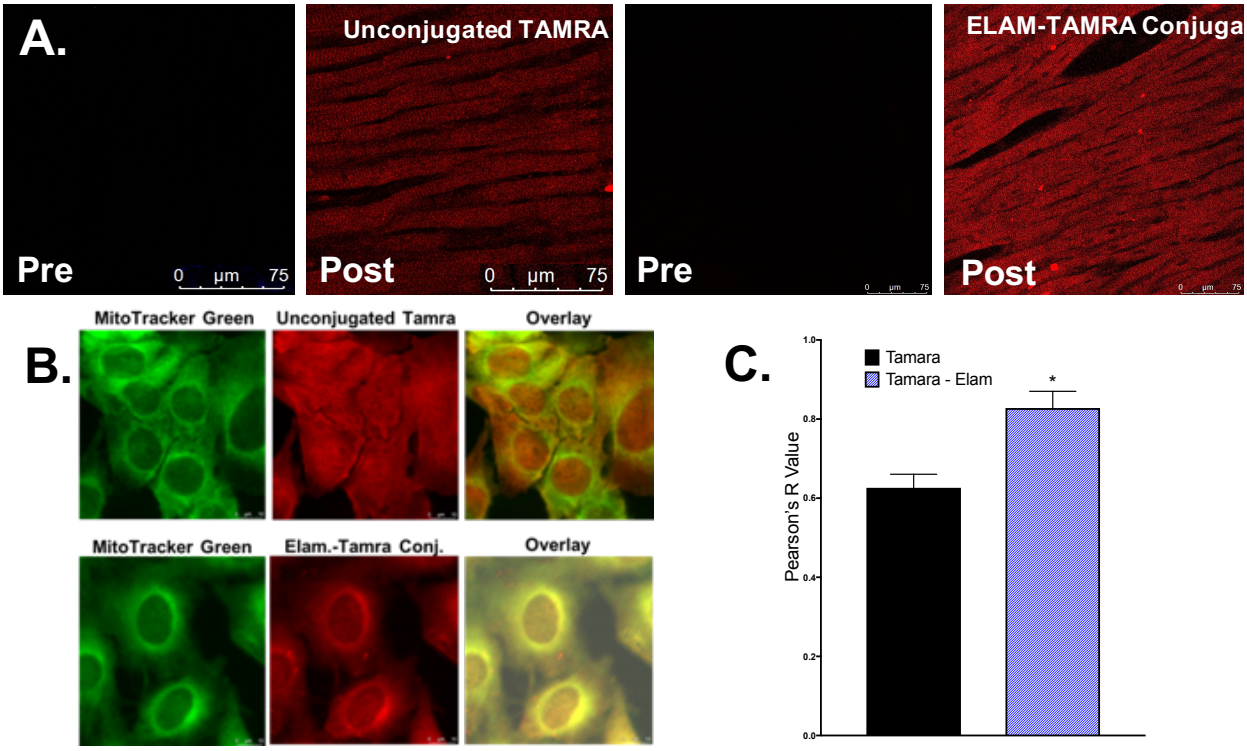

Supplemental Figure 1. Elamipretide localizes to mitochondria. (A) multiphoton images from the pre and post perfused, intact heart with unconjugated TAMRA and the TAMRA-elamipretide conjugate. (B) Confocal images of C2C12 mouse myoblasts showing the TAMRA-elamipretide conjugate localizes specifically to mitochondria whereas unconjugated TAMRA does not. (C) Pearson's correlation analysis of co-localization with mitotracker green (from panel B).

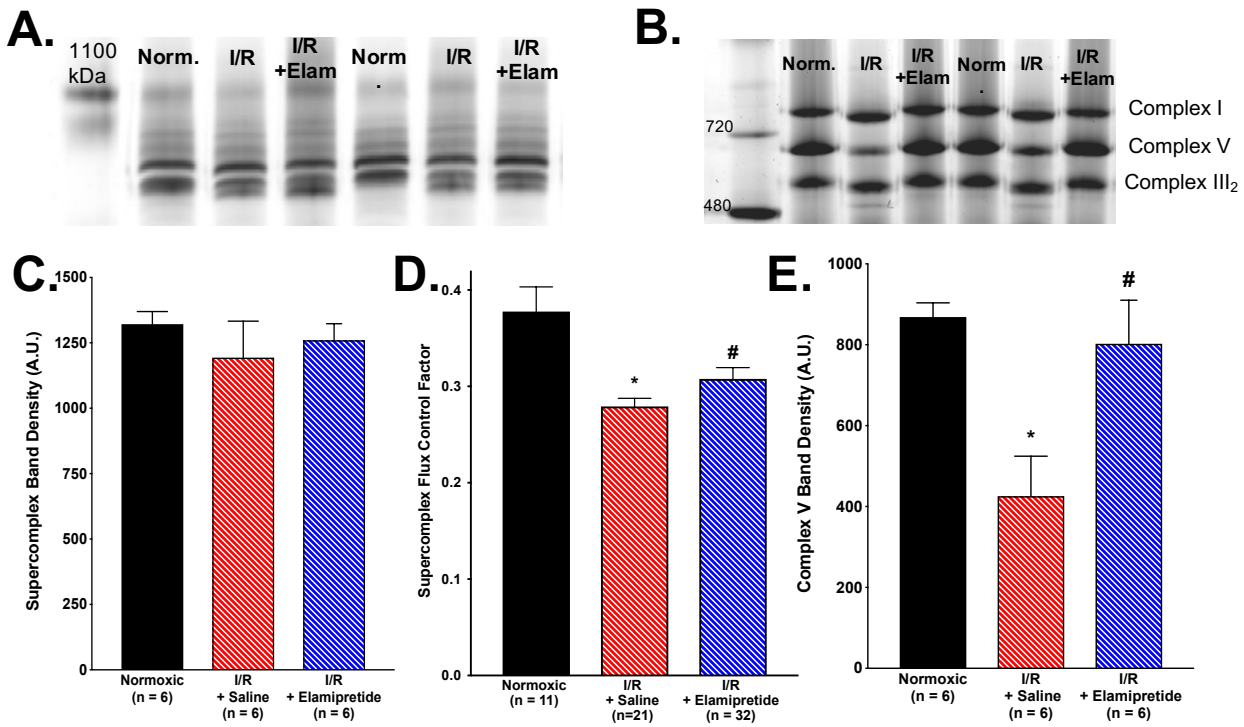

Supplemental Figure 2: Effect of I/R and Elamipretide treatment on respiratory supercomplexes from BN-PAGE studies. Representative super complex blots (A) and blots from complexes I, III, and V (B). There were no statistically significant differences across groups in super complex density (C) while we observed I/R-induced decrements in super complex flux control factor (D) and complex V density (E) that were both alleviated with Elamipretide treatment.

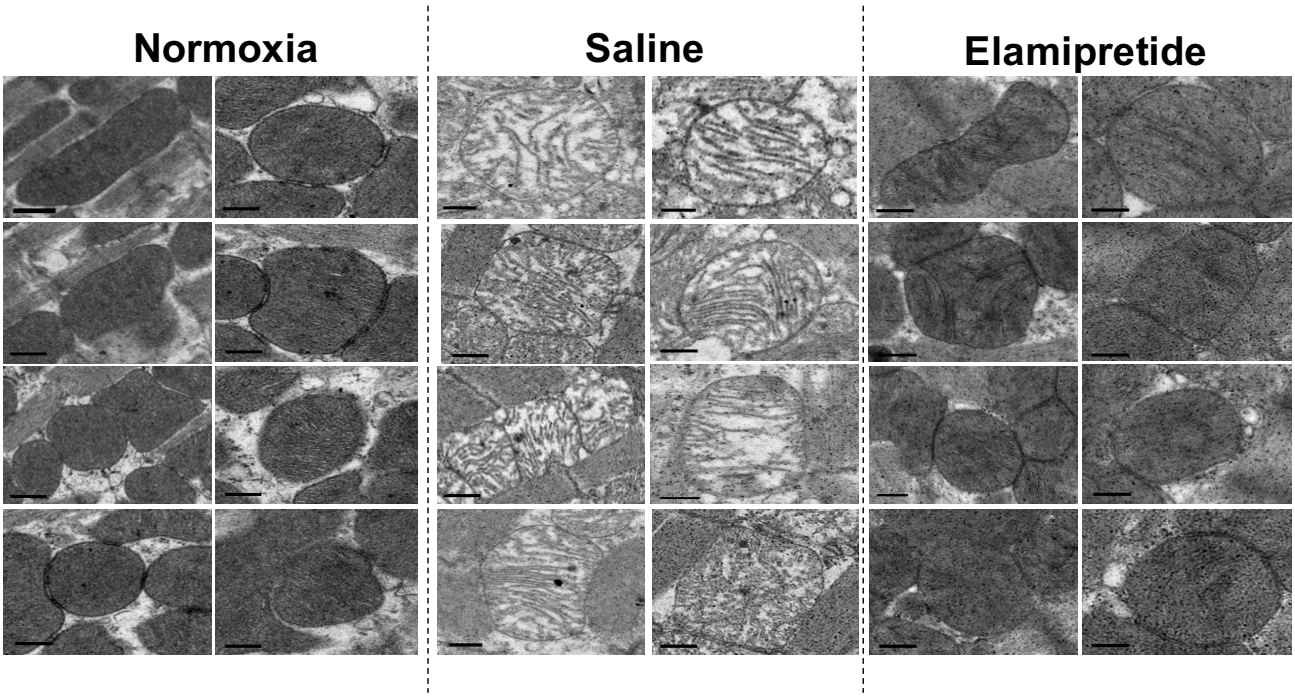

Supplemental Figure 3. TEM images of mitochondria from normoxic (A), I/R + saline (B), and I/R + Elamipretide hearts. Scale bars represent 500nm.

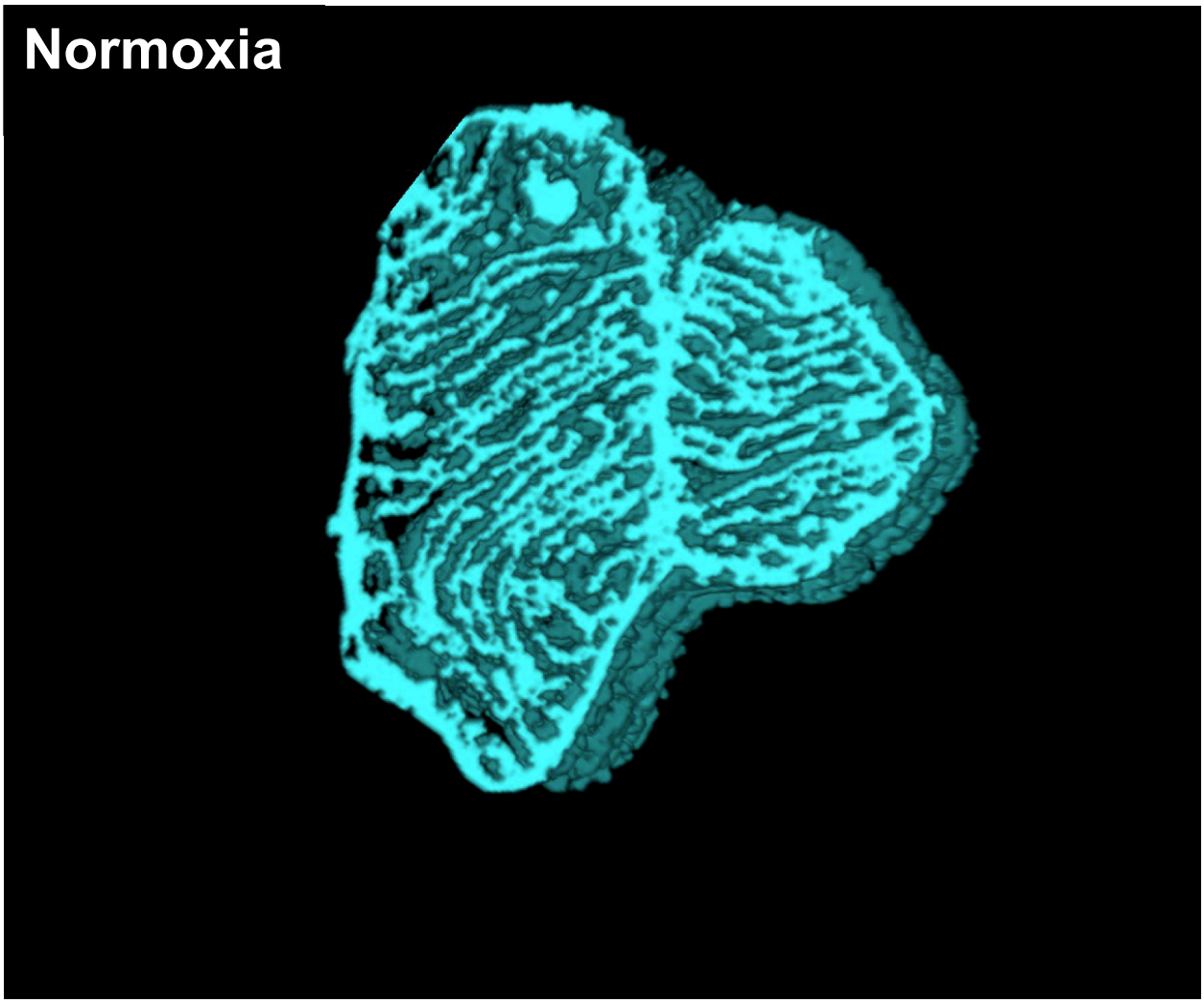

Supplemental Figure 4. Representative SBF-SEM movie of mitochondria from normoxic hearts.

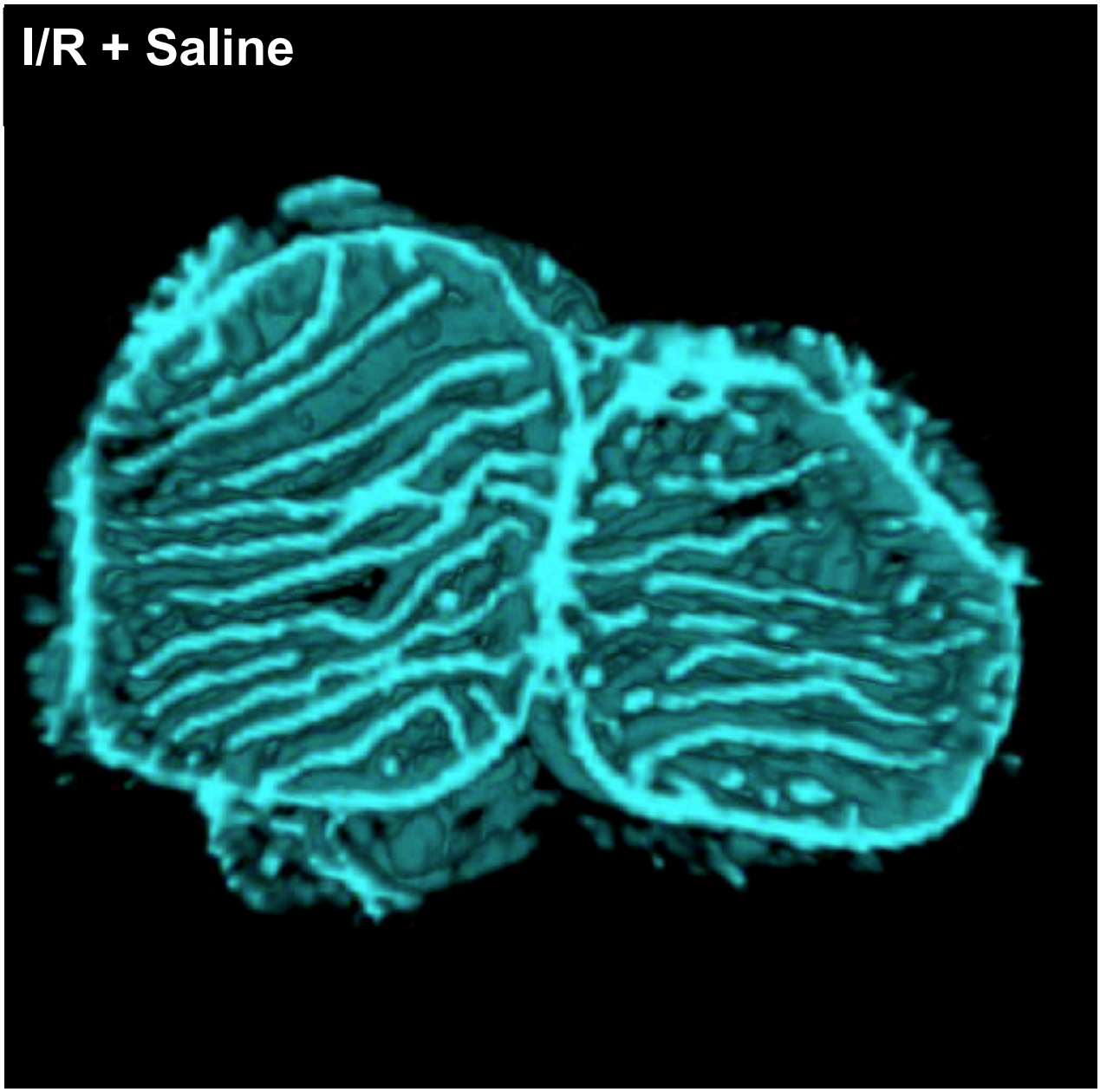

Supplemental Figure 5. Representative SBF-SEM movie of mitochondria from I/R + saline hearts.

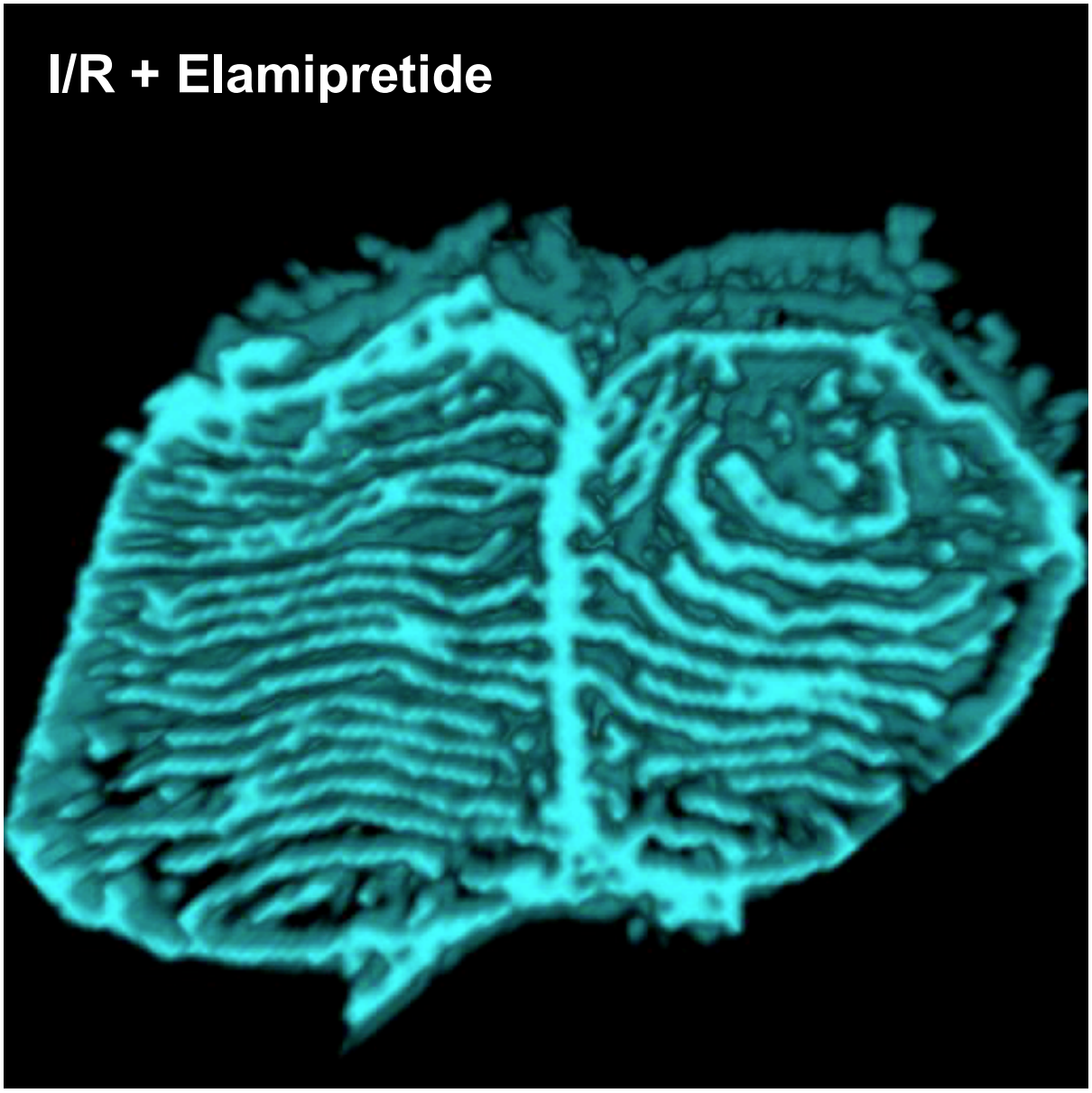

Supplemental Figure 6. Representative SBF-SEM movie of mitochondria from I/R + saline hearts.

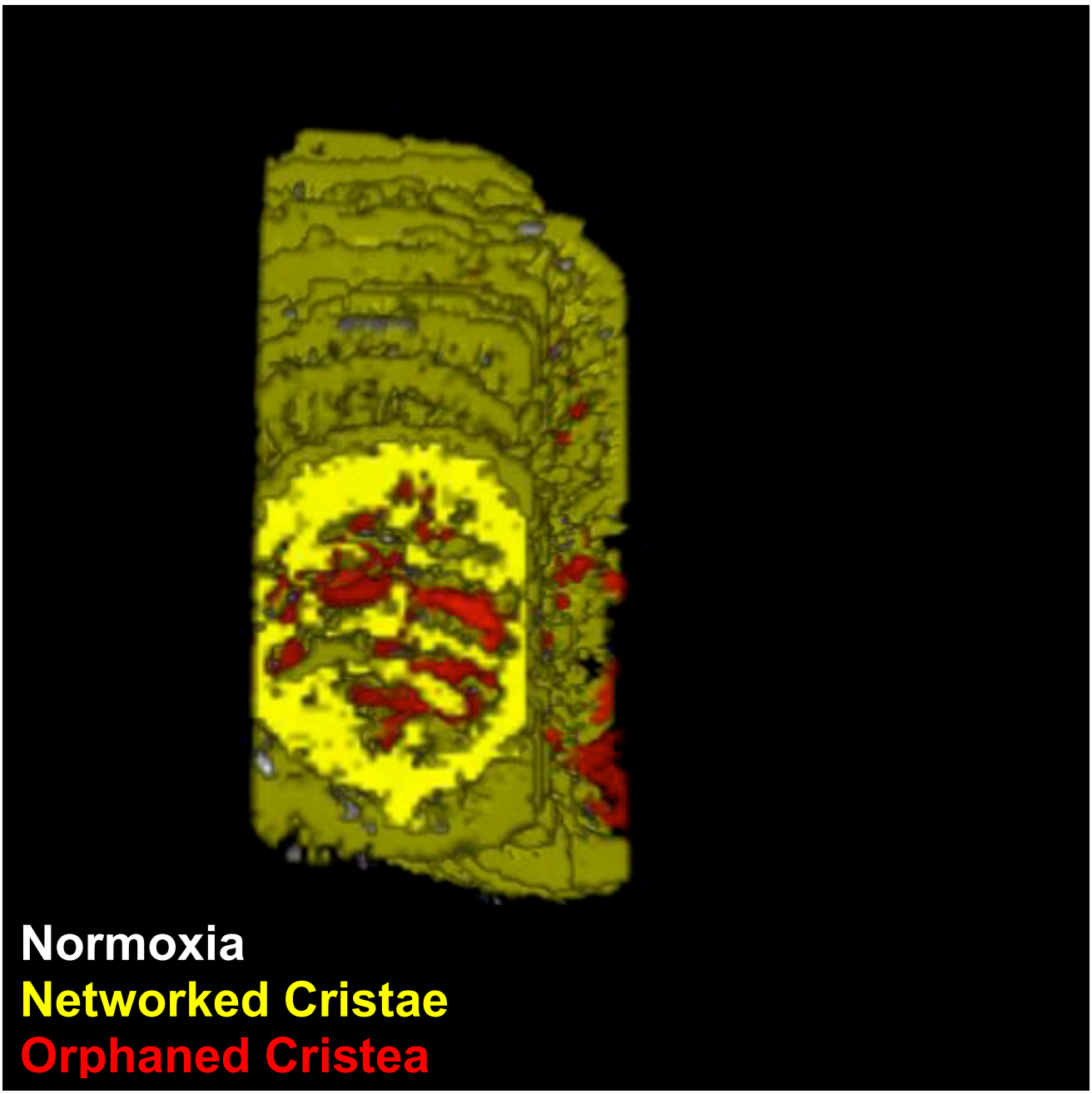

Supplemental Figure 7. Representative SBF-SEM movie of cristae networking within one cross-sectioned normoxic mitochondrion. Yellow cristae are networked while red cristae are orphaned.

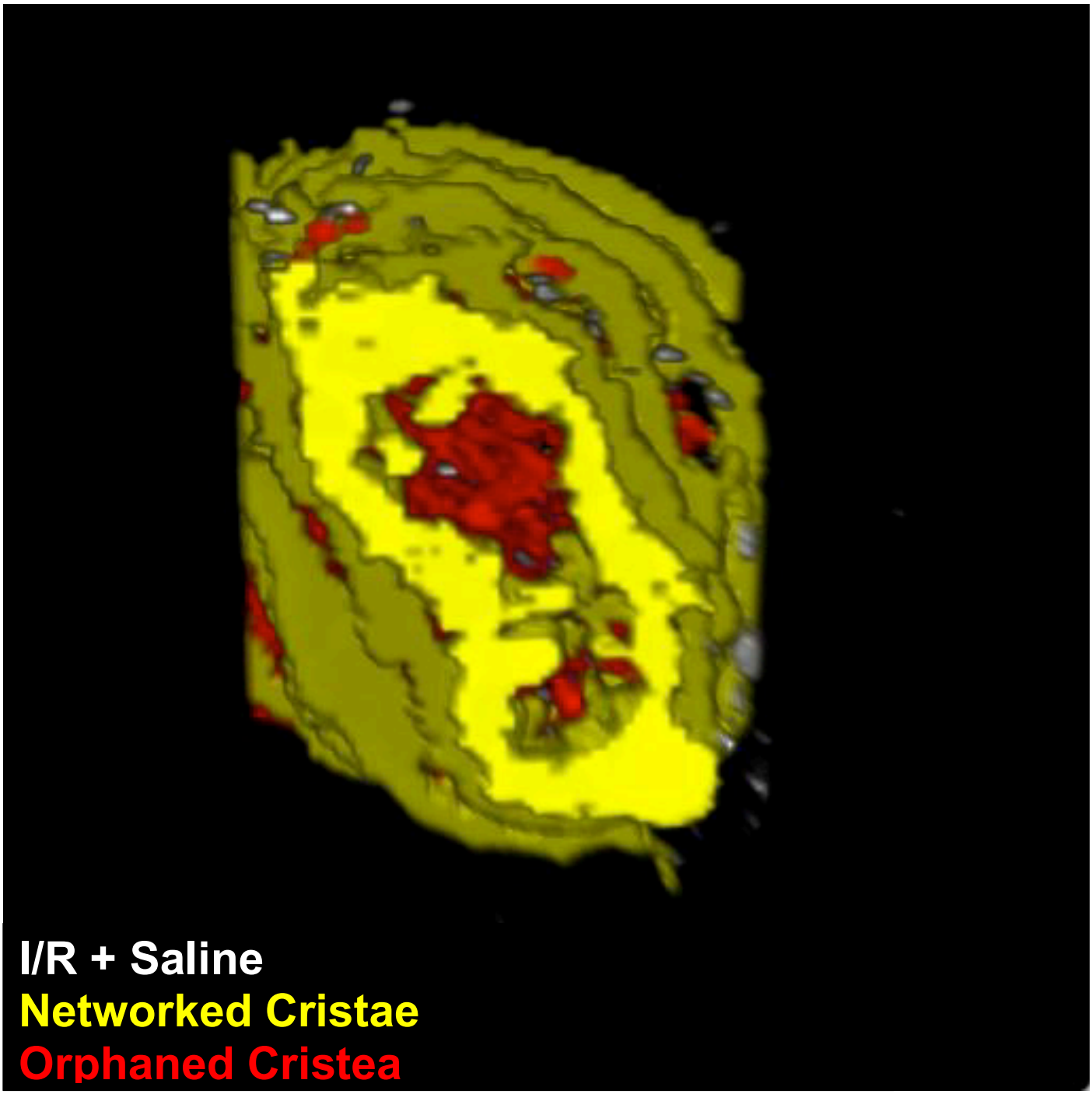

Supplemental Figure 9. Representative SBF-SEM movie of cristae networking within one cross-sectioned I/R + saline mitochondrion. Yellow cristae are networked while red cristae are orphaned.

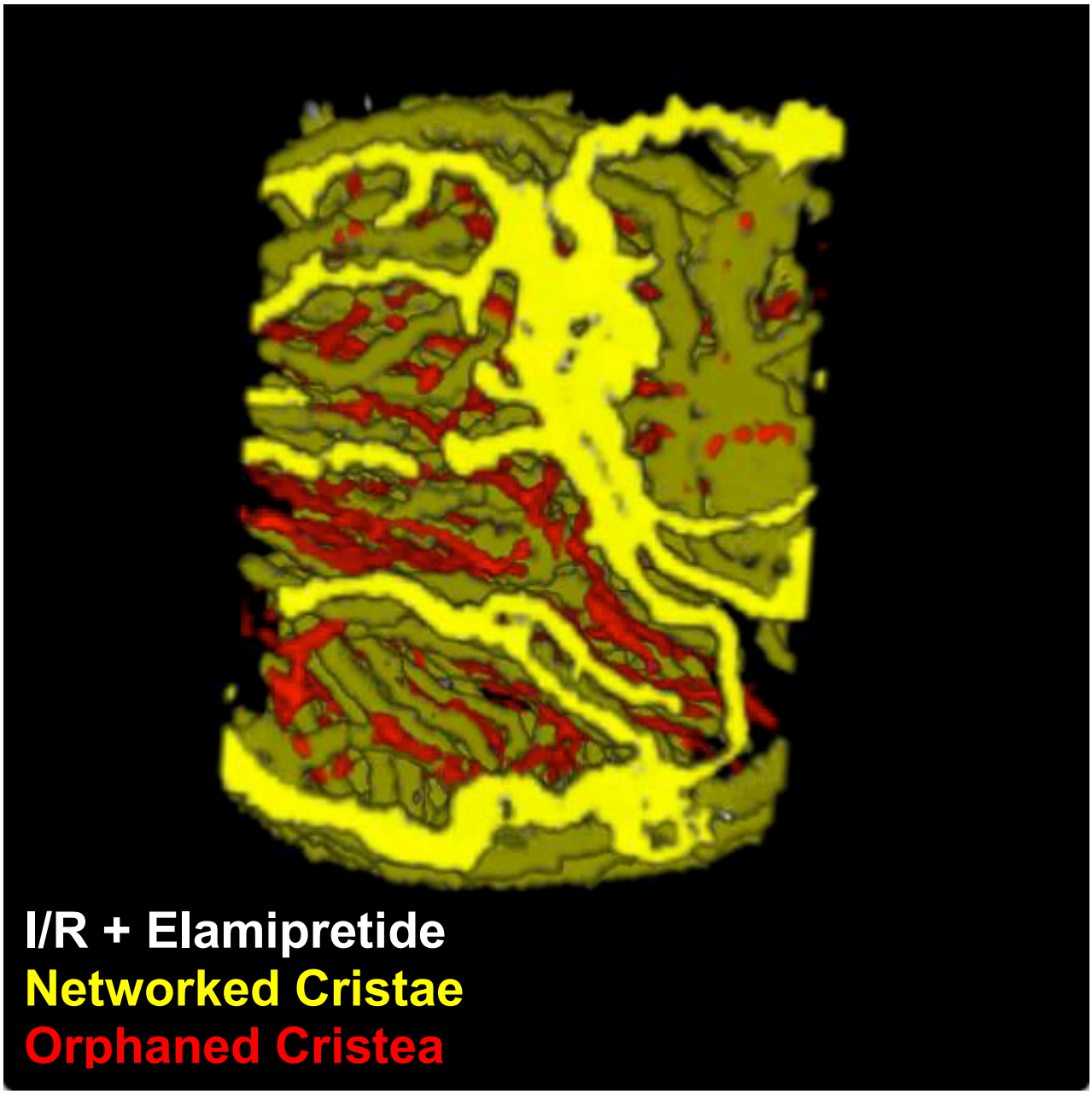

Supplemental Figure 9. Representative SBF-SEM movie of cristae networking within one cross-sectioned I/R + saline mitochondrion. Yellow cristae are networked while red cristae are orphaned.

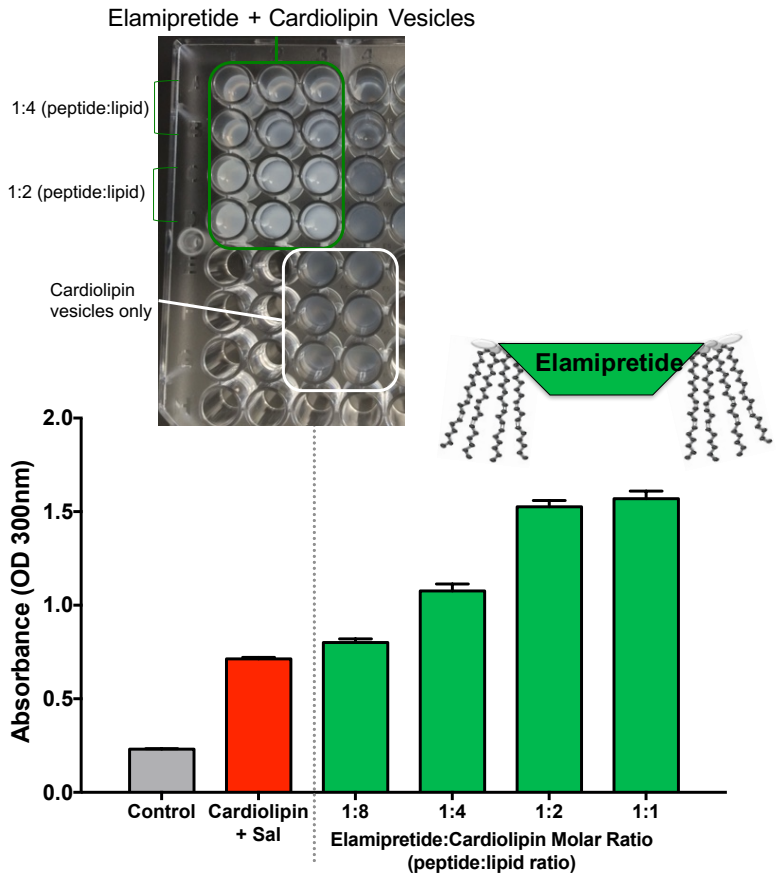

Supplemental Figure 10: Elamipretide aggregates cardiolipin-containing lipid vesicles. Elamipretide was added to cardiolipin vesicles at the indicated peptide:lipid ratios. We observed lipids "crash" out of solution with elamipretide treatment and subsequently measured the absorbance of each well. Maximal absorbance was measured at a 1 peptide to 2 lipid ratio.

Chapter 4

A novel peptide protects mitochondrial structure-function: Implications for cationic, lipophilic peptides as endogenous assembly factor mimetics

Mitchell E. Allen[1], Edward Ross Pennington[2], Aloka B. Bandara[1], Alexander H. Thomson[1], Justin B. Perry[1], Tom Green[3], Terence Ryan[4], Webster L. Santos[5,6], Joe McClung[3], Saame Raza Shaikh[2], and David A. Brown[1,6,7,8]

[1]Department of Human Nutrition, Foods, and Exercise, Virginia Tech, Blacksburg, VA; [2]Department of Nutrition, University of North Carolina, Chapel Hill, NC; [3]Department of Physiology, East Carolina University, Greenville NC; [4]Department of Applied Physiology and Kinesiology, University of Florida; [5]Department of Chemistry, Virginia Tech, Blacksburg VA; [6]Virginia Tech Center for Drug Discovery, [7]Virginia Tech Faculty of Health Sciences, and [8]Virginia Tech Metabolic Phenotyping Core Virginia Tech, Blacksburg VA.

Corresponding Author
David A. Brown, Ph.D.
Virginia Tech Corporate Research Center
1981 Kraft Drive
1035 Integrated Life Sciences Building
Blacksburg, VA 24060
540-231-8146 (phone)
brownda@vt.edu

Abstract

Mitochondrial structure and function are inextricably linked, with decrements in structure-function noted across diseases. Alternating cationic, lipophilic motifs are known to stabilize mitochondrial protein assembly, and are a shared feature of many mitochondria-targeted peptides. In this study, we determined if a new peptide, RYKF, restored mitochondrial structure-function in pathological mitochondria. We then complemented these studies with biomimetic mitochondrial membrane models to test RYKF-cardiolipin interactions. Vectors and adenoviruses inducing RYKF expression were utilized in C2C12 myoblasts and peptide expression was confirmed with a GFP reporter. Vector-mediated RYKF expression significantly improved maximal mitochondrial respiration after a metabolic stressor while Adeno-RYKF trended to improve function. In contrast, exogenous RYKF peptide treatment did not protect maximal respiration from peroxide injury. Transmission electron microscopy was employed to study isolated mitochondria from rat left ventricle treated with RYKF after a freeze thaw injury. Decrements in cristae complexity and mitochondrial networks were observed with injury, and RYKF pre-treatment significantly improved these morphological deficits. Synthetic lipid membranes were constructed to model healthy and diseased inner mitochondrial membranes and test for RYKF-cardiolipin interactions. Confocal imaging of lipid membranes suggested RYKF aggregates cardiolipin. In diseased membranes containing 25% less cardiolipin, RYKF restored the biophysical integrity of the membranes toward the healthy control. These data suggest RYKF may be aggregating CL-containing membranes, and in turn, mimicking an endogenous mitochondrial assembly factor that stabilizes cristae ultrastructure and bioenergetic function. Mitochondria-targeted peptides represent a promising therapeutic approach to treat diseases characterized by mitochondrial dysmorphology.

Introduction

In the early 1940s, Dr. Albert Claude concluded "the mechanism by which molecular oxygen is utilized […] in the cell can be ascribed in large measure, if not entirely, to a definite morphological entity" [1]. This proclamation was ahead of its time as Dr. Claude was among the first scientists to hypothesize mitochondrial form and function were interrelated. A decade later, the advent of high resolution electron microscopy enabled investigators to study the basic morphology of mitochondria for the first time [2]. Today, advances in imaging technologies permit detailed insight into mitochondrial structure-function and how their interdependent relationship contributes to health and disease.

Mitochondria are double membraned organelles composed of a limiting outer membrane (OM) and protein-rich inner membrane (IM). The IM is characterized by the presence of cardiolipin (CL), a unique phospholipid exclusively found within the IM. Specifically, CL is located in the inner leaflet where it imparts negative membrane curvature and drives protein-protein interactions [3, 4]. Accordingly, CL physically interacts with protein complexes at the curves of the IM. CL is also essential for the formation and maintenance of cristae, the invaginations of the IM [5]. Cristae house the electron transport chain (ETC), an assembly of CL-dependent protein complexes that drive ATP production [6]. Cristae are dynamic structures that switch from a contracted, "orthodox" shape to an expanded, "condensed" morphology upon activation of the ETC [7, 8]. To this end, Cogliati et al. described cristae as "dynamic biochemical reactors" that reorganize their structure according to the energetic needs of the cell [9]. The loss of CL is concomitant with cristae dysmorphology and these structural decrements have been noted across pathologies [10]. In pre-clinical models, exogenous CL perfusion protects against diseases characterized by CL loss [11]. However, the clinical translation of this therapy is unknown. To

date, there are no FDA-approved therapeutics to treat diseases characterized by CL loss and the concomitant decrements in cristae ultrastructure.

Conserved LYR tripeptide sequences plus a highly conserved, downstream phenylalanine motif (LYR + F) have been identified in a superfamily of eukaryotic proteins [12]. These endogenously expressed, conserved peptide sequences and their larger proteins are known to interact with mitochondrial scaffolding proteins and aid in respiratory complex assembly [13] [14]. Similarly, elamipretide is a tetrapeptide in clinical trials for mitochondrial diseases, and consists of D-arginine-dimethyltyrosine-lysine-phenylalanine [(D)R-Dmt-K-F)]. We previously reported elamipretide improves mitochondrial structure-function by aggregating the mitochondrial-specific lipid cardiolipin. In this study we tested the hypothesis that a novel peptide sequence, RYKF, may show similarity to the endogenously expressed, conserved LYR + F motifs that stabilize mitochondrial protein assembly. In this study, we utilized RYKF to test the hypothesis that non-natural cationic, lipophilic peptides mimic endogenous mitochondrial assembly factors and preserve bioenergetic structure-function during disease.

Methods

Animals. Male Sprague-Dawley rats (aged 2-3 months) were used in this study. All animal procedures were approved by the Institutional Animal Care and Use Committees at Virginia Tech. The animals were housed in a temperature and light-controlled environment and received food and water ad libitum. Prior to excision of the heart, animals received an i.p. injection of ketamine/xylazine (90mg/kg/10mg/kg, respectively). Hearts were excised (after the diminution of animal reflexes) via midline thoracotomy and placed in ice-cold saline.

R-Y-K-F Synthesis. Synthesis of the RYKF peptide was achieved by solid phase peptide synthesis using N-α-Fmoc protected L-amino acids (Novabiochem) (3 equiv), Pyoxim (Peptides International) (3 equiv) in DMF as coupling reagent, and DIEA (Aldrich) (6 equiv) on Rink amide MBHA resin (100–200 mesh) (Novabiochem) with 0.52 mmol/g loading. The Fmoc group was deprotected with 20% piperidine in DMF. The solid phase synthesis was performed on a vacuum manifold (Qiagen) outfitted with 3-way Luer lock stopcocks (Sigma) in either Poly-Prep columns or Econo-Pac polypropylene columns (Bio-Rad). The resin was mixed in solution by bubbling nitrogen during all coupling and washing steps. The acetyl-capped peptide was prepared by deprotecting the Fmoc group with 20% piperidine in DMF followed by washing the resin (3x DMF, 3x DCM). A 1:1 acetic anhydride:piperidine mixture was added to the resin and bubbled for 5 minutes. The resin was then washed (3x DMF, 3x DCM, 3x DMF, 3x DCM). Finally, the resin was treated with 85:5:5:5 TFA (trifluoroacetic acid, Acros)/H2O/TIS (triisopropylsilane, Acros)/EDT (ethanedithiol, Sigma-Aldrich) (v/v/v/v) for 4 h. The supernatant was dried under reduced pressure, and the crude peptide was triturated from cold diethyl ether. The peptides were

purified using a Jupiter 4 lm Proteo 90 Å semiprep column (Phenomenex) using a solvent gradient composed of 0.1% TFA in Milli-Q water and HPLC grade acetonitrile. The identity of the peptide was determined by LC/MS Peptide purity was determined using a Jupiter 4 lm Proteo 90 Å analytical column (Phenomenex). HPLC Solvent A: 0.1% TFA in Milli-Q water, Solvent B: HPLC grade acetonitrile. Expected m/z of H-RYKF-NH2, 612.3616, observed m/z, 612.3641. Expected m/z of Ac-RYKF-NH2, 654.3722, observed m/z, 654.3713.

Cell lines and culture conditions. Mus musculus myoblast cell line C2C12 (American Tissue Culture Collection, Manassas, VA) was used for expressing the peptide RYKF. Media and reagents for growing and maintaining cells were purchased from Life Technologies Corporation (Carlsbad, CA). The cells were maintained in Dulbecco's modification of Eagle medium (DMEM) supplemented with 10% (by volume) fetal bovine serum and 1% penicillin-streptomycin. Cells were sustained in a humidified incubator at 37ºC and 5% CO_2. A 0.25% trypsin-EDTA solution was used for detachment of cells.

Escherichia coli strain DH5α chemically Competent cells (Life Technologies Corporation) were used for constructing the recombinant expression plasmids. Bacteria carrying the plasmids were maintained in Luria Bertani (LB; Sigma-Aldrich, St. Louis, MO) agar or broth, and sustained in a humidified incubator at 37ºC and 5% CO_2.

Construction of the recombinant vector to express RYKF peptide. The IgKzsGreen1 furin cleavage/RYKF peptide sequence was PCR amplified and cloned at EcoRI/HindIII site of the plasmid pCMV5-MCS (Addgene, Watertown, MA). The resulting recombinant plasmid was

designated as pCMV5::RYKF and harvested from E. coli DH5α grown at 100 µg/ml ampicillin (Sigma-Aldrich). The vector pCMV5-MCS without the peptide sequence was also harvested using the same procedure and used as a control in the assays described below.

Construction of the recombinant vector to express RYKF peptide with the aid of a mitochondrial targeting sequence. The RYKF sequence together with a mitochondria targeting sequence (MTS) was cloned into the plasmid vector pCMV5 maxi (Addgene) to produce the recombinant vector (designated) CMV5-6a2MTS::RYKF. This plasmid did not possess a gene to express green fluorescence but was expected to express RYKF peptide. A control plasmid constructed by cloning the MTS region together with a green fluorescence gene but without an RYKF sequence was designated CMV5-6a2MTS:2sGreen. This second plasmid was expected to produce fluorescence but with no expression of RYKF

Transfection of C2C12 cells with the recombinant plasmids. Two different transfection reagents were used separately to facilitate the transfection, i.e., Lipofectamine 2000 (Life Technologies Corporation, and Xfect (Takara Bio USA, Inc., Mountain View, CA). Approximately 1 million C2C12 cells/well incubated overnight in growth medium in 6-well plates were transfected with 2 or 5 µg of DNA of pCMV5::RYKF, pCMV5-MCS, CMV5-6a2MTS::RYKF, or CMV5-6a2MTS:2sGreen using the procedures provided by the manufacturers. The transfection procedure using Xfect reagent was briefly as follows. Two to five µg of plasmid DNA was added into 100 µl final volume of Xfect Reaction Buffer; 1.5 µl of Xfect polymer was added to the DNA-buffer mixture; mixture was incubated at room temperature for 10 min; DNA-buffer-polymer mixture was added into the wells containing 1 ml of complete growth medium; and after 4 h of incubation at standard culture conditions, the medium was replaced with fresh medium. Transfection using

Lipofectamine 2000 was briefly as follows. Two µg of plasmid DNA were diluted in 0.5 ml of growth medium without serum and mixed; 10 µl of Lipofectamine 2000 was diluted in 0.5 ml of growth medium without serum; two of the above components were combined and the mixture was incubated at room temperature for 20 min; cell monolayers grown overnight were washed with 1ml of pre-warmed growth medium without serum; the cell monolayer was overlaid with the diluted DNA-lipofectamine mixture and incubated for 5 h; and 1 ml of growth medium containing twice the concentration of serum without removing the transfection mixture was added. Under both transfection procedures, after 48 to 72 hours of incubation, cells were harvested and viewed by confocal microscopy.

Construction of adenovirus stains carrying RYKF peptide. Adenovirus Expression System 3 (Takara Bio USA, Inc.) was used as the carrier. The pAd-X PRLS promoterless vector was used as the backbone plasmid. CMV-GOI-hgHterminator cassette was cloned into pAd-X PRLS vector via IN-Fusion cloning. The adenovirus strain manipulated to carry the IgKzsGreen1 furin cleavage/RYKF peptide cartridge was designated as Adeno::RYKF. The control adenovirus strain expressing only the green fluorescent protein (GFP) was designated as Adeno::GFP.

Transduction of C2C12 cells with Adenovirus stains carrying RYKF peptide. C2C12 cells were plated on 6-well plates approximately $4x10^5$ cells/well in 1 ml medium and incubated overnight. Cells were subsequently transduced with Adeno::RYKF or Adeno::GFP strains at 1:100 cell:adenovierus ratio using reagents and a procedure provided by ibidi GmbH (ibidi USA, Inc., Madison, WI). Briefly, adenoviruses were thawed on ice; 2.7 µl of ibiBoost™ Adenovirus Transduction Enhancer was mixed with 0.5 ml of culture medium; appropriate volumes of adenoviral particles were added into the solution and mixed by flicking the tube; solution was

incubated for 30 minutes with shaking at 400 rpm at room temperature; culture medium was removed from the cells and the pre-incubated adenovirus/ibiBoostTM mixture was added; after 4 h of incubation at standard culture conditions, adenovirus/ibiBoostTM mixture was replaced with 1 ml of fresh medium. After 48 to 72 hours of incubation, cells were harvested and viewed by confocal microscopy. The transfection reagent polybrene (Sigma-Aldrich) was used at 5 μg/ml in culture medium during transfection. To assess the effect of ibiBoost^{TM} Adenovirus Transduction Enhancer, experimental groups with or without this reagent were used.

Examination of fluorescence production by using confocal microscopy. Approximately 50,000 cells were plated on MatTek glass cover slips (MatTek Corporation, Ashland, MA) and incubated overnight at 37°C and 5% CO_2. Fluorescence signals were analyzed by recording stained 63x images using a confocal laser scanning microscope.

Cellular Respiration: Exogenous RYKF Treatment. Oxygen consumption rate (OCR) was measured in XF96 and XFe96 Seahorse Extracellular Flux Analyzers (Agilent Technologies, Santa Clara, California, USA) according to our previously published methods [15]. Briefly, C2C12 cells were seeded in Seahorse microplates at 1.5 x 100 cells per well. Cells were incubated overnight (37°C, 5% CO_2) to adhere. After incubation, cells were treated with saline or 100nM-10uM RYKF for 3 hours at 37°C, 5% CO_2. Following pre-treatment, 500uM H_2O_2 was added to the wells to injure the cells for 4 hours. The media was then removed and 180uL of Seahorse XF Media (XF Base Medium, 10mM pyruvate, 10mM glucose, 2mM glutamax, pH 7.4, 37°C) was added to each well. The microplate was then placed into the Seahorse Extracellular Flux Analyzer and a mitochondrial stress test was completed. After baseline measurements, sequential injections of

oligomycin (1ug/mL), FCCP (2uM), and antimycin A (2uM) were added to assess the bioenergetic status of the cells. Statistical analyses were then performed by normalizing the data to antimycin A respiratory values.

Mitochondrial studies. For mitochondrial morphology studies, mitochondria were isolated from the left ventricles of Sprague Dawley- male rats according to our previously published methods [16]. Mitochondria were processed for imaging and treatment according to methods described in [17]. Briefly, mitochondria were diluted to 0.5mg/mL in PBS and incubated for 20 minutes at room temperature with saline or 10uM RYKF. Following incubation, mitochondria were subjected to 3 cycles of a 1-minute freeze (dry ice with 70% ethanol), 1 minute thaw (55°C) injury. Mitochondria were then pelleted using a centrifuge at 12,000g for 10 minutes at 4°C. The pellet was subsequently fixed with 1% glutaraldehyde in PBS for 90 minutes at room temperature, washed with PBS, and fixed in 1% osmium tetroxide for 2 hours at 4°C. After fixation, the pellets were dehydrated with graded ethanol and infiltrated with propylene oxide and resin. The pellets were cured in the resin for 48 hours at 60°C. The blocks were thinly sectioned to 60nm and adhered to nickel grids for 30minutes at 60°C to prepare for imaging. Following sectioning, the grids were rinsed in water and stained with 2% uranyl acetate for 5 minutes.

Transmission Electron Microscopy. Mitochondrial pellets from rat left ventricle (see above for isolation protocol) were imaged using transmission electron microscopy (Virginia Tech Morphology Service Core Laboratory, Virginia-Maryland College of Veterinary Medicine). Samples were imaged according to our previously published methods (Described in chapter 3). Briefly, samples were imaged at a magnification of 25,000X and resolution of

0.0022um x 0.0022um. The images were processed in the Gatan Inc. Software and stored on a personal storage device. Mitochondrial complexity index and intramitochondrial networking were calculated from the images as described below.

Mitochondrial Complexity Index. Transmission electron micrographs of isolated mitochondria were used to calculate the mitochondrial complexity index using previously published methods [18]. Briefly, lines were drawn through the major (longest length) and minor (width) axes of the mitochondria. The number of times cristae intersected the axes were counted to calculate the cristae complexity.

Mitochondrial Networking. Transmission electron micrographs of isolated mitochondria were used to calculate mitochondrial networking. All networking calculations were completed according to our previously defined methods (described in chapter 3). Briefly, the yellow flood-fill macro (Image J) was used to highlight the networked cristae. A single flood-fill click on the most bottom left cristae was performed to initiate the connectivity within mitochondria. The yellow highlighted cristae were thresholded and converted to white. The mean grey value was then calculated. The percent connectivity was measured by dividing the thresholded mean grey value (networked cristae) by the total mean grey value (total mitochondrial grey value prior to flood fill macro use).

Construction of biomimetic giant unilamellar vesicles. Biomimetic giant unilamellar vesicles (GUVs) were constructed via electroformation as previously described [19], and contained 39.9 mol% 18:0-22:6 PC, 30.0 mol% 16:0-20:4 PE, 20 mol% $(18:2)_4$CL, 5 mol% $(18:1)_2$PI, 3 mol% $(18:1)_2$PS, 2 mol% cholesterol, and 0.1 mol% nonyl acridine orange (NAO). Briefly, 10 μg of total

lipid was spread onto the conductive side of an indium tin oxide coated glass slide. The lipid-coated slide was subjected to dark vacuum for 1 hr to remove excess solvent. Electroformation occurred at room temperature using a buffer containing 10 mM HEPES (pH 7.4) and 250 mM sucrose. Upon completion, samples were prepared for microscopy as previously described [19]. For select experiments in which the CL concentration was altered, the total CL concentration was decreased 25-50% by mass. For experiments involving the addition of peptide, a final concentration of 20 uM peptide was added to the vesicles immediately prior to imaging.

Construction of biomimetic lipid monolayers. All phospholipids were handled with extreme care to prevent oxidation under low light conditions and a gentle stream of nitrogen gas. Fresh lipid stocks in chloroform (HPLC grade, Fisher Scientific) were used for all studies. Initially, biomimetic mitochondrial lipid monolayers were generated by co-dissolving lipids (40 mol% 18:0-22:6 PC, 30.0 mol% 16:0-20:4 PE, 20 mol% $(18:2)_4$CL, 5 mol% $(18:1)_2$PI, 3 mol% $(18:1)_2$PS, 2 mol% cholesterol) in chloroform (10 μg/μL). The trough was washed three times with 70% ethanol, Milli-Q water, and subphase prior to collecting surface pressure-area isotherms. Lipid monolayers were constructed by spotting 10 μg of lipid on a subphase of 10 mM sodium phosphate buffer (pH 7.4). For select experiments in which CL's concentration was altered, the total CL concentration was decreased 25-50% by mass. For experiments involving the addition of peptide, a final concentration of 1 uM peptide was injected underneath the subphase immediately after spotting lipid. Pressure-area isotherms were generated using a Mini Langmuir-Blodgett Trough (KSV NIMA, Biolin Scientific, Paramus, NJ) as previously demonstrated [20]. Secondary analysis of raw surface pressure-are isotherms were performed at a physiological surface pressure of 30 mN/m as previously shown [20].

Statistical Analysis. Data are reported at mean ± SEM. Comparisons between treatment groups were first analyzed by one-way ANOVA. If statistical differences were detected, values between 2 groups were compared with student's t-test. Statistical significance was established at $p < 0.05$.

Results

RYKF is expressed in recombinant cell lines. We constructed RYKF-encoding plasmids tagged with green fluorescent protein (GFP) to confirm RYKF cellular expression and stability. Green fluorescence was observed in recombinant C2C12 cells transfected with the plasmid pCMV5::RYKF. Approximately 90% of cells transfected with 2 μg of the pCMV5::RYKF plasmid using Xfect reagent produced fluorescence (Figure 1). Significantly less fluorescence was observed in transfections performed using the reagent Lipofectamine 2000 (data not shown). Importantly, cells transfected with the control pCMV-MCS plasmid DNA did not fluoresce (Figure 1A). Similarly, we transduced C2C12 cells with adenovirus constructs to confirm RYKF cellular uptake and stability. We observed that cells transduced with Adeno::GFP and Adeno:RYKF fluoresce green, whereas cells not transduced with an adenovirus did not fluoresce (data not shown). These studies confirm RYKF was delivered to and expressed in our cultured cells.

Exogenous RYKF treatment does not protect cellular respiration from peroxide injury. Data from cellular respiration studies are presented in Figure 2. Mitochondrial function was determined in cultured C2C12 cultured myoblasts stressed with 500uM H_2O_2. This injury significantly decreased maximal respiration by 62.5% in the vehicle (saline) control group (Figure 2A). Pre-treatment with exogenous RYKF peptide at final concentrations of 100nM, 1uM, and 10uM did not significantly protect mitochondrial respiration from the peroxide injury (Figure 2A) ($p < 0.05$).

Vector-mediated RYKF expression of RYKF protects cells from peroxide injury. Vectors containing RYKF were delivered to cultured C2C12 myoblasts to determine if endogenous expression of RYKF protected mitochondrial function. A peroxide stressor (500uM H_2O_2) significantly impaired maximal respiration by 50% (Figure 2B). This functional decrement in

mitochondrial function was significantly improved by 37% in cells treated with the RYKF vector ($p < 0.05$).

Viral expression of RYKF does not significantly protect cells from hypoxia nutrient deprivation (HND) injury. To complement our vector studies, we virally transfected cells with RYKF to determine if endogenously expressed RYKF protected mitochondrial function (Figure 2C). Hypoxia plus nutrient deprivation (HND) injury significantly decreased maximal respiration by 35%. RYKF expression enhanced maximal mitochondrial respiration by 10%, but this improvement was not statistically significant (Figure 2C). Notably, there were no differences in maximal respiration between non-injured controls and non-injured cells expressing RYKF ($p < 0.05$).

RYFK protects mitochondrial cristae complexity from freeze thaw injury. To complement our mitochondrial function studies, we devised a series of imaging experiments to determine if RYKF affected bioenergetic morphology (Figure 3). Freeze thaw injury significantly decreased the cristae complexity of isolated mitochondria by 24% (Figure 3A). When isolated mitochondria were pre-treated with 10uM RYKF prior to freeze thaw, we observed a significant 19% improvement in cristae complexity ($p < 0.05$), suggesting RYKF protects against cristae loss.

RYKF preserves intramitochondrial networking after freeze thaw injury. The maintenance of cristae morphology during disease is associated with improved mitochondrial connectivity and networking (Described in chapter 3, chapter 3). Accordingly, we examined how a freeze thaw injury affected intramitochondrial networking in isolated mitochondria. In healthy, non-injured

mitochondria, 60% of cristae were connected (Figure 3B). However, freeze thaw injury significantly impaired intramitochondrial networking in vehicle control (saline) mitochondria and led to a 39% decrease in cristae connectivity (Figure 2B). Pre-treatment with 10uM RYKF prior to freeze thaw injury significantly enhanced mitochondrial networking by 35% ($p < 0.05$).

RYKF maintains biophysical properties of mitochondrial membranes. To gain insight into how RYKF preserves cristae morphology, we synthesized biomimetic inner mitochondrial membranes to test for peptide-lipid interactions (Figure 3). Inner membrane models were composed of physiological phospholipid levels, including 20% cardiolipin content. The lipid compositions (described in methods) were consistent with those observed across mammalian mitochondria [21]. We previously observed a 25% loss of cardiolipin content after ischemia-reperfusion injury (Described in chapter 3, chapter 3). Accordingly, we modeled this loss in our biomimetic membranes and examined the effects in a Langmuir Trough to study molecular area-pressure isotherms on lipid monolayers (i.e. lipid packing). The 25% loss of cardiolipin (disease model) resulted in a significant decrease in the mean molecular area at physiological membrane pressure (30mN/m) (Figure 4B). Addition of 1uM RYKF to the disease modeled membrane completely restored the mean molecular area back to healthy levels.

We complimented these studies by synthesizing giant unilamellar lipid vesicles (GUVs) of similar composition. We utilized NAO to study cardiolipin fluorescence in the lipid vesicles (Figure 3). In the absence of protein and peptide, we observed that cardiolipin is uniformly distributed around the cross-sectional surface of the lipid vesicle. However, after the addition of RYKF, cardiolipin fluorescence clusters (Figure 4A).

Discussion

We utilized RYKF to test the hypothesis that alternating cationic, lipophilic peptides mimic endogenous mitochondrial assembly factors that preserve bioenergetic structure-function during disease. Our evidence suggests that RYKF protects mitochondrial structure-function from metabolic stress. The findings presented here are novel for several reasons. First, we demonstrate

that endogenous expression of cationic, lipophilic peptides improves mitochondrial function and this was associated with preserved cristae ultrastructure. Next, we developed a novel method to calculate the connectivity of cristae networks in isolated mitochondria. Finally, RYKF preserves the biophysical integrity of the inner membrane despite losses of CL.

Effects of RYKF on mitochondrial function. We observed that endogenous RYKF expression protected mitochondrial function (albeit modestly in viral studies) whereas exogenous RYKF treatment had no effect (Figure 2). Taken together, these data suggest exogenous RYKF is not cell permeable or is being degraded by intracellular processes prior to reaching mitochondria. Interestingly, previous data has reported mitochondria-targeting peptides are cell permeable but need a non-natural arginine (D-R) for intracellular stability [22]. Because we tested a peptide containing the natural arginine (L-R), this may explain why we did not observe protection with exogenous RYKF treatment in our cellular model. Indeed, we previously reported mitochondria-targeting peptides containing a D-arginine residue protect cellular respiration from the same peroxide stressor employed in the present study [23]. To this end, the data suggest exogenous RYKF treatment is not protected from cellular degradation mechanisms while endogenously expressed RYKF appears to be intracellularly stable as confirmed by our RYKF-GFP reporter. Although our confocal microscopy studies confirmed the presence and stability of RYKF in cells, we did not verify the peptide localized to mitochondria. The images presented in Figure 1 suggest RYKF-GFP fluorescence is peri-nuclear and consistent with mitochondria-targeted dyes, but further studies examining their overlay is are needed to confirm this hypothesis.

RYKF protects cristae ultrastructure. Because the relationship between mitochondrial structure and function is interdependent, we next employed transmission electron microscopy (TEM) to study how RYKF affects cristae morphology (Figure 3). Treatment with RYKF significantly improved injury-induced decrements in cristae complexity. These data suggest RYKF pre-treatment protected against the loss of cristae, and are consistent with previous reports that freeze thaw-induced membrane rupturing causes decrements in mitochondrial ultrastructure and cristae loss [24, 25].

As both a cause and consequence of impaired morphology, freeze thaw mitochondria are known to produce more reactive oxygen species (ROS), which subsequently causes bioenergetic dysfunction and cell death [26, 27]. These decrements in structure-function are reportedly improved by mitochondria-targeted antioxidants like Mitoquinone (MitoQ) [28]. Although we report RYKF similarly improves mitochondrial structure-function, the naturally-occurring peptide does not seem to exert protection as a ROS scavenger (Perry, unpublished). This is supported by studies reporting that mitochondria-targeted peptides without dimethyltyrosine do not scavenge ROS [29]. Additionally, we previously concluded that a putative non-natural analog of RYKF, elamipretide, does not scavenge ROS in cell-free systems while others report the peptide decreases ROS in diseased mitochondria but has no effect on healthy tissues [30-32]. Future studies employing cell free systems and mitochondria-targeted antioxidants like MitoQ as positive controls are needed to confirm this hypothesis. Instead, our findings that RYKF preserves cristae complexity in isolated mitochondria and enhances respiration supports an alternative mechanism in which endogenous peptide expression stabilizes bioenergetic structure.

We further examined cristae morphology in freeze-thaw mitochondria by analyzing mitochondrial networks (Figure 3B). Recent evidence suggests mitochondria exist in a highly

connected reticulum that rapidly conducts electrical current to distribute energy throughout cells [33]. Accordingly, mitochondrial diseases are characterized by the loss of connectivity and network fragmentation [34]. In the present study, we found that pre-treatment with RYKF significantly preserved intramitochondrial networks after freeze thaw injury. These data are consistent with other findings reporting that the maintenance of bioenergetic structure and cristae-shaping factors preserves mitochondrial connectivity [35]. To our knowledge, these studies are among the first to quantify the connectivity of cristae within a single mitochondrion. These analyses provide a map of where electrical currents, metabolites, ATP, and other mitochondrial contents may be transmitted by the cristae.

However, despite the novelty in routing the pathways that potentially distribute mitochondrial content, we acknowledge there are limitations to these analyses. For example, it is unknown which substances within mitochondria are being transmitted along interconnected networks within and between mitochondria. To this end, Skulachev reported mitochondria propagate their membrane potential along electrically-coupled networks [36, 37] while others have complemented these findings by demonstrating pH flashes can spread between contiguous networks [35]. Taken together, these data may suggest RYKF supports the transmission of membrane potential and protons within isolated mitochondria. Moreover, the present study did not investigate how RYKF impacts networking across multiple mitochondria. We previously reported elamipretide, a potential non-natural analog of RYKF, enhanced the interconnectedness of networks composed of three to nine mitochondria in pathological systems (described in chapter 3). Given the resemblance between elamipretide and RYKF, it is tempting to speculate that RYKF would exert comparable effects. However, future studies are needed to conclusively determine whether or not RYKF can similarly enhance network connectivity in cell or whole tissue models.

RYKF effects on the Inner Membrane Lipid Organization. Given the critical role cardiolipin (CL) plays in stabilizing cristae form and function, we next created mitochondrial membrane models to test the hypothesis that RYKF interacts with CL to stabilize inner membrane morphology (Figure 3). In our giant unilamellar vesicles (GUV) mimicking the phospholipid environment of cristae (20% CL), we observed a uniform distribution of CL (Figure 4A). Interestingly, when RYKF was added to GUVs, CL clustered into domains, suggesting the peptide physically aggregates CL. These results are consistent with previous reports from our group (Described in chapter 3) and others [38] demonstrating cationic, lipophilic peptides like RYKF and elamipretide interact with anionic lipids such as CL.

To gain greater insight into how RYKF-CL interactions affect the biophysical properties of the cristae, we synthesized mitochondrial inner membranes to study lipid packing at a physiological pressure (30nM/m) (Figure 4B). In previous studies, we observed a 25% loss of both total and 18:2 CL content after ischemia-reperfusion injury (Described in chapter 3). Accordingly, we synthesized our mitochondrial membranes to mimic this diseased-induced loss of CL and subsequently, studied the lipid area. The diseased membranes exhibited a significantly less mean molecular area ($P<0.05$), suggesting that membranes containing 25% less CL lose their biophysical integrity. These results are consistent with a number of studies reporting CL loss drastically impairs inner membrane architecture [39]. Interestingly, diseased membranes treated with RYKF demonstrated a mean molecular area comparable to healthy controls that contained 20% CL. These studies were protein free, and the enzymatic and molecular machinery needed for CL biosynthesis was not present. Thus, we ruled out the possibility that RYKF promoted de novo CL synthesis to sustain the biophysical integrity of the inner membrane.

Instead, we propose a mechanism in which RYKF mimics an endogenous mitochondrial assembly factor. We hypothesize RYKF aggregates CL to adhere the damaged membrane, and in turn, this molecular adhesion stabilizes the inner membrane assembly and maintains the lipid area. Our findings that endogenously expressed RYKF protected mitochondrial function are congruent with this hypothesis. Additionally, the observed RYKF-mediated improvements in cristae complexity and networking after freeze thaw support this mechanism as the peptide prevented injury-induced inner membrane disintegration and subsequent cristae fragmentation. However, there are current limitations to this hypothesis as we have not definitively proven RYKF-mediated membrane remodeling is CL-dependent. Future studies are needed to investigate the effects of RYKF in GUVs and biomimetic inner membranes devoid of CL.

Further evidence supporting our hypothesis is illustrated by the presence of conserved tripeptide LYR motifs found in a superfamily of eukaryotic proteins [12, 13]. These LYR proteins also contain a highly conserved phenylalanine (F) residue downstream of the LYR motif (LYR + F). Together, this endogenously expressed, conserved peptide sequence is remarkably similar to RYKF. LYR + F sequences are located near the N-terminus of ~15kDa polypeptides and are known to interact with mitochondrial protein complexes. Indeed, LYR tripeptide sequences are reportedly involved in the assembly of complexes I, II, III, and V of the ETC [13], and the conserved, downstream phenylalanine residue (LYR + F) may be needed for complex I activity and stability [14]. Furthermore, the LYR proteins have been demonstrated to interact with mitochondrial scaffolding proteins, and recently, this interaction was suggested to help coordinate the assembly of ETC complexes with substrate availability [40]. Although our studies did not directly test the effects of RYKF on ETC complex assembly or the ability to interact with mitochondrial scaffolding proteins, our data suggest endogenous RYKF expression similarly

improves ETC function and cristae stability. Taken together, RYKF may exert protection by mimicking conserved, endogenously expressed peptide sequences like LYR + F that facilitate proper mitochondrial protein assembly and ETC function. Our current and previously reported data suggest RYKF and its non-natural analog, elamipretide, aggregate CL and in turn, stabilize cristae ultrastructure and improve mitochondrial function. To our knowledge, it is unknown if LYR or LYR + F sequences similarly interact with CL to indirectly promote ETC structure-function or if the conserved sequences directly stabilize respiratory proteins independent of CL. Because LYR and LYR + F sequences are hydrophobic, cationic, and their larger proteins aid in fatty acid synthesis, it is tempting to speculate that they interact with anionic lipids like CL. However, future studies are needed to confirm these hypotheses.

Limitations

In addition to the limitations already described, there are other drawbacks to our study we would like to acknowledge. First, we did not test the effects of RYKF on non-injured cells (except viral studies) and isolated mitochondria. We have not observed any effects of elamipretide, the non-

natural analog of RYKF, in healthy controls across experimental models. These findings are supported by our viral control studies in which RYKF expression did not affect mitochondrial function in non-injured cells. Furthermore, our mitochondrial networking analyses are limited by their 2D scope. Mitochondria and their cristae are 3D structures. The acquired electron micrographs are from multiple 60nm (z) slices, yet whether or not the cristae (~30nm diameter) were networked at some point above or below each slice is unknown. However, these novel analyses provide a quicker and significantly cheaper approach to measuring mitochondrial networks. Finally, we subjected isolated mitochondria to freeze thaw and did not perform mass spectrometry to measure cardiolipin content following the injury. Therefore, we cannot certify that the observed freeze thaw-induced losses of cristae complexity and networking were due to losses of cardiolipin. This may also limit our interpretations of the biomimetic membrane studies. We modelled our diseased mitochondrial membranes after a previously observed 25% loss of cardiolipin following ischemia-perfusion injury. It is unknown whether a similar loss of cardiolipin occurs after freeze thaw injury. Despite the inconsistencies across models, mitochondrial morphology is similarly affected in both ischemia reperfusion and freeze thaw as we have demonstrated both injuries significantly impair cristae density and networking. Thus we believe our comparisons across models are valid.

Conclusions

We provide evidence that the alternating cationic, lipophilic tetrapeptide sequence, RYKF, protects mitochondrial structure-function. Interestingly, we observed similar CL-RYKF interactions and improved cristae morphology that was associated with respiratory chain protection

when RYKF was endogenously expressed. Given that conserved, tripeptide sequences of alternating cationic, lipophilic motifs stabilize respiratory complex assembly and function in humans, our data suggest RYKF may be mimicking an endogenous mitochondrial assembly factor. Future studies are needed to corroborate this hypothesis and the role mitochondrial phospholipids like cardiolipin play. In all, these data demonstrate the potential of mitochondria-targeted peptides to alter inner membrane organization, improve abhorrent bioenergetic structure-function, and treat diseases characterized by mitochondrial dysmorphology.

Acknowledgements

We are very grateful for the support provided by Kathy Lowe of the Virginia Tech Electron Microscopy Core. Without her guidance and technical expertise, our electron microscopy studies and morphological analyses would not have been possible.

Conflict of Interest

DAB has received consulting income and research grants from Stealth Biotherapeutics.

Funding

These studies were supported by research grants from the National Institutes of Health, NHLBI 1R01HL123647 (to SRS and DAB), Stealth Biotherapeutics (to DAB and SRS), USDA National Institute of Food and Agriculture Hatch Project 1017927 (to DAB), and a Translational Obesity

Research Fellowship from the Virginia Tech Interdisciplinary Graduate Education Program (to MEA).

References

1. Hogeboom GH, C.A., Hotchkiss RD, *The distribution of cytochrome oxidase and succinoxidase in the cytoplasm of the mammaliam liver cell* J Biol Chem, 1946. **165**.
2. GE, P., *The fine structure of mitochondria* The Anatomical Record 1952. **114**(3): p. 427-451.
3. J, W., *Structural biology: Up close with membrane lipid-protein complexes.* Science, 2011. **334**: p. 320-321.
4. C, H.J.a.U., *Cellular microcompartments constitute general subcellular functional units in cells* Biological Chemistry, 2013. **394**: p. 151-161.

5. Bazán S, M.E., Mallampalli VK, Heacock P, Sparagna GC, Dowhan W, *Cardiolipin-dependent reconstitution of respiratory supercomplexes from purified Saccharomyces cerevisiae complexes III and IV.* Journal of Biological Chemistry, 2013. **288**(1): p. 401-411.
6. Gilkerson RW, S.J., Capaldi, *The cristal membrane of mitochondria is the principal site of oxidative phosphorylation.* FEBS Letters, 2003. **546**: p. 355-358.
7. Hackenbrock, C., *Ultrastructural bases for metabolically linked mechanical activity in mitochondria* Journal of Cell Biology 1966. **2**: p. 269-297.
8. Hackenbrock, C., *Ultrastructural bases for metabolically linked mechanical activity in mitochondria. II. Electron transport-linked ultrastructural transformations in mitochondria.* Journal of Cell Biology 1968. **37**(2): p. 345-369.
9. Cogliati, E., Scorrano, *Mitochondrial Cristae: Where Beauty Meets Functionality.* Cell Press, 2016. **41**(3).
10. Chicco, A.J. and G.C. Sparagna, *Role of cardiolipin alterations in mitochondrial dysfunction and disease.* Am J Physiol Cell Physiol, 2007. **292**(1): p. C33-44.
11. Paradies, G., et al., *Decrease in mitochondrial complex I activity in ischemic/reperfused rat heart: involvement of reactive oxygen species and cardiolipin.* Circ Res, 2004. **94**(1): p. 53-9.
12. H, A., *Eukaryotic LYR Proteins Interact with Mitochondrial Protein Complexes.* Biology, 2015. **4**(1): p. 133-150.
13. H, A., *The superfamily of mitochondrial Complex1_LYR motif-containing (LYRM) proteins.* Biochemical Societal Transactions, 2013. **41**(5): p. 1335-1341.
14. Angerer H, R.M., Mańkowska M, Steger M, Zwicker K, Heide H, Wittig I, Brandt U, Zickermann V, *The LYR protein subunit NB4M/NDUFA6 of mitochondrial complex I anchors an acyl carrier protein and is essential for catalytic activity.* Proceedings of the National Academy of Sciences, USA, 2014. **111**(14): p. 5207-5212.
15. Dai, W., et al., *Cardioprotective Effects of Mitochondria-Targeted Peptide SBT-20 in two Different Models of Rat Ischemia/Reperfusion.* Cardiovasc Drugs Ther, 2016.
16. Sloan RC, M.F., Frasier CR, Patel HD, Bostian PA, Lust RM, Brown DA, *Mitochondrial permeability transition in the diabetic heart: contributions of thiol redox state and mitochondrial calcium to augmented reperfusion injury* Journal of Molecular and Cellular Cardiology 2012. **52**: p. 1009-1018.
17. Fonseca SB, P.M., Mourtada R, Gronda M, Horton KL, Hurren R, Minden MD, Schimmer AD, Kelley SO, *Rerouting chlorambucil to mitochondria combats drug deactivation and resistance in cancer cells.* Chem Biol, 2011. **18**(4): p. 445-453.
18. Williams, P.A., et al., *Retinal ganglion cell dendritic degeneration in a mouse model of Alzheimer's disease.* Neurobiol Aging, 2013. **34**(7): p. 1799-806.
19. Sullivan, E.M., et al., *Docosahexaenoic acid lowers cardiac mitochondrial enzyme activity by replacing linoleic acid in the phospholipidome.* J Biol Chem, 2018. **293**(2): p. 466-483.
20. Pennington, E.R., et al., *Distinct membrane properties are differentially influenced by cardiolipin content and acyl chain composition in biomimetic membranes.* Biochim Biophys Acta, 2017. **1859**(2): p. 257-267.
21. Paradies, G. and F.M. Ruggiero, *Age-related changes in the activity of the pyruvate carrier and in the lipid composition in rat-heart mitochondria.* Biochim Biophys Acta, 1990. **1016**(2): p. 207-12.

22. Horton KL, S.K., Froseca SB, Guo Q, Kelley S, *Mitochondria-Penetrating Peptides.* Cell Press, 2008 **15**: p. 375-382.
23. Dai W, C.E., Alleman RJ, Perry JB, Allen ME, Brown DA, Kloner RA, *Cardioprotective effects of mitchondria-targeted peptide SBT-20 in two different models of rat ischemia/reperfusion.* Cardiovasuclar Drugs and Therapy 2016.
24. Woolley DM, R.D., *Ultrastructural injury to human spermatozoa after freezing and thawing.* Journal of reproduction and fertility, 1978. **53**(2): p. 389-394.
25. Bowers WD Jr, H.R., Daum RC, Ashbaugh P, Nilson E, *Ultrastructural studies of muscle cells and vascular endothelium immediately after freeze-thaw injury.* Crybiology 1973. **10**(1): p. 9-21.
26. Hanai A, Y.W., Ravikumar TS, *Induction of apoptosis in human colon carcinoma cells HT29 by sublethal cryo-injury: mediation by cytochrome c release.* International Journal of Cancer, 2001. **93**(4): p. 526-533.
27. Mori Y, S.H., Nei T, *Freezing injury in the yeast respiratory system.* Cryobiology, 1986. **23**(1): p. 64-71.
28. Liu L, W.M., Yu TH, Cheng Z, Li M, Guo QW, *Mitochondria-targeted antioxidant Mitoquinone protects post-thaw human sperm against oxidative stress injury.* National journal of andrology 2016. **22**(3): p. 205-211.
29. Zhao, K., et al., *Cell-permeable peptide antioxidants targeted to inner mitochondrial membrane inhibit mitochondrial swelling, oxidative cell death, and reperfusion injury.* J Biol Chem, 2004. **279**(33): p. 34682-90.
30. Brown, D.A., et al., *Reduction of Early Reperfusion Injury With the Mitochondria-Targeting Peptide Bendavia.* J Cardiovasc Pharmacol Ther, 2013.
31. Dai, W., et al., *Bendavia, a mitochondria-targeting peptide, improves postinfarction cardiac function, prevents adverse left ventricular remodeling, and restores mitochondria-related gene expression in rats.* J Cardiovasc Pharmacol, 2014. **64**(6): p. 543-53.
32. Siegel, M.P., et al., *Mitochondrial-targeted peptide rapidly improves mitochondrial energetics and skeletal muscle performance in aged mice.* Aging Cell, 2013. **12**(5): p. 763-71.
33. Glancy, B., et al., *Mitochondrial reticulum for cellular energy distribution in muscle.* Nature, 2015. **523**(7562): p. 617-20.
34. Vincent AE, W.K., Davey T, Philips J, Ogden RT, Lawess C, Warren C, Hall MG, Ng YS, Falkous G, Holden T, Deehan D, Taylor RW, Turnbull DM, Picard M, *Quantitative 3D Mapping of the Human Skeletal Muscle Mitochondrial Network.* Cell Reports, 2019. **26**(4): p. 996-1009.
35. Santo-Domingo J, G.M., Poburko D, Scorrano L, Demaurex N, *OPA1 promotes pH flashes that spread between contiguous mitochondria without matrix protein exchange.* EMBO J, 2013. **32**(13): p. 1927-1940.
36. Amchenkova AA, B.L., Chentsov YS, Skulachev VP, Zorov DB, *Coupling membranes as energy-transmitting cables. I. Filamentous mitochondria in fibroblasts and mitochondrial clusters in cardiomyocytes.* Journal of Cell Biology, 1988. **107**(2): p. 481-495.
37. VP, S., *Mitochondrial filaments and clusters as intracellular power-transmitting cables.* Trends in Biochemical Sciences, 2001. **26**(1): p. 23-29.

38. Birk, A.V., et al., *Targeting Mitochondrial Cardiolipin and the Cytochrome C/Cardiolipin Complex to Promote Electron Transport and Optimize Mitochondrial Atp Synthesis.* Br J Pharmacol, 2013.
39. Acehan D, M.A., Xu Y, Ren M, Stokes DL, Schlame M, *Cardiolipin Affects the Supramolecular Organization of ATP Synthase in Mitochondria.* Biophysics Journal, 2011. **100**(9): p. 2184–2192.
40. Van Vranken JG, N.S., Clowers KJ, Jeong MY, Ouyang Y, Berg JA, Gygi JP, Gygi SP, Winge DR, Rutter J, *ACP Acylation Is an Acetyl-CoA-Dependent Modification Required for Electron Transport Chain Assembly.* Molecular Cell, 2018. **71**(4): p. 567-580.

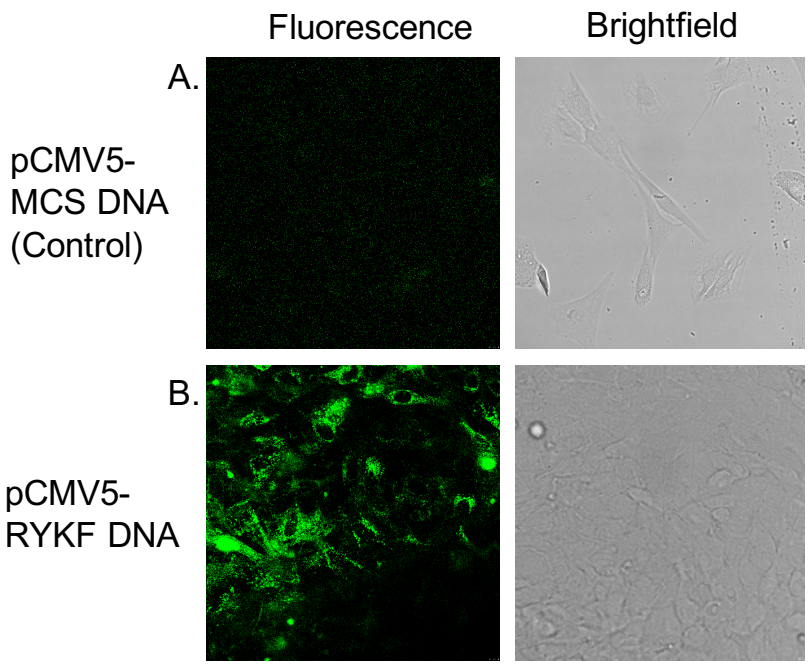

Figure 1. Confocal microscopic images of of C2C12 mouse myoblasts transfection with control (A) or recombinant (B) plasmids. The pCMV5-MCS plasmid was used for cloning, and the IgKzsGreen1 furin cleavage/RYKF peptide was PCR amplified and cloned at the EcoRI/HindIII site. Approximately 1 million cells were transfected with 2ug Xfect in 6 well plates. (A) The pCMV5-MCS control vector does not fluoresce green inside cells, whereas (B) the recombinant pCMV5-RYKF DNA vector fluoresces green, confirming RYKF expression in ~90% of cells.

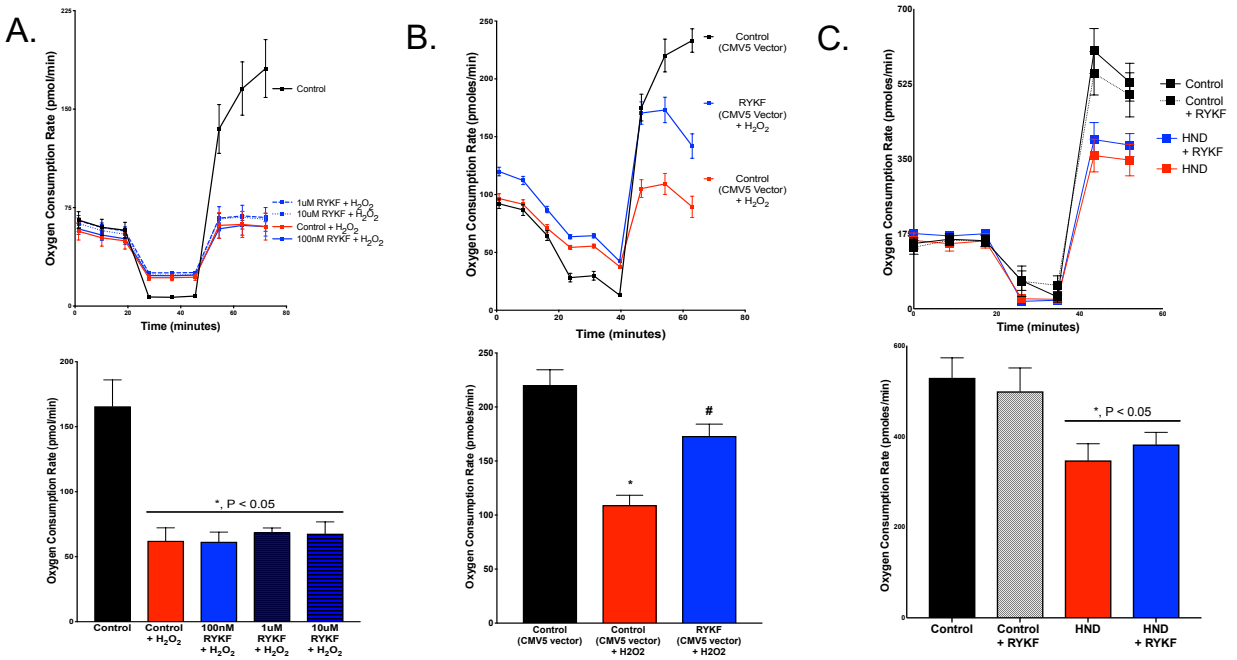

Figure 2. Effects of exogenous treatment and endogenous expression of RYKF on mitochondrial function in cultured cells. Seahorse traces are normalized to antimycin a values in top panel with corresponding FCCP (maximal) respiratory rates in bottom panel. Order of injections was oligomycin (2uM), FCCP (1uM), Antimycin A (2uM). (A) 3 hour pre-treatment with 10uM RYKF did not protect against peroxide-induced decrements in C2C12 myoblast maximal respiration. N = 11 per group. (B) Endogenously expressing RYKF with vector-mediated delivery significantly protected C2C12 maximal respiration from a peroxide injury. N = 16-32 per group. (C) Endogenously expressing RYKF via viral transfection trended to but did not significantly protect C2C12 maximal respiration from hypoxia nutrient deprivation (HND) injury. N = 11 per group. *, P<0.05 v control; #, P<0.05 versus injured control.

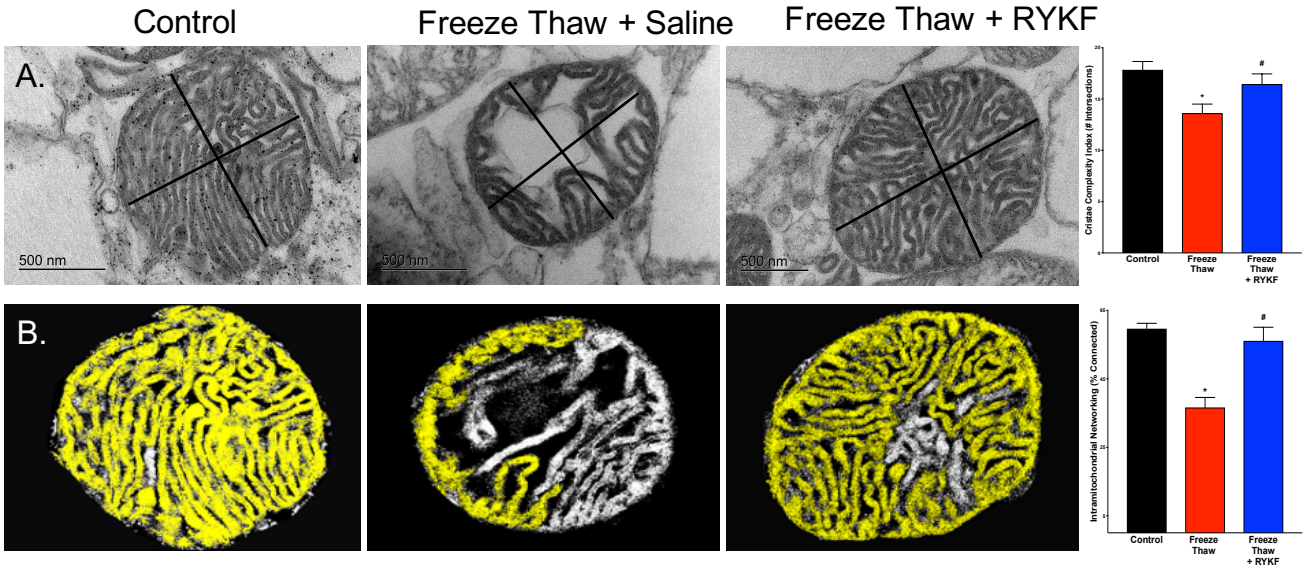

Figure 3. TEM images of mitochondria illustrating the effects of RYKF on mitochondrial structure. Isolated mitochondria from rat left ventricle were pre-treated with 10uM RYKF for 30min and subjected to 3 cycles of a 1min freeze 1min thaw injury. (A) Mitochondria were analyzed for cristae complexity by counting the number of cristae intersections along the horizontal and vertical axes. N = 26-42 mitochondria per group. (B) Intramitochondrial networking was calculated using the yellow flood fill tool in image j as previously described (Allen et al). N = 20 mitochondria per group. *, P<0.05 v control; #, P<0.05 versus freeze thaw.

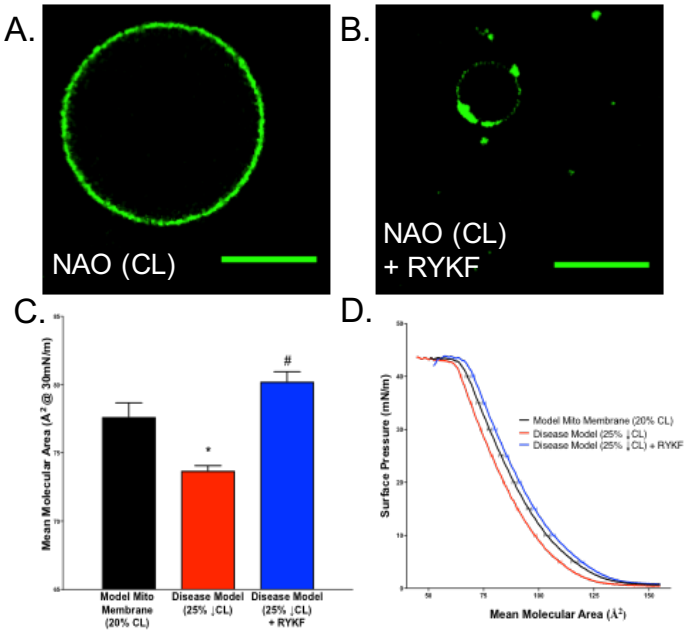

Figure 4. RYKF reorganizes biomimetic mitochondrial inner membrane lipids. (A-B) GUV imaging of cardiolipin (CL) with NAO. 20uM RYKF was added to GUVs in (B). N = 30-75 GUVs per group. We previously observed a 25% loss of total and 18:2 CL content in the ischemia-reperfused heart (Allen et al, 2019). This loss in CL content was recapitulated in diseased membrane models (C-D). Pressure-area isotherms at physiological membrane pressure (30mN/m) show the effects of losing CL content and RYKF (1uM) interactions to augment lipid area despite CL losses. N = 3-6 biomimetic membranes per group. *, P<0.05 v control; #, P<0.05 versus disease model.

Chapter 5

Conclusion

Mitochondrial structure-function plays a critical role in health and disease. The cristae, invaginations of the inner membrane, host the oxidative phosphorylation (OXPHOS) machinery that produces energy. Healthy cristae are "dynamic biochemical reactors" capable of reorganizing their structure to facilitate the electrochemical processes needed to produce ATP [1]. Indeed, upon activation of OXPHOS the IM shifts from a contracted, "orthodox" state to a wider, "condensed" morphology [2, 3]. The ability of cristae to properly complete these dynamic morphological shifts is dependent on lipids and proteins that regulate their structure and function. Namely, cardiolipin, MICOS, OPA1, and ATP synthase dimers all collaborate to maintain cristae shape [1, 4].

Defects in one or a combination of these cristae shaping factors causes severe impairments in mitochondrial structure-function that lead to a variety of diseases. Notably, decrements in cristae shaping factors underlie debilitating mitochondrial diseases. To date, there are no FDA approved treatments for mitochondrial disease, but several compounds aiming to improve mitochondrial function are currently being developed. These therapeutics can improve electron flow through the respiratory chain, scavenge mitochondrial ROS, or stabilize mitochondrial lipids. However, their effects on cristae shaping factors and overall mitochondrial structure are relatively understudied. In an effort to understand which therapeutics have the best opportunity to treat which diseases, further studies are desperately needed to define the relationships between specific morphological decrements, disease, and therapeutics. As these investigations are realized, medicines can be tailored to specific diseases and improve patient outcomes.

In the present work, we studied elamipretide, a cell-permeable tetrapeptide in clinical trials for genetic and age-related mitochondrial disease. Importantly, we demonstrated elamipretide aggregates the cristae shaping factor cardiolipin. To this end, cardiolipin aggregation was associated with restored inner membrane biophysical integrity, preserved cristae ultrastructure, protected cristae networks, and improved respiration across electron transport chain complexes. We also observed similar cardiolipin interactions and subsequent protection of mitochondrial structure-function with a naturally-occurring peptide sequence, RYKF. Taken together, our findings suggest cationic, lipophilic peptides may mimic endogenous mitochondrial assembly factors. However, future studies are needed to corroborate this hypothesis and the role mitochondrial phospholipids like cardiolipin play.

Several aspects of our findings are novel to the field. First, we showed that improvements in pathological bioenergetics is observed with elamipretide across electron transport system complexes. Second, elamipretide reduced the emission of mitochondrial reactive oxygen species through a modest reduction in reverse electron transport and preservation of some (but not all) native respiratory complexes. Third, these functional improvements were associated with augmented mitochondrial structure, particularly as it pertains to the cristae network. Fourth, structure-function improvements with elamipretide are observed without preventing the acute loss of cardiolipin. Fifth, mechanistic experiments with biophysical models of the mitochondrial inner membrane in cardiac health and disease provided unpreceded insight into the consequences of cardiolipin loss, and demonstrated that acute elamipretide and RYKF treatment aggregates mitochondrial membranes in a cardiolipin-dependent manner. Finally, we developed a novel method to calculate the connectivity of cristae networks in mitochondria.

Collectively, these data demonstrate the potential of mitochondria-targeted peptides to alter inner membrane organization, improve abhorrent bioenergetic structure-function, and treat diseases characterized by mitochondrial dysmorphology. Our findings support the development of a new class of mitochondria-targeted peptides comprised of alternating cationic, lipophilic motifs. These peptides represent a promising therapeutic approach for mitochondrial diseases characterized by underlying cristae dysmorphology. Our findings suggest RYKF and elamipretide alike may be mimicking conserved, endogenously expressed mitochondrial assembly factors. Importantly, the presented work supports the continued development of mitochondria-targeting molecules for a variety of mitochondrial diseases, particularly those characterized by the loss of cardiolipin and cristae.

References

1. Cogliati, E., Scorrano, *Mitochondrial Cristae: Where Beauty Meets Functionality.* Cell Press, 2016. **41**(3).

2. Hackenbrock, C., *Ultrastructural bases for metabolically linked mechanical activity in mitochondria* Journal of Cell Biology 1966. **2**: p. 269-297.
3. Hackenbrock, C., *Ultrastructural bases for metabolically linked mechanical activity in mitochondria. II. Electron transport-linked ultrastructural transformations in mitochondria.* Journal of Cell Biology 1968. **37**(2): p. 345-369.
4. Quintana-Cabrera, M., Rigoni, Soriano, *Who and how in the regulation of mitochondrial cristae shape and function.* Biochemical and Biophysical Research Communications, 2018. **500**: p. 94-101.